

Assessing Enzyme-Catalysed Phosphorylation of Nucleosides to Aid Synthetic Approaches to Novel Antiviral Nucleotides

By

Crispin Dye

A thesis submitted to the Victoria University of Wellington in fulfilment of the requirements
for the degree of Master of Drug Discovery and Development

Victoria University of Wellington

(2022)

Abstract

Nucleoside analogues acting as chain terminators of viral RNA and DNA polymerases represent an effective therapeutic strategy for the inhibition of viral replication and treatment of viral infections. These compounds must be anabolised into their triphosphate forms before inclusion into the nascent nucleic acid chain by the relevant polymerase thus their action is somewhat reliant on intracellular phosphorylation machinery. The synthetic addition of α -, β -, and γ -phosphate groups to the 5'-carbons of these compounds may provide a means to circumvent this reliance and produce more effective antiviral nucleoside analogues. This can be achieved through the utilisation of enzymes as a synthetic tool, enzymes capable of phosphorylating nucleoside analogues can be expressed in and purified from bacterial cell lines for use in the synthetic process.

The present study has optimised the catalytic reaction of human UCK1 for synthetic purpose and assessed the activity of the enzyme against a range of nucleoside analogues. A range of nucleoside kinase enzymes were recombinantly expressed and purified with the goal of developing an enzymatic reaction process with synthetic utility. A linear regression model capable of calculating the substrate turnover of UCK from ^{31}P NMR spectra of reaction samples was developed, and optimal conditions for a PK-coupled UCK reaction were identified (12.5 mM substrate, 1.5 mg/mL UCK, 3 mg/mL PK) using this model. Under the previously stated reaction conditions UCK1 was found to phosphorylate 71.68% of cytidine and 14.12% of uridine in the sample in a thirty-minute duration, translating to a production of 2.90 mg of CMP and 0.57 mg of UMP from 1 mL reaction volume. Assessment of UCK1 activity against unnatural substrates of the enzyme revealed 13.67% conversion of 5-methyl-U to the corresponding monophosphate. UCK1 was also shown to have phosphorylative activity against aza-C and riboaminopyrrole via LCMS analysis, at a level below the sensitivity of the ^{31}P NMR-based model. The results of this study reinforce the importance of the sugar moiety in nucleoside binding to UCK and indicate a low tolerability of the enzyme for modifications to the substrate at this moiety. These results also suggest the potential of UCK1 to be used as a tool in the synthesis of nucleobase-modified nucleoside analogues.

The reaction process developed in the present study represents a significant step towards the development of an efficient means of synthesising phosphorylated derivatives of nucleoside analogues through enzyme-catalysed reaction. Future efforts on this research should focus on the development of an effective means of isolating product compound from the reaction mixture and increasing the scale of reaction to be synthetically useful.

Acknowledgments

To begin I'd like to thank my supervisors, Dr Lawrence Harris and Dr Tom Scully, for the opportunity to work on this fascinating project which has all but consumed my life over the past year. To Lawrence, your guidance and feedback has been invaluable. To Tom, I'll be forever grateful for your mentorship in the lab, patience in dealing with my incessant questions, and belief in my abilities.

Thank you to the Ferrier Research Institute and the Victoria University of Wellington for providing a great learning environment and the opportunity to work with so many brilliant scientists. Thanks to Assoc Prof Simon Hinkley for helping me decide on and settle into the MDDD programme. Additional thanks to Prof Emily Parker for providing me with laboratory and office space to work from, to Eleanor and Jo for all their work behind the scenes to keep the lab running smoothly, and to Jan Vorster for all the help with my NMR analysis.

To my classmates and lab mates, thanks for making my time at VUW so pleasant. I've thoroughly enjoyed my time working with both the Parker and Harris lab groups, my gratitude goes out to each member of these teams for the advice, support, and good company that you have provided. To my MDDD course mates, thanks for making the course enjoyable. For those that are still studying good luck, and for those that have graduated congratulations.

To my parents, thanks for all the advice, support, and motivation you have provided me throughout my academic study.

A special thanks to my partner Isabelle, for both encouraging me to undertake this course to begin with and for supporting me through all the stress of thesis-writing and many late nights of study. I truly could not have done this without you.

Finally, thanks to all my friends and family who have supported me throughout this journey.

Contents

Abstract.....	i
Acknowledgments.....	ii
Contents	iii
List of Figures	viii
List of Tables	xiii
List of Abbreviations	xiv
1.0 Background.....	1
1.1 Nucleosides and Nucleic Acids.....	1
1.1.1 Nucleosides	1
1.1.2 Nucleic Acids	1
1.2 RNA Viruses.....	2
1.2.1 Replication of RNA Viruses	2
1.2.2 RNA-Dependant RNA Polymerase.....	2
1.2.3 Reverse Transcriptase	3
1.3 Antiviral Nucleoside Analogues	3
1.3.1 Mechanism of Action.....	3
1.3.2 Anabolic Activation of Nucleoside Analogues.....	4
1.3.3 Application of Prodrug Strategy to Nucleoside Analogues	4
1.3.4 Endogenous Chain Terminators	5
1.4 Strategies for Nucleoside Analogue Drug Development	6
1.4.1 Nucleoside Analogue Drug Design.....	6
1.4.2 Synthetic Addition of Phosphate Groups	7
1.5 Enzymes Catalysing Ribonucleoside Phosphorylation	8
1.5.1 α -Phosphate Addition.....	8
1.5.2 β -Phosphate Addition.....	10
1.5.3 γ -Phosphate Addition.....	11
1.6 Enzymatic Catalysis as a Synthetic Tool	11
1.6.1 Production of Enzymes for Synthetic Use	11
1.6.2 Use of ^{31}P Nuclear Magnetic Resonance Spectroscopy to Assess Synthetic Utility	12
1.6.3 Activity of Uridine-Cytidine Kinase Against Unnatural Nucleosides	12
1.7 Aims of the Present Study.....	13
2.0 Materials and methods	14
2.1 General Microbial Strains and Materials	14
2.1.1 Bacterial Strains	14

2.1.2	Plasmids	15
2.1.3	Media	15
2.1.4	Media Supplements	16
2.1.5	Enzymes	16
2.1.6	Buffer Solutions	16
2.2	Microbial Growth and Maintenance	18
2.2.1	General Maintenance	18
2.2.2	1 L Bacterial Culture Growth	18
2.2.3	Induction of Protein Expression	18
2.3	General Molecular Biology	19
2.3.1	Isolation of Plasmid DNA	19
2.3.1.1	Plasmid Isolation from E. coli	19
2.3.1.2	Plasmid Isolation from Filter Paper (PBS-Based Soaking Extraction)	19
2.3.1.3	Plasmid Isolation from Filter Paper (TAE-Based Soaking Extraction)	19
2.3.1.4	Plasmid Isolation from Filter Paper (TAE-Based Shredded Paper Extraction)	19
2.3.2	DNA Analysis	19
2.3.2.1	Agarose Gel Electrophoresis	19
2.3.2.2	Nanodrop Measurement of DNA Concentration	20
2.3.2.3	DNA Sequencing	20
2.3.3	Transformation of Competent Cells	20
2.3.3.1	Transformation of BL21 Cells	20
2.3.3.2	Transformation of Stellar™ Cells	20
2.3.4	Lysis of Bacterial Cultures	20
2.3.4.1	Chemical Lysis	20
2.3.4.2	Sonication Lysis	21
2.4	Protein Purification	21
2.4.1	Spin Column Purification	21
2.4.2	Immobilised Metal Affinity Chromatography (IMAC) Purification	21
2.4.3	Anion Ion Exchange Chromatography (IEC) Purification	22
2.4.4	Protein Dialysis	23
2.4.5	Protein Concentration	23
2.4.6	Protein Storage	23
2.4.7	Production of Pyruvate Kinase	23
2.5	Protein Analysis	24
2.5.1	Polyacrylamide Gel Electrophoresis	24
2.5.2	Measurement of Protein Concentration	24
2.6	Enzyme Bioactivity Assays	24

2.6.1	General Reaction Process.....	24
2.7	Analysis of Catalytic Activity.....	25
2.7.1	Small Molecule Analysis	25
2.7.1.1	Liquid Chromatography-Mass Spectrometry.....	25
2.7.1.2	Nuclear Magnetic Resonance Spectroscopy	25
2.7.2	Enzyme Turnover Quantification.....	25
3.0	Results: Protein Production.....	27
3.1	Selection of Kinases.....	27
3.2	Adenosine Kinase (<i>Anopheles gambiae</i>)	27
3.2.1	Transformation of BL21	27
3.2.2	Protein Purification	29
3.3	Uridine Cytidine Kinase 1 (human).....	32
3.3.1	Transformation of BL21	32
3.3.2	Protein Purification	32
3.4	Uridine Cytidine Kinase 2 (human).....	36
3.4.1	FLAG-tagged UCK2.....	36
3.4.1.1	Transformation.....	36
3.4.1.2	Purification.....	36
3.4.2	His-tagged UCK2.....	39
3.4.2.1	Transformation.....	39
3.4.2.2	Purification.....	40
3.5	Adenylate Kinase (<i>Escherichia coli</i>)	42
3.5.1	Transformation.....	42
3.5.2	Protein Expression	42
3.6	Guanylate Kinase (<i>Plasmodium falciparum</i>).....	44
3.6.1	Transformation.....	44
3.6.2	Protein Expression	45
3.7	Uridine Monophosphate-Cytidine Monophosphate Kinase (human)	50
3.7.1	FLAG-tagged CMPK.....	50
3.7.1.1	Transformation.....	50
3.7.1.2	Purification.....	50
3.7.2	His-tagged CMPK.....	53
3.7.2.1	Transformation.....	53
3.7.2.2	Purification.....	54
4.0	Reaction Optimisation.....	57
4.1	Introduction.....	57
4.2	Standards.....	57

4.2.1	Adenosine Triphosphate	58
4.2.2	Uridine	58
4.2.3	Uridine Monophosphate.....	59
4.2.4	Adenosine Monophosphate.....	59
4.2.5	Adenosine Diphosphate	60
4.2.6	Phosphoenolpyruvate	60
4.2.7	Mixed Standards	61
4.2.8	Heat Study.....	62
4.2.9	pH study	65
4.3	Confirmation of Enzymatic Activity.....	66
4.3.1	ADK.....	66
4.3.2	GUK.....	67
4.3.3	UCK1	69
4.3.4	UCK2 (FLAG-tag).....	70
4.3.5	CMPK (FLAG-tag).....	71
4.4	Optimisation of Component Concentration	72
4.5	Reaction Duration Study	74
4.6	Substrate Excess Study	75
4.7	Use of Pyruvate Kinase.....	77
4.8	Confirmation of Enzymatic Activity.....	79
4.8.1	ADK.....	79
4.8.2	GUK.....	80
4.8.3	UCK1	81
4.8.4	UCK2 (His-tag).....	83
4.8.5	CMPK (His-tag).....	84
4.7	Quantification Model	86
4.7.1	NMR	86
4.7.2	Linear Regression Modelling.....	88
4.7.3	Accuracy of Model at Higher Component Concentrations	90
4.8	UCK1 Concentration Study	91
4.9	PK Concentration Study.....	92
4.10	Addition Strategy Study.....	93
4.11	Identification of Optimised Conditions.....	94
5.0	Results: Activity Against Unnatural Nucleosides.....	95
5.1	Introduction.....	95
5.2	Activity Against Natural Substrates.....	95
5.2.1	Analysis via ³¹ P NMR	96

5.2.2	Analysis via LCMS.....	97
5.3	Activity Against Unnatural Substrates.....	100
5.3.1	Analysis via ³¹ P NMR.....	101
5.3.2	Analysis via LCMS.....	102
6.0	Discussion.....	107
6.1	Protein Production	107
6.1.1	Heterologous Protein Expression.....	107
6.1.2	Mode of Bacterial Lysis	107
6.1.3	IMAC Protein Purification.....	108
6.1.4	IEC Protein Purification.....	109
6.2	Optimisation of Catalytic Activity.....	110
6.2.1	Choice of Phosphate Donor	110
6.2.2	Utility of Phosphate Donor Regeneration.....	110
6.2.3	Observed Activity of Nucleoside Monophosphate Kinases.....	111
6.2.4	Duration of Reaction.....	111
6.2.5	Potential Phosphate Contamination	111
6.2.6	Choice of Component Concentration.....	113
6.3	Activity Against Unnatural Substrates.....	114
6.3.1	Predicted Utility of Ribonucleoside Kinases	114
6.3.2	Impact of Substrate Solubility.....	114
6.3.3	Activity of UCK1.....	114
6.3.4	Activity of UCK2.....	116
6.4	Quantification Curve.....	116
6.5	Limitations of Present Study.....	117
6.6	Future Development.....	117
6.6.1	Synthetic Utility	117
6.6.2	‘One-pot’ Reaction Development	118
7.0	Concluding Remarks.....	119
	References.....	120

List of Figures

Figure 1.1: Chemical structures of the endogenous nucleosides that act as structural constituents of nucleic acids.....	1
Figure 1.2: Chemical structure of tenofovir disoproxil.....	5
Figure 1.3: Chemical structures of a range of clinically approved nucleoside analogue drugs	7
Figure 1.4: Organic synthesis of ddhCTP.....	8
Figure 1.5: General scheme depicting the anabolic pathway of conversion of cytidine to cytidine triphosphate.....	9
Figure 1.6: General scheme of the catalytic mechanism of nucleoside kinases	10
Figure 3.1: Comparison of gel electrophoresis results of different AgAK plasmid extraction methods	28
Figure 3.2: Picture of representative agar plates produced from transformation of Stellar™ cells with TAE-based AgAK plasmid extracts.....	28
Figure 3.3: Picture of representative agar plate produced from transformation of BL21 cells with AgAK plasmid extract from Stellar™ cells	29
Figure 3.4: IMAC purification of cell lysate derived from AgAK BL21 liquid culture.....	29
Figure 3.5: PAGE of eluent from His SpinTrap™ purification of AgAK BL21 cell lysate.....	30
Figure 3.6: IEC purification of cell lysate derived from AgAK BL21 liquid culture.....	31
Figure 3.7: PAGE of fractions collected from IEC of AgAK BL21 cell lysate.....	31
Figure 3.8: Picture of representative agar plate produced from transformation of BL21 cells with UCK1 plasmid extract from Mach1 cells	32
Figure 3.9: PAGE of UCK1 BL21 cell lysate and His SpinTrap™ eluent.....	33
Figure 3.10: IMAC purification of cell lysate derived from 150 mL UCK1 BL21 liquid culture.....	34
Figure 3.11: PAGE of eluent from IMAC purification of UCK1 BL21 cell lysate.....	34
Figure 3.12: IMAC purification of cell lysate derived from 3 L UCK1 BL21 liquid culture.....	35
Figure 3.13: PAGE of eluent from large scale IMAC purification of UCK1 BL21 cell lysate	35
Figure 3.14: Picture of representative agar plate produced from transformation of BL21 cells with UCK2 (FLAG-tag) plasmid extract from Stbl3 cells.....	36
Figure 3.15: IEC purification of cell lysate derived from UCK2 (FLAG-tag) BL21 liquid culture.....	37
Figure 3.16: PAGE of fractions collected from IEC of UCK2 (FLAG-tag) BL21 cell lysate.....	37
Figure 3.17: Double-purification IEC of cell lysate derived from UCK2 (FLAG-tag) BL21 liquid culture	38
Figure 3.18: Double-purification IEC of cell lysate derived from UCK2 (FLAG-tag) BL21 liquid culture	38

Figure 3.19: PAGE of fractions collected from double-purification IEC of UCK2 (FLAG-tag) BL21 cell lysate	39
Figure 3.20: Picture of representative agar plates produced from transformation of BL21 cells with pure UCK2 (His-tag) plasmid	39
Figure 3.21: PAGE of eluent from His SpinTrap™ purification of UCK2 (His-tag) BL21 cell lysate	40
Figure 3.22: IMAC purification of cell lysate derived from 3 L UCK2 (His-tag) BL21 liquid culture	41
Figure 3.23: PAGE of eluent from large scale IMAC purification of UCK2 (His-tag) BL21 cell lysate	41
Figure 3.24: Picture of representative agar plate produced from transformation of BL21 cells with EcADK plasmid extract from DH5-Alpha cells	42
Figure 3.25: PAGE of EcADK BL21 cell lysate and His SpinTrap™ eluent	43
Figure 3.26: IMAC purification of cell lysate derived from 150 mL EcADK BL21 liquid culture	44
Figure 3.27: PAGE of eluent from IMAC purification of EcADK BL21 cell lysate.....	44
Figure 3.28: Picture of representative agar plate produced from transformation of BL21 cells with PfGUK plasmid extract from Stbl3 cells	45
Figure 3.29: PAGE of PfGUK BL21 cell lysate and His SpinTrap™ eluent	46
Figure 3.30: IMAC purification of cell lysate derived from PfGUK BL21 liquid culture	47
Figure 3.31: PAGE of eluent from IMAC purification of PfGUK BL21 cell lysate	47
Figure 3.32: PAGE of eluent from His SpinTrap™ purification of PfGUK BL21 cell lysate	48
Figure 3.33: IEC purification of cell lysate derived from PfGUK BL21 liquid culture	49
Figure 3.34: PAGE of fractions collected from IEC of PfGUK BL21 cell lysate	49
Figure 3.35: Picture of representative agar plate produced from transformation of BL21 cells with CMPK (FLAG-tag) plasmid extract from Stbl3 cells	50
Figure 3.36: IEC purification of cell lysate derived from CMPK (FLAG-tag) BL21 liquid culture	51
Figure 3.37: PAGE of fractions collected from IEC of CMPK (FLAG-tag) BL21 cell lysate.....	51
Figure 3.38: Double-purification IEC of cell lysate derived from CMPK (FLAG-tag) BL21 liquid culture	52
Figure 3.39: Double-purification IEC of cell lysate derived from CMPK (FLAG-tag) BL21 liquid culture	53
Figure 3.40: PAGE of fractions collected from double-purification IEC of CMPK (FLAG-tag) BL21 cell lysate	53
Figure 3.41: Picture of representative agar plates produced from transformation of BL21 cells with pure CMPK (His-tag) plasmid	54
Figure 3.42: PAGE of eluent from His SpinTrap™ purification of CMPK (His-tag) BL21 cell lysate	54
Figure 3.43: IMAC purification of cell lysate derived from 3 L CMPK (His-tag) BL21 liquid culture	55

Figure 3.44: PAGE of eluent from large scale IMAC purification of CMPK (His-tag) BL21 cell lysate	56
Figure 4.1: ^{31}P NMR spectrum derived from 25 mM ATP in rNK reaction buffer, 5% D_2O	58
Figure 4.2: ^{31}P NMR spectrum derived from 25 mM uridine solution, 5% D_2O	58
Figure 4.3: ^{31}P NMR spectrum derived from 25 mM UMP in rNK reaction buffer, 5% D_2O	59
Figure 4.4: ^{31}P NMR spectrum derived from 25 mM AMP in rNK reaction buffer, 5% D_2O	59
Figure 4.5: ^{31}P NMR spectrum derived from 25 mM ADP in rNK reaction buffer, 5% D_2O	60
Figure 4.6: ^{31}P NMR spectrum derived from 137.5 mM PEP in rNK reaction buffer, 5% D_2O	60
Figure 4.7: ^{31}P NMR spectrum derived from 12.5 mM uridine, 13.75 mM PEP, 2.5 mM ATP in rNK reaction buffer, 5% D_2O	61
Figure 4.8: ^{31}P NMR spectrum derived from 25 mM UMP, 25 mM PEP, 25 mM ATP in rNK reaction buffer, 5% D_2O	62
Figure 4.9: ^{31}P NMR spectrum derived from 25 mM ATP in rNK reaction buffer, 5% D_2O	62
Figure 4.10: ^{31}P NMR spectrum derived from 25 mM UMP in rNK reaction buffer, 5% D_2O	63
Figure 4.11: ^{31}P NMR spectrum derived from 25 mM AMP in rNK reaction buffer, 5% D_2O	63
Figure 4.12: ^{31}P NMR spectrum derived from 25 mM ADP in rNK reaction buffer, 5% D_2O	63
Figure 4.13: ^{31}P NMR spectrum derived from 137.5 mM PEP in rNK reaction buffer, 5% D_2O	64
Figure 4.14: ^{31}P NMR spectrum derived from 12.5 mM uridine, 13.75 mM PEP, 2.5 mM ATP in rNK reaction buffer, 5% D_2O	64
Figure 4.15: ^{31}P NMR spectrum derived from 25 mM UMP, 25 mM PEP, 25 mM ATP in rNK reaction buffer, 5% D_2O	64
Figure 4.16: ^{31}P NMR spectrum derived from 25 mM UMP, 25 mM PEP, 25 mM ATP in rNK reaction buffer (pH 6.5), 5% D_2O	65
Figure 4.17: ^{31}P NMR spectrum derived from 25 mM UMP, 25 mM PEP, 25 mM ATP in rNK reaction buffer (pH 7.5), 5% D_2O	65
Figure 4.18: ^{31}P NMR spectrum derived from 25 mM UMP, 25 mM PEP, 25 mM ATP in rNK reaction buffer (pH 8.5), 5% D_2O	66
Figure 4.19: ^{31}P NMR spectrum derived from ADK activity test reaction sample.....	67
Figure 4.20: ^{31}P NMR spectrum derived from ADK activity test negative control sample.....	67
Figure 4.21: Image of PfGUK reaction mixture approximately two minutes following the addition of GMP	68
Figure 4.22: ^{31}P NMR spectrum derived from GUK activity test reaction sample.....	68
Figure 4.23: ^{31}P NMR spectrum derived from GUK activity test negative control sample.....	69
Figure 4.24: ^{31}P NMR spectrum derived from UCK1 activity test reaction sample	69
Figure 4.25: ^{31}P NMR spectrum derived from UCK1 activity test negative control sample	70
Figure 4.26: ^{31}P NMR spectrum derived from UCK2 (FLAG-tag) activity test reaction sample.....	70

Figure 4.27: ^{31}P NMR spectrum derived from UCK2 (FLAG-tag) activity test negative control sample	71
Figure 4.28: ^{31}P NMR spectrum derived from CMPK (FLAG-tag) activity test reaction sample.....	72
Figure 4.29: ^{31}P NMR spectrum derived from CMPK (FLAG-tag) activity test negative control sample	72
Figure 4.30: Comparative bar graph depicting difference in integrals of relevant peaks between reaction and control sample of PK activity study. Full data described in Table 4.5.....	78
Figure 4.31: Comparative bar graph depicting difference in integrals of relevant peaks between reaction and control sample of ADK activity study. Full data described in Table 4.6.	80
Figure 4.32: Comparative bar graph depicting difference in integrals of relevant peaks between reaction and control sample of GUK activity study. Full data described in Table 4.7.	81
Figure 4.33: Comparative bar graph depicting difference in integrals of relevant peaks between reaction and control sample of UCK1 activity study. Full data described in Table 4.8.	82
Figure 4.34: Comparative bar graph depicting difference in integrals of relevant peaks between reaction and control sample of UCK2 activity study. Full data described in Table 4.9.	84
Figure 4.35: ^{31}P NMR spectrum derived from CMPK (His-tag) activity test negative control sample	85
Figure 4.36: ^{31}P NMR spectrum derived from CMPK (His-tag) activity test reaction sample.....	86
Figure 4.37: Changes in peak integrals of peaks attributed to UMP and PEP as simulated substrate conversion increases	87
Figure 4.38: Changes in mean peak chemical shift as simulated substrate conversion increases	88
Figure 4.39: Relationship between peak ratio and simulated substrate conversion of samples of quantification curve	89
Figure 4.40: Change in mean error of calculated substrate conversion across full quantification curve	89
Figure 4.41: Effectiveness of substrate conversion quantification curve at calculating conversion at higher component concentrations at the same component ratio	90
Figure 4.42: Change in mean substrate conversion efficiency (% of total substrate in solution phosphorylated) of UCK1 against uridine with change in UCK1 concentration.....	91
Figure 4.43: Mean substrate conversion efficiency (% of total substrate in solution phosphorylated) of UCK1 against uridine across different weight to weight ratios of PK to UCK1 in solution	93
Figure 4.44: Mean substrate conversion efficiency (% of total substrate in solution phosphorylated) of UCK1 against uridine across different UCK1 addition strategies	94
Figure 5.1: Molecular structures of unnatural nucleosides used in the present study.....	95
Figure 5.2: Mean substrate conversion efficiency (% of total substrate in solution phosphorylated) of UCK1 and UCK2 against uridine and cytidine.....	97
Figure 5.3: Comparison of CMP-targeting EIC spectra of UCK2-cytidine reactions and cytidine control sample	98

Figure 5.4: Mean areas of integrated nucleoside monophosphate LCMS peaks in reactions of UCK1 and UCK2 against uridine and cytidine as substrates	100
Figure 5.5: Comparison of substrate conversion efficiency (% of total phosphorylated substrate in solution) of UCK1 against 5-methyl-U, uridine, and cytidine.....	102
Figure 5.6: Areas of integrated nucleoside monophosphate LCMS peaks in reactions of UCK1 against unnatural substrates.....	105
Figure 5.7: Comparison of mean nucleoside monophosphate peak area of UCK1 against unnatural and natural substrates.....	105
Figure 6.1: Comparison of protein purification efficiencies of UCK1 purifications utilising different modes of lysis	108
Figure 6.2: Representative ³¹ P NMR spectra depicting UMP and phosphate peaks in potentially phosphate-contaminated experiments	112

List of Tables

Table 2.1: List of E. coli strains utilised in the present study	15
Table 2.2: List of plasmids utilised in the present study	15
Table 2.3: Description of method program for IMAC protein purification via AKTA pure 25	22
Table 2.4: Description of method program for IEC protein purification via AKTA pure 25	22
Table 4.1: Literature analysis of reaction conditions for nucleoside kinase catalytic activity	57
Table 4.2: Data from ^{31}P NMR spectra of samples from component concentration study	74
Table 4.3: Data from ^{31}P NMR spectra of samples from reaction duration study	75
Table 4.4: Data from ^{31}P NMR spectra of samples from substrate excess study	77
Table 4.5: Data from ^{31}P NMR spectra of samples from PK activity study	78
Table 4.6: Data from ^{31}P NMR spectra of samples from ADK activity study	80
Table 4.7: Data from ^{31}P NMR spectra of samples from GUK activity study	81
Table 4.8: Data from ^{31}P NMR spectra of samples from UCK1 activity study	83
Table 4.9: Data from ^{31}P NMR spectra of samples from UCK2 activity study	84
Table 5.1: Identification details of key compounds of enzymatic reaction mixture	98
Table 5.2: Results of EIC analysis of LCMS data aimed at detecting phosphorylated substrate in natural substrate reaction samples.....	99
Table 5.3: Identification details of unnatural substrates and monophosphate derivatives thereof in enzymatic reaction mixtures	103
Table 5.4: Results of EIC analysis of LCMS data aimed at detecting phosphorylated substrate in unnatural substrate reaction samples.....	104

List of Abbreviations

ADK	adenylate kinase
ADP	adenosine diphosphate
AgAK	<i>Anopheles gambiae</i> AK
AK	adenosine kinase
AMP	adenosine monophosphate
ANOVA	analysis of variance
ATP	adenosine triphosphate
CMP	cytidine monophosphate
CMPK	UMP-CMP kinase
ddhC	3'-deoxy-3',4'-didehydro-cytidine
ddhCTP	3'-deoxy-3',4'-didehydro-cytidine triphosphate
dH₂O	distilled deionised H ₂ O
DNA	deoxyribonucleic acid
DTT	dithiothreitol
EcADK	<i>Escherichia coli</i> ADK
EDTA	ethylenediaminetetraacetic acid
EIC	extracted ion chromatogram
FLAG-tag	FLAG TM -tag, DYKDDDDK-tag
GMP	guanosine monophosphate
GUK	guanylate kinase
HCV	hepatitis C virus
HEPES	4-(2-hydroxyethyl)-1-piperazineethanesulfonic acid
His-tag	polyhistidine-tag
HIV	human immunodeficiency virus
HSD	honestly significant difference
IEC	ion exchange chromatography
IMAC	immobilised metal affinity chromatography
IPTG	isopropyl β-D-1-thiogalactopyranoside
LB	lysogeny broth
LCMS	liquid chromatography mass spectrometry

MOPS	3-(<i>N</i> -morpholino)propanesulfonic acid
NDP	nucleoside diphosphate
NDPK	NDP kinase
NMP	nucleoside monophosphate
NMR	nuclear magnetic resonance
NTP	nucleoside triphosphate
PAGE	polyacrylamide gel electrophoresis
PBS	phosphate-buffered saline
PEP	phosphoenolpyruvate
<i>Pf</i>GUK	<i>Plasmodium falciparum</i> GUK
PK	pyruvate kinase
RdRp	RNA-dependant RNA polymerase
RNA	ribonucleic acid
rNK	ribonucleoside kinase
RT	reverse transcriptase
SOC	super optimal broth with catabolite suppression
TAE	Tris-acetate-EDTA
Tris	tris(hydroxymethyl)aminomethane
UCK	uridine-cytidine kinase
UCK1	human UCK1
UCK2	human UCK2
UDP	uridine diphosphate
UMP	uridine monophosphate
UV	ultraviolet

1.0 Background

1.1 Nucleosides and Nucleic Acids

1.1.1 Nucleosides

The nucleosides are a class of biomolecule characterised by their structure. This structure includes a nitrogenous base, either a purine or pyrimidine, covalently bound to the 1'-carbon of a pentose sugar in a β -furanose formation.¹ A chain of up to three phosphate groups may be esterified to the 5'-hydroxyl of the pentose sugar, in this case the compounds are referred to as nucleotides, or nucleoside monophosphates (NMPs), diphosphates (NDPs), or triphosphates (NTPs). NTPs, among other roles, serve as key structural constituents of the nucleic acids, deoxyribonucleic acid (DNA) and ribonucleic acid (RNA).¹ There are four endogenous nucleosides involved in the synthesis of each of DNA and RNA, the structures of which can be seen in *Figure 1.1*. The nucleosides that form the structures of DNA and RNA are differentiated by the constituents of the 2'-carbon of the pentose sugar moieties, as the nomenclature suggests DNA is composed of nucleotides lacking an oxygen at this position.²

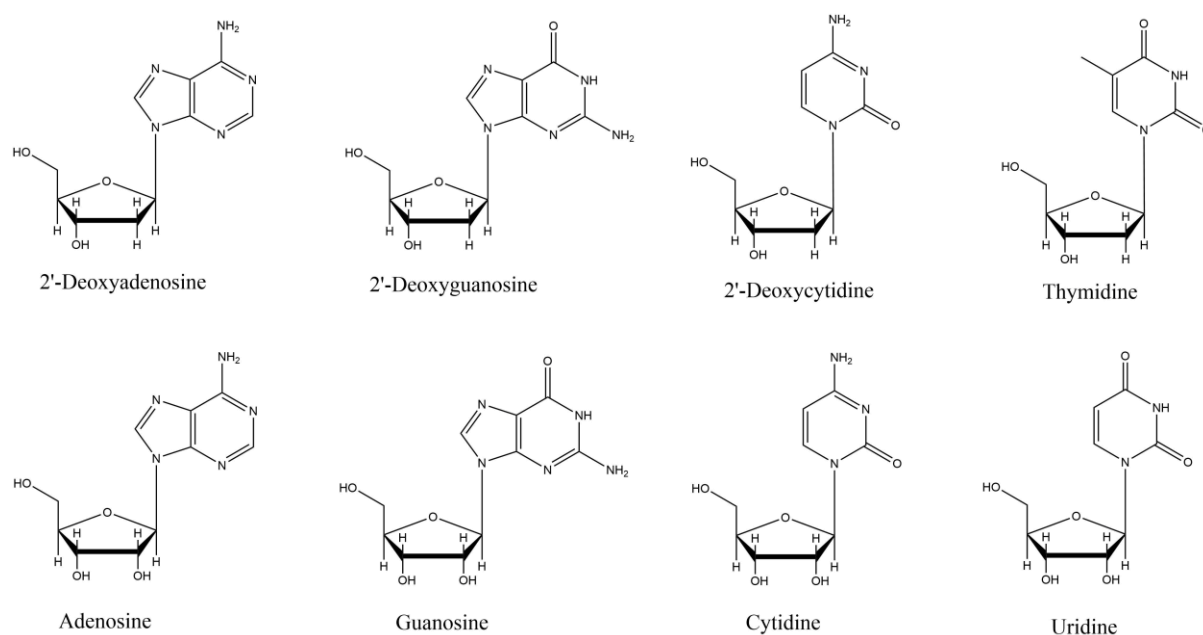


Figure 1.1: Chemical structures of the endogenous nucleosides that act as structural constituents of nucleic acids. DNA (top row), RNA (bottom row).

1.1.2 Nucleic Acids

The nucleic acids, DNA and RNA, are linear polymers composed of nucleoside monophosphate monomers joined by phosphodiester bonds between the 5'- and 3'-carbon atoms of adjacent monomers.

The specific localisation of these phosphodiester bonds on the nucleotide monomers results in a directional polymer, the termini of the polymer are referred to as the 3' and 5' ends.³ Synthesis of nucleic acids occurs in the 5' to 3' direction, NTP monomers are added to the elongating strand in enzyme-catalysed reactions in which the 3'-oxygen of the nascent strand nucleophilically attacks the 5'- α -phosphate of the unincorporated nucleotide to form a phosphodiester bond. Following this bond formation the 5'- β - and γ -phosphates of the newly bound nucleotide are released as pyrophosphate.^{3, 4} The mechanism of this catalysis is highly conserved across the DNA and RNA polymerases, divalent metal ions coordinated to aspartic acid residues of the polymerase position the incoming nucleotide and promote proton loss from the 3'-hydroxyl group, facilitating nucleophilic attack of the α -phosphate and phosphodiester bond formation.⁵

1.2 RNA Viruses

1.2.1 Replication of RNA Viruses

Viruses can be classified as either RNA or DNA viruses by the specific nucleic acid that composes the viral genome.⁶ These classifications can be further divided by the specific structures of said genomes, which defines the manner in which the viral genome will replicate. RNA viruses for example may be classified as double-stranded RNA, single-strand (+)-sense RNA, or single-strand (-)-sense RNA viruses. Of the single-strand (+)-sense RNA viruses exists the subclass of retroviruses which utilise a DNA intermediate for transcription of the genome.⁷ The genomic replication of RNA viruses can be generally considered to occur through either RNA-dependant RNA polymerase (RdRp) or reverse transcriptase (RT), depending on the class of virus.⁸ These enzymes represent promising drug targets for the inhibition of viral replication and treatment of infection by RNA viruses as they do not appear in the human genome.⁹

1.2.2 RNA-Dependant RNA Polymerase

RdRp is a virally encoded enzyme that catalyses the addition of ribonucleoside triphosphates to a nascent RNA chain via the formation of phosphodiester bonds, in an RNA-template dependant manner.¹⁰ The selectivity of RdRp for nucleotides with 2'-hydroxyl functionality, such as the ribonucleotides, is derived from a highly conserved aspartic acid residue at the active site, the side chain of which forms a hydrogen bond with the 2'-hydroxyl group.¹¹ As may be expected, many substrate-mimic RdRp inhibitors retain the 2'-hydroxyl functionality of the typical substrate.¹²⁻¹⁴ Although there is significant variation in the sequences encoding these proteins across viral families, the active sites

are highly conserved indicating the potential broad-spectrum utility of inhibitors binding to these pockets.^{15, 16}

1.2.3 Reverse Transcriptase

RT, also known as RNA-dependant DNA-polymerase, is represented within both viral and eukaryotic genomes where it functions to synthesise DNA polymers based on an RNA template.⁴ As a virally encoded enzyme the role of RT is similar to that of RdRp, it is a mediator of viral genomic replication. In eukaryotes RT is responsible for maintaining the length of telomeres, repeat nucleotide sequences that have protective function at the ends of linear chromosomes.¹⁷ RT is utilised by retroviruses to transcribe their genomic RNA into double-stranded DNA which is then incorporated into the genome of the host.⁴

RT-mediated transcription has a high error rate resulting in large genetic variation across retroviral genomes and RT genes.¹⁸ It has however been shown that despite this high mutation rate the catalytic site of RT is highly conserved, supporting its potential as a drug target for antiviral therapeutics.¹⁹ A specific feature of RT enzymes that exhibits high levels of conservation between isoforms is the presence of a tyrosine or phenylalanine residue in close proximity to the active site.²⁰ This highly conserved residue provides the selectivity of RT for deoxyribonucleoside triphosphates as substrate.²⁰ ²¹ This selectivity for nucleotides lacking 2'-hydroxyl functionality is also observed in the binding of unnatural substrates to the RT active site. The human immunodeficiency virus (HIV), which uses RT in its replication cycle, has been the target of intense research and as of 2010 all approved nucleoside analogue inhibitors of HIV RT lacked a hydroxyl group at the 2'-carbon.²²

1.3 Antiviral Nucleoside Analogues

1.3.1 Mechanism of Action

A key unifying feature of RdRp and RT, and indeed all enzymes catalysing nucleic acid synthesis, is the stepwise addition of NTPs to the nascent nucleic acid chain. Analogues of the endogenous nucleosides normally utilised in this process have shown inhibitory function against these enzymes and thus potential as anti-viral therapeutic agents.²³⁻²⁵ The majority of antiviral nucleoside analogues exhibit the same mode of action, they act as chain terminators interfering with nucleic acid synthesis and inhibiting viral replication through the induction of early termination of the nascent nucleic acid chain.²⁶ Chain terminators act as substrates for nucleic acid polymerases, competing with endogenous NTPs for inclusion into the polymer. After inclusion into the polymeric chain, structural differences between chain terminators and the typical substrates inhibit further elongation of said chain resulting in

incomplete replication.²⁷ Lack of the 3'-hydroxyl group required for RNA polymerisation is commonly observed in the molecular structures of chain terminators, such molecules are referred to as obligatory RNA chain terminators and incorporation of the triphosphate derivative of these into the elongating polymer results in the immediate termination of transcription. Nucleoside analogues retaining 3'-hydroxyl function may also act as chain terminators if incorporation of the triphosphate derivative of the molecule into the RNA polymer results in sufficient steric hinderance to the formation of subsequent phosphodiester bonds. In this case such compounds are referred to as non-obligatory chain terminators.²⁶

1.3.2 Anabolic Activation of Nucleoside Analogues

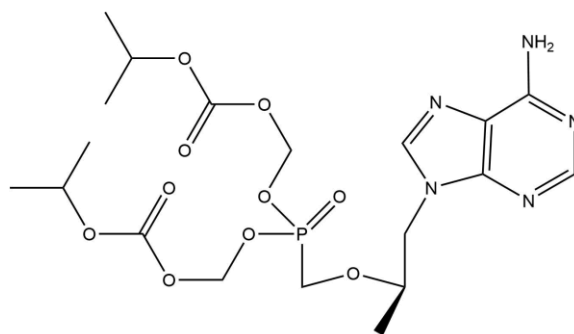
Just as the natural substrates of RdRp and RT must be in triphosphate form prior to the enzymatic catalysis of their addition to the nascent nucleic acid chain, antiviral nucleoside analogues that inhibit these enzymes must be activated through conversion to their triphosphate analogue forms prior to therapeutic activity.^{28, 29} This activation requires anabolism by cellular phosphorylative machinery, enzymes known as kinases, in a series of steps, any which may act as a rate-limiting step. The drug must function as a substrate for not only the target enzyme, but also the specific intracellular kinases necessary for its stepwise anabolism into the triphosphate form.²⁹ This reliance on intracellular machinery for activation of nucleoside analogues can also result in these drugs exhibiting unpredictable pharmacokinetics, as factors influencing the activity of these kinases will also impact activation.³⁰ Thus, the development of nucleoside analogues with a phosphorylated 5'-oxygen may serve to improve the effectiveness of this drug class through reduced reliance on intracellular enzyme activity. Nucleoside analogue 5'-phosphates may also be used in the assessment of nucleoside kinase affinity for these compounds, the results of which can provide insight into the ability of the drug to be anabolically activated in vivo.

1.3.3 Application of Prodrug Strategy to Nucleoside Analogues

A druglike compound that must be activated through biotransformation prior to the exertion of its therapeutic effect is referred to as a prodrug.³¹ The development of prodrug derivatives of a drug represents a strategy that may serve to improve pharmacodynamic and pharmacokinetic properties, which may in turn result in improved therapeutic utility of the compound.³² Given the previously described need for nucleoside analogue chain terminators to be anabolised into their triphosphate forms prior to incorporation into the nascent nucleic acid chain, these compounds, and indeed their monophosphate and diphosphate forms, could be considered to be prodrugs themselves.

As previously mentioned, the development of nucleoside analogues with phosphorylated 5'-oxygen atoms may improve the therapeutic utility of the parent compounds through decreased reliance on endogenous enzyme activity. The presence of phosphate groups will also act to adversely affect drug delivery to the target protein however, as the highly polar phosphate moieties will prevent passive diffusion across the membrane and limit cell entry.³³ The development of prodrugs of nucleoside analogue phosphates may provide a means to mitigate the adverse impact of the phosphate groups on cell entry while retaining the functionality of these moieties at the active site of the target protein. It is generally prodrugs deriving from the monophosphate forms of nucleoside analogues that are synthesised, as it is the initial conversion to the monophosphate form that is generally considered to be the rate-limiting step in the overall nucleoside to nucleoside triphosphate anabolic process.^{33, 34} This strategy has been proven effective with the uridine monophosphate (UMP) analogue prodrug sofosbuvir (*Figure 1.3*), used to treat hepatitis C virus (HCV) infection. This compound was shown to travel to the target tissue where it was able to enter cells and be converted to its corresponding active triphosphate form, which had inhibitory action against HCV RdRp.³⁵

There are a wide range of synthetic routes that have been used to successfully synthesise prodrugs of nucleoside and nucleotide analogues.³³ Certain approaches to prodrug synthesis, similar to the synthesis of bis-pivaloyloxymethyl prodrugs such as tenofovir disoproxil (*Figure 1.2*), may require the use of a nucleoside monophosphate as a reagent within the synthetic process.^{36, 37} Thus, despite the poor pharmacokinetics of phosphorylated nucleoside analogue drugs, the monophosphate forms have utility in the overall synthetic process of deriving therapeutic agents from antiviral nucleoside analogues.



Tenofovir disoproxil

Figure 1.2: Chemical structure of tenofovir disoproxil.

1.3.4 Endogenous Chain Terminators

Recently a novel viral RdRp inhibitor, 3'-deoxy-3'4'-didehydro-cytidine triphosphate (ddhCTP), has been discovered and shown to be endogenously produced in humans.^{13, 38} ddhCTP is produced from cytidine triphosphate through the catalytic activity of viperin, an interferon-inducible enzyme that

exhibits broad-spectrum antiviral activity.^{13, 39} ddhCTP has been shown to inhibit the replication of a range of flaviviruses while not affecting human cell viability, indicating a lack of inhibition of mammalian RNA polymerases.¹³

The broad-spectrum antiviral activity of ddhCTP against flaviruses, lack of deleterious interaction with mammalian nucleic acid polymerases, and high levels of conservation observed across RdRp active sites suggest that the compound itself or similar compounds may have utility as antiviral drugs.

1.4 Strategies for Nucleoside Analogue Drug Development

1.4.1 Nucleoside Analogue Drug Design

The structural modification of nucleosides to produce therapeutic analogues can occur at any of the three key moieties, the phosphate group(s), the sugar, or the nucleobase.

Nucleoside analogues with modified sugars have been extensively explored as antiviral agents with many reaching clinical use for this purpose.^{40,41} A wide range of sugar-moiety modifications have been successfully incorporated into therapeutic agents, such as stereochemical alterations, substitution or elimination of the 2' and 3' substituents, and substitution of the ribose oxygen (*Figure 1.3*).⁴²⁻⁴⁶ Base-modified nucleoside analogues have also found clinical success, halogenation of the nucleobase moiety is a base modification strategy that has seen clinical success with antiviral agents such as idoxuridine, trifluridine, and brivudine (*Figure 1.3*).⁴⁷⁻⁴⁹

One strategy for the development of novel drugs for the inhibition of a specific therapeutic target is the rational design of compounds with chemical structures similar to a compound known to inhibit this target. In the case of nucleoside analogue RdRp inhibitor development, the previously described ddhCTP may represent a useful 'starting compound' from which structurally related compounds can be derived for investigation.

The group of nucleoside analogues to be used as targets for synthetic enzyme-catalysed phosphorylation in the proposed research are cytidine and uridine analogues with modifications to the ribose sugar moiety and/or the nucleobase. Although not always the case, the initial conversion from nucleoside to nucleoside monophosphate is generally the rate-limiting step of the overall nucleoside to nucleoside triphosphate pathway.^{30, 34} Thus, this step represents the primary focus of the presently discussed research.

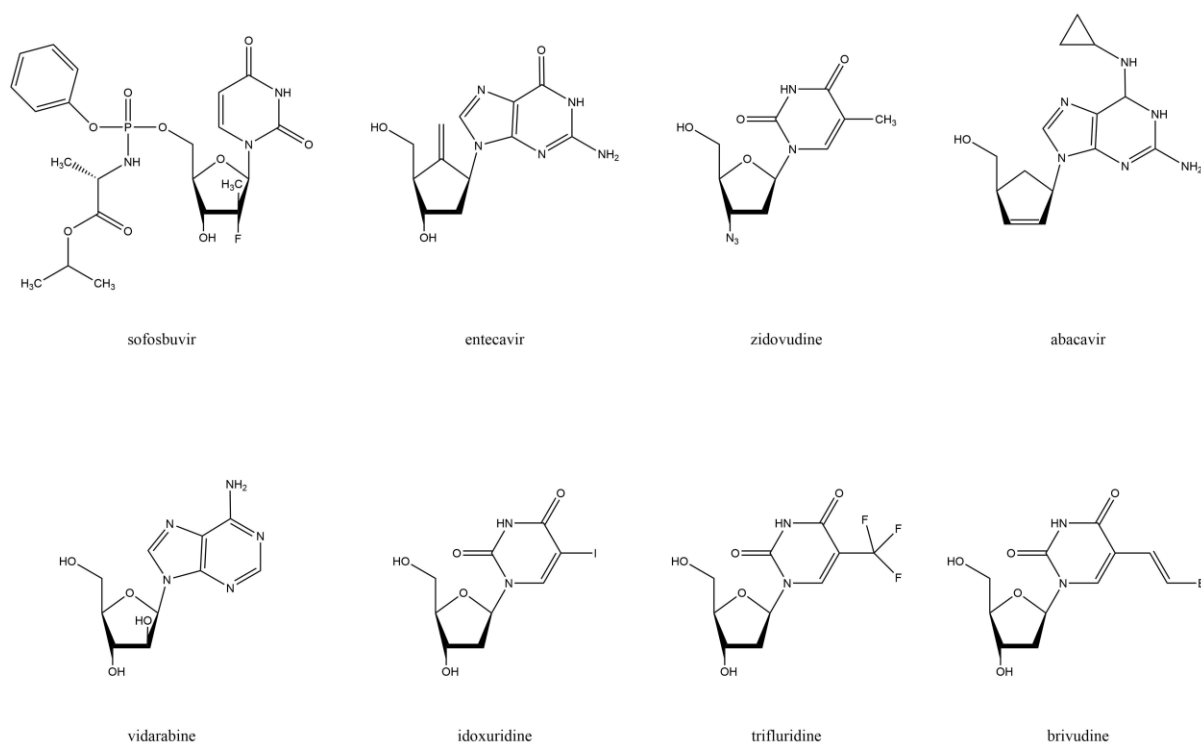


Figure 1.3: Chemical structures of a range of clinically approved nucleoside analogue drugs.

1.4.2 Synthetic Addition of Phosphate Groups

There are two general strategies towards the addition of phosphate groups to nucleoside analogues in the laboratory, this can be achieved either through a typical organic synthetic route or through utilisation of enzyme-mediated phosphorylation. Synthesis of nucleoside 5'-phosphates through organic synthetic methods has been achieved, however early synthetic strategies were often difficult and inefficient due to a range of factors including the necessary regioselectivity for the 5'-hydroxyl, side reactions of the nucleobases, and intrinsic reactivity of phosphoanhydride bonds as occurs between the α - β or β - γ phosphates of NTPs.⁵⁰⁻⁵³

A recently published study has provided synthetic routes to access the mono-, di-, and triphosphate forms of 3'-deoxy-3'.4'-didehydro-cytidine (ddhC) from the commercially available starting material, 4-*N*-benzoylcytidine (*Figure 1.4*).⁵⁴ The synthetic strategies utilised within this study may be applicable to other nucleoside analogues, thus could represent an improved means to synthetically produce 5'-phosphate derivatives of such compounds during the drug development process. Poor total yields resulting from a multi-step synthetic process such as described may impact the feasibility of this approach, however. Further limiting the practical utility of synthetic strategies such as described for ddhCTP is the time- and resource-consuming nature of this process.

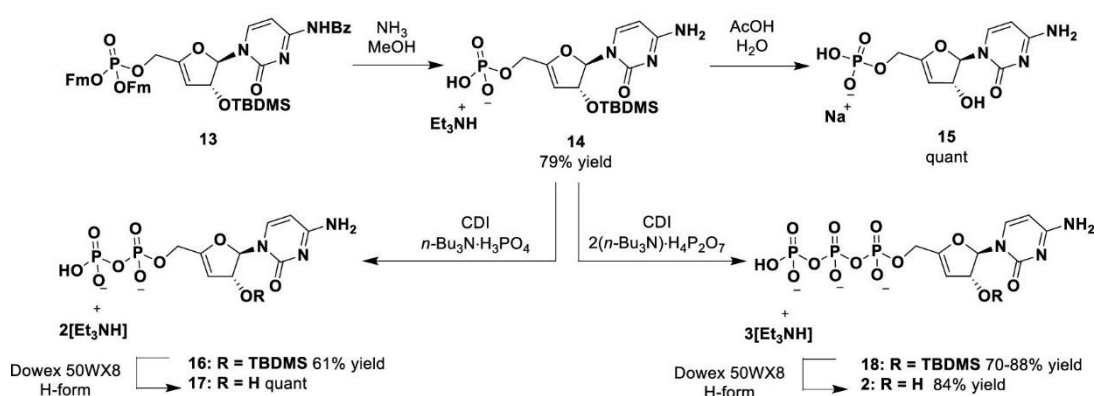


Figure 1.4: Organic synthesis of ddhCTP. Adapted with permission from Wood et al. (2021)⁵⁴

Synthesis of phosphorylated nucleoside analogue derivatives via enzymatic catalysis may thus represent a better strategy than total chemical synthesis. A 1974 study showed that enzymatic catalysis provided an effective means for the production of nucleoside 5'-monophosphates from the non-phosphorylated derivative compounds at a gram scale.⁵⁵ More recently, Li et al. were able to optimise cytidine kinase activity to result in close to 100% yield of cytidine 5'-monophosphate, illustrating the potential of nucleoside kinases to serve as synthetic tools capable of producing target compounds at high yield.⁵⁶

1.5 Enzymes Catalysing Ribonucleoside Phosphorylation

1.5.1 α -Phosphate Addition

Enzymes that catalyse the transfer of the γ -phosphate of an NTP to the 5'-oxygen atom of nucleosides to form NMPs are known as nucleoside kinases, this classification can be further divided into the deoxyribonucleoside kinases and ribonucleoside kinases (rNKs).⁵⁷

The first two steps in the nucleoside to NTP anabolic pathway are catalysed by enzymes specific to the nucleobase of the substrate, however catalysis of the diphosphate to triphosphate conversion by nucleoside diphosphate kinase (NDPK) has a much broader substrate scope (Figure 1.5)^{30, 58}.

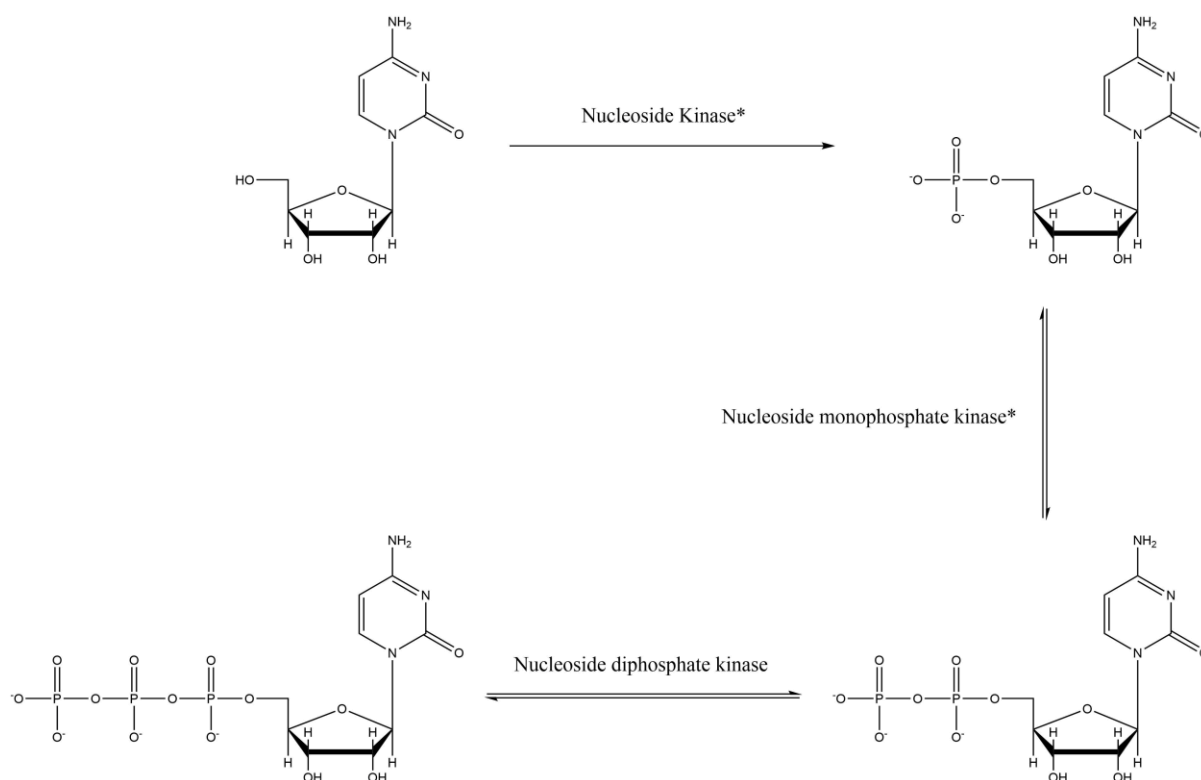


Figure 1.5: General scheme depicting the anabolic pathway of conversion of cytidine to cytidine triphosphate. All nucleosides follow this general scheme. * = substrate-specific enzymes

In human cells the rNKs responsible for phosphorylation of the pyrimidine ribonucleosides are the uridine-cytidine kinases (UCK), UCK1 and UCK2.⁵⁹ Both UCK1 and UCK2 have been shown to phosphorylate a variety of nucleobase-modified cytidine and uridine analogues with varying efficiency.⁶⁰ It must be noted however that tight binding of the ribose moiety to the enzyme is essential for substrate binding, thus changes in the hydrogen bonding interactions observed between ribose hydroxyl groups and active site residues may limit the activity of these enzymes towards sugar-modified analogues.⁵⁹

The phosphorylation of the purine ribonucleoside adenosine is catalysed by the enzyme adenosine kinase (AK).⁶¹ The adenosine kinase with the highest known affinity for adenosine as substrate is that of *Anopheles gambiae* (AgAK). AgAK has been successfully utilised in the enzyme-catalysed phosphorylation of the antiviral adenosine analogue galidesivir.⁶² This protein thus represents another potential tool for use in the production of nucleoside analogue monophosphates. The high specificity for adenosine exhibited by AgAK may limit its utility in the phosphorylation of pyrimidine nucleoside analogues.⁶³

The catalytic mechanisms of AK and UCK enzymes can be explained as a general scheme (Figure 1.6). After substrate binding, a catalytic site Asp residue acts as a base, deprotonating the 5'-hydroxyl group of the nucleoside. The O⁻ of the 5' carbon then nucleophilically attacks the 5'-γ-phosphate of the NTP

to form a pentavalent transition state, which is stabilised by an active site divalent metal ion and other active site residues. This divalent atom also acts to enhance the phosphate donor NDP as a leaving group, resulting in formation of substrate monophosphate.^{59, 64}

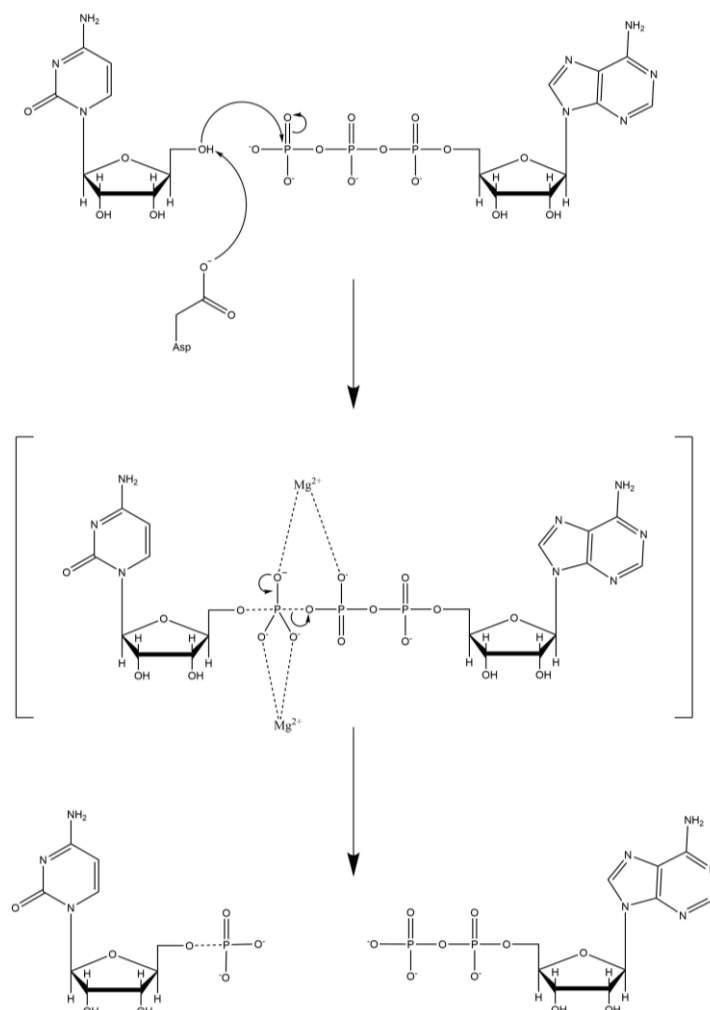


Figure 1.6: General scheme of the catalytic mechanism of nucleoside kinases. Cytidine is used as an example substrate. ATP is used as an example phosphate donor.

1.5.2 β -Phosphate Addition

The enzymes catalysing the conversion of nucleoside monophosphates to the corresponding diphosphates are known as the nucleoside monophosphate kinases.

The enzyme uridine-monophosphate cytidine-monophosphate kinase (CMPK) catalyses the phosphorylation of both UMP and cytidine monophosphate (CMP), and has also been shown to phosphorylate adenosine monophosphate (AMP) at a reduced efficiency.³⁴ CMPK has been shown to phosphorylate the sugar-modified cytidine analogue ara-C-monophosphate at similar efficiency to CMP.

The phosphorylation of AMP is also catalysed by the enzyme adenylate kinase (ADK), with greater efficiency than CMPK.³⁴ The human ADK isoforms AK5 and AK8 have been shown to efficiently phosphorylate a variety of sugar modified NMP analogues, thus indicating their potential for use in the enzyme catalysed synthesis of nucleoside analogue diphosphates.⁶⁵

Guanosine monophosphate is converted to its diphosphate form by guanylate kinase (GUK) enzymes.³⁴ The GUK isoform expressed by *Drosophila melanogaster* has been shown to have phosphorylative activity against guanosine monophosphate (GMP) analogues with modified sugar moieties.⁶⁶ The GUK isoform expressed by *Plasmodium falciparum* (PfGUK) has been shown as active against AMP, activity not observed from other GUK isoforms.⁶⁷

1.5.3 γ -Phosphate Addition

NDPKs catalyse the final phosphorylative step in the nucleoside to NTP anabolic pathway. As previously stated, these enzymes are non-specific with regard to the nucleobase of their NDP substrate, although variations in activity towards differing substrates do occur.⁶⁸ This lack of specificity extends to variations in both the nucleobase and sugar moieties of the nucleoside, thus these enzymes have potential phosphorylative capability towards nucleoside analogues.⁶⁹ The high conservation between active sites of different NDPKs and lack of substrate specificity indicates that any one of these enzymes may have use as a synthetic tool for the presently discussed purpose.^{68, 70, 71}

1.6 Enzymatic Catalysis as a Synthetic Tool

1.6.1 Production of Enzymes for Synthetic Use

A highly utilised strategy for the production of enzymes for use in drug development, and indeed other applications, is the transformation of *E. coli* cells with a recombinant plasmid encoding the target protein and subsequent purification of said protein from cell lysate.⁷² The BL21 strain of *E. coli* cells are designed for recombinant protein expression and widely used for this purpose.⁷³ These recombinant proteins are often genetically modified to include a polyhistidine or other form of affinity tag motif allowing isolation of the protein from cell lysate with specialised columns. In the case of polyhistidine tags (His-tag) an immobilized metal affinity chromatography (IMAC) is used with a Ni²⁺-based column. Although effective, the utility of His-tags for IMAC purification may be limited by the potential for co-elution of native *E. coli* proteins.⁷⁴ Another class of affinity tag that can be utilised to provide highly specific protein purification is a FLAG[™] tag (FLAG-tag).⁷⁵ The FLAG-tag, also known as the DYKDDDDK-tag, is a peptide tag that allows purification via immunoaffinity chromatography.

Although FLAG-tag use may result in higher purity of protein extract their use is limited by the high cost of the necessary equipment.⁷⁶

1.6.2 Use of ³¹P Nuclear Magnetic Resonance Spectroscopy to Assess Synthetic Utility

³¹P nuclear magnetic resonance (NMR) spectroscopy is an analytical chemistry technique that can be used to detect and characterise phosphorus-containing compounds within a sample.⁷⁷ ³¹P provides a good target for NMR spectroscopy, largely due to its natural 100% abundance and nuclei spin of ½.⁷⁸

³¹P NMR has been previously used to characterise phosphorylative reactions catalysed by nucleotide kinases such as AK and pyruvate kinase (PK), indicating its potential utility in characterising the phosphorylation of nucleoside analogues.^{79, 80} Although ³¹P NMR has utility in detecting the presence of nucleoside mono, di, and triphosphates the technique cannot distinguish between nucleotides with differing sugar or nucleobase moieties.⁸¹ This may be a limitation in assessing the enzyme-catalysed addition of β and γ-phosphates to nucleotides due to the concurrent presence of both donor and substrate di or triphosphates. In the case of α-phosphate addition this should not limit utility, as there is no need for nucleotide monophosphate in the reaction mixture aside from the product compound.⁸²

The presence of adenosine triphosphate (ATP) in the reaction mixture is necessary due to the need for a phosphate donor compound, however the ATP resonance peaks may overlap with those of the product or substrate compounds making assessment of activity difficult. This limitation can be mitigated through the inclusion of PK and phosphoenolpyruvate (PEP) in the reaction mixture.⁸³ PK acts to convert PEP and adenosine diphosphate (ADP) into ATP and pyruvic acid, thus serves to regenerate ATP within the reaction mixture and reduce the initial ATP concentration required.⁸⁴

The chemical shifts of resonance peaks observed in ³¹P NMR spectra can be affected by a range of factors, including pH, interaction with enzymes, and interaction with cations such as Mg²⁺.^{80, 85, 86} With regard to nucleosides, as solution pH increases and phosphate groups become deprotonated a downfield shift in the resonance peaks is observed.⁸⁵

1.6.3 Activity of Uridine-Cytidine Kinase Against Unnatural Nucleosides

Both UCK1 and UCK2 have been shown as having phosphorylative activity against a range of unnatural nucleotides.⁶⁰ Some nucleoside analogue drugs have been indicated to be preferentially phosphorylated by UCK2 over UCK1 in vivo, although this may be due to differing cellular localisations of the isoforms rather than increased activity of one over the other.⁸⁷⁻⁸⁹

Structural studies of UCK2 have provided insight into the mechanism of this phosphorylation, although this may not necessarily apply to UCK1 the similarities of the enzymes substrates and mechanisms implies a similarity of active site structure. The presence of a 2'-hydroxyl group on the substrate is essential for UCK activity, hydrogen bonding interactions between this moiety and the Arg-166 and Asp-84 residues of UCK2 are responsible for this selectivity.^{59, 60} Hydrogen bonds are also formed between the substrate 5'-hydroxyl group and the UCK2 Asp-62 residue.⁵⁹ The structure of the sugar moiety of the substrate may be important for activity beyond these interactions, as it has been suggested that binding of this moiety to the UCK2 active site induces a conformational change thus allowing the nucleobase moiety to bind.⁵⁹ The importance of the sugar moiety in this binding may indicate that modifications here will be less well tolerated than modifications to the nucleobase moiety.

1.7 Aims of the Present Study

The present study exists as part of a larger research project that seeks to achieve the development of novel inhibitors of viral replication through the investigation of the antiviral activities of ddhC and analogues thereof. As part of this larger project there is need for the production of 5'-phosphorylated derivatives of these compounds, as previously stated these phosphorylated derivatives have potential use in both synthetic processes and the assessment of biological activity.

The present study aims to assess the utility of a range of nucleoside kinase enzymes in the synthesis of 5'-phosphorylated nucleoside analogues, as progress towards the ultimate goal of developing a scalable 'one-pot' synthetic methodology for the enzyme-catalysed production of nucleoside mono-, di- and triphosphates.

Further to this, the present study aims to develop a method for the quantification of nucleoside kinase turnover using ³¹P NMR and utilise this method to elucidate how the chemical structure of the substrate affects enzyme activity.

2.0 Materials and methods

2.1 General Microbial Strains and Materials

2.1.1 Bacterial Strains

The *E. coli* strains used in the present study are described in *Table 2.1*.

Strain	Description	Source
BL21	Chemically competent	Produced in-house
Stellar™	Chemically competent	Takara Bio
Mach1 (UCK1)	Contains plasmid encoding His-tagged human UCK1	Purchased from Addgene (Addgene plasmid # 42374 ; http://n2t.net/addgene:42374 ; RRID:Addgene_42374)
Stbl3 (UCK2)	Contains plasmid encoding Flag-tagged human UCK2	Purchased from Addgene (Addgene plasmid # 20661 ; http://n2t.net/addgene:20661 ; RRID:Addgene_20661) ⁹⁰
DH5alpha (<i>EcADK</i>)	Contains plasmid encoding His-tagged <i>E. coli</i> ADK	Purchased from Addgene (Addgene plasmid # 73625 ; http://n2t.net/addgene:73625 ; RRID:Addgene_73625) ⁹¹
DH5alpha (<i>PfGUK</i>)	Contains plasmid encoding His-tagged <i>P. falciparum</i> GUK	Purchased from Addgene (Addgene plasmid # 25571 ; http://n2t.net/addgene:25571 ; RRID:Addgene_25571)
Stbl3 (CMPK)	Contains plasmid encoding Flag-tagged human CMPK	Purchased from Addgene (Addgene plasmid # 20537 ; http://n2t.net/addgene:20537 ; RRID:Addgene_20537) ⁹⁰
BL21 (<i>AgAK</i>)	Contains plasmid encoding His-tagged <i>A. gambiae</i> AK	Produced as part of the present study. Described in <i>Section 3.2.1</i>
BL21 (UCK1)	Contains plasmid encoding His-tagged human UCK1	Produced as part of the present study. Described in <i>Section 3.3.1</i>
BL21 (UCK2 – FLAG-tag)	Contains plasmid encoding FLAG-tagged human UCK2	Produced as part of the present study. Described in <i>Section 3.4.1.1</i>
BL21 (UCK2 – His-tag)	Contains plasmid encoding His-tagged human UCK2	Produced as part of the present study. Described in <i>Section 3.4.2.1</i>
BL21 (<i>EcADK</i>)	Contains plasmid encoding His-tagged <i>E. coli</i> ADK	Produced as part of the present study. Described in <i>Section 3.5.1</i>

BL21 (PfGUK)	Contains plasmid encoding His-tagged <i>P. falciparum</i> GUK	Produced as part of the present study. Described in <i>Section 3.6.1</i>
BL21 (CMPK – FLAG-tag)	Contains plasmid encoding FLAG-tagged human CMPK	Produced as part of the present study. Described in <i>Section 3.7.1.1</i>
BL21 (CMPK – His-tag)	Contains plasmid encoding His-tagged human CMPK	Produced as part of the present study. Described in <i>Section 3.7.2.1</i>

Table 2.1: List of *E. coli* strains utilised in the present study. Includes both externally and internally sourced bacterial strains.

2.1.2 Plasmids

The plasmid vectors used in the present study are described in *Table 2.2*.

Plasmid	Vector Backbone	Relevant Characteristics	Source
AgAK	pDEST14	Encodes His-tagged <i>A. gambiae</i> AK	Gift from Vern Schramm, obtained directly from Schramm lab ⁶³
UCK1A	pNIC28-Bsa4	Encodes His-tagged human UCK1	Purchased from Addgene (Addgene plasmid # 42374 ; http://n2t.net/addgene:42374 ; RRID:Addgene_42374)
pWZL Neo Myr Flag UCK2	pWZL-Neo-Myr-Flag-DEST	Encodes FLAG-tagged human UCK2	Purchased from Addgene (Addgene plasmid # 20661 ; http://n2t.net/addgene:20661 ; RRID:Addgene_20661) ⁹⁰
UCK2_Twist	pET-28a(+)	Encodes His-tagged human UCK2	Designed in-house and purchased from Twist Bioscience
pWZL Neo Myr Flag CMPK	pWZL-Neo-Myr-Flag-DEST	Encodes FLAG-tagged human CMPK	Purchased from Addgene (Addgene plasmid # 20537 ; http://n2t.net/addgene:20537 ; RRID:Addgene_20537) ⁹⁰
CMPK_Twist	pET-28a(+)	Encodes His-tagged human CMPK	Designed in-house and purchased from Twist Bioscience
Pf-GUK1	pET28a-LIC	Encodes His-tagged <i>P. falciparum</i> GUK	Purchased from Addgene (Addgene plasmid # 25571 ; http://n2t.net/addgene:25571 ; RRID:Addgene_25571)
pET22-HT/plsA	pET22b	Encodes His-tagged <i>E. coli</i> ADK	Purchased from Addgene (Addgene plasmid # 73625 ; http://n2t.net/addgene:73625 ; RRID:Addgene_73625) ⁹¹

Table 2.2: List of plasmids utilised in the present study.

2.1.3 Media

All media was sterilised through autoclaving at 121 °C for 15 minutes. Sterilised media was cooled to room temperature prior to addition of supplements and/or experimental use. Media components were dissolved in distilled deionised water (dH₂O) unless otherwise stated.

Prior to the pouring of agar plates, solid media was heated via repeat iterations of microwaving for 30 seconds until a consistency desirable for pouring was achieved.

Lysogeny broth (LB) medium: Peptone-140 10 g/L, yeast extract 5 g/L, NaCl 10 g/L

Note: LB media purchased as premixed powder, Luria Broth Base (Miller's LB Broth Base), sourced from Invitrogen.

Super Optimal broth with Catabolite repression (SOC) medium: Dextrose 3.603 g/L, KCl 0.186 g/L, MgSO₄ 4.8 g/L, tryptone 20 g/L, yeast extract 5 g/L

Note: SOC media purchased premade from Sigma-Aldrich

Solid lysogeny broth (LB) medium: Ppeptone-140 10 g/L, yeast extract 5 g/L, NaCl 10 g/L, Select Agar™ 20 g/L.

Note: LB media purchased as premixed powder, Luria Broth Base (Miller's LB Broth Base), sourced from Invitrogen.

Note: Select Agar™ sourced from Invitrogen.

2.1.4 Media Supplements

Supplements were dissolved in dH₂O unless otherwise stated. Antibiotic stock solutions were made to 1000× the required concentration in media. All supplements sterilised through filtration with 0.22 µm filter.

1000× ampicillin: 100 mg/mL

1000× kanamycin: 50 mg/mL

2.1.5 Enzymes

Pierce™ Universal Nuclease for Cell Lysis was sourced from ThermoFisher Scientific. Recombinant kinases were produced in-house, through transformation of *E. coli* BL21 cells.

2.1.6 Buffer Solutions

All buffer solutions were generated through dissolution of ingredients into dH₂O. Solution pH was adjusted using HCl or NaOH solutions of varying concentration. Ingredients were added to dH₂O

equivalent to 40% of final solution volume, solutions were diluted to desired concentration and volume following adjustment to desired pH.

TAE buffer: Tris 40 mM, acetic acid 20 mM, EDTA 1 mM – pH 7.5

AgAK IEC equilibration buffer: HEPES 50 mM, NaCl 100 mM – pH 8

AgAK IEC elution buffer: HEPES 50 mM, NaCl 500 mM – pH 8

AgAK IMAC equilibration buffer: HEPES 50 mM, 300 mM NaCl, imidazole 20 mM – pH 8

AgAK IMAC elution buffer: HEPES 50 mM, 300 mM NaCl, imidazole 500 mM – pH 8

AgAK lysis buffer: HEPES 50 mM, NaCl 300 mM, DTT 1 mM – pH 7.5

CMPK IEC equilibration buffer: Tris 20 mM, NaCl 50 mM – pH 8.5

CMPK IEC elution buffer: Tris 20 mM, NaCl 500 mM – pH 8.5

CMPK IMAC equilibration buffer: Tris 20 mM, imidazole 25 mM – pH 7.5

CMPK IMAC elution buffer: Tris 20 mM, imidazole 500 mM – pH 7.5

CMPK lysis buffer: HEPES 50 mM, NaCl 500 mM – pH 7.5

EcADK IMAC equilibration buffer: Tris 50 mM, NaCl 250 mM, imidazole 20 mM – pH 7.5

EcADK IMAC elution buffer: Tris 50 mM, NaCl 250 mM, imidazole 250 mM – pH 7.5

EcADK lysis buffer: Tris 50 mM, NaCl 250 mM – pH 7.5

PfGUK IEC equilibration buffer: Tris 25 mM, NaCl 100 mM – pH 7.5

PfGUK IEC elution buffer: Tris 25 mM, NaCl 500 mM – pH 7.5

PfGUK IMAC equilibration buffer: Tris 25 mM, NaCl 150 mM, imidazole 20 mM – pH 7.2

PfGUK IMAC elution buffer: Tris 25 mM, NaCl 150 mM, imidazole 250 mM – pH 7.2

PfGUK lysis buffer: Tris 25 mM, NaCl 150 mM – pH 7.5

UCK1 IMAC equilibration buffer: Tris 20 mM, imidazole 25 mM – pH 7.5

UCK1 IMAC elution buffer: Tris 20 mM, imidazole 500 mM – pH 7.5

UCK1 lysis buffer: HEPES 50 mM, NaCl 500 mM – pH 7.5

UCK2 IEC equilibration buffer: Sodium phosphate 20 mM, NaCl 100 mM – pH 7.4

UCK2 IEC elution buffer: Sodium phosphate 20 mM, NaCl 500 mM – pH 7.4

UCK2 IMAC equilibration buffer: Tris 20 mM, imidazole 25 mM – pH 7.5

UCK2 IMAC elution buffer: Tris 20 mM, imidazole 500 mM – pH 7.5

UCK2 lysis buffer: HEPES 50 mM, NaCl 500 mM – pH 7.5

rNK reaction buffer: Tris 50mM, MgCl₂ 5mM, KCl 100 mM – pH 7.5

2.2 Microbial Growth and Maintenance

2.2.1 General Maintenance

LB media was used for all growth and maintenance of bacterial strains. Typical growth temperature was 37 °C. Liquid cultures were provided aeration through shaking at 200 rpm. Long-term maintenance was achieved through the mixing of overnight culture with 50% glycerol in a 1:1 ratio and storage of 1mL aliquots of the resulting mixture at -80 °C.

To ensure maintenance of plasmids bearing antibiotic resistance markers within bacterial populations of specific strains, the appropriate antibiotic(s) were added to liquid and solid media used for growth and maintenance of the relevant strains.

2.2.2 1 L Bacterial Culture Growth

1 L bacterial cultures were prepared using a pre-culture methodology. 50 mL of liquid LB broth was inoculated with the relevant bacteria and grown in a shaking incubator (37 °C, 200 rpm) for approximately 16 hours. 15 mL of this culture was then added to 1 L of liquid LB broth (containing the appropriate antibiotic) which was placed in a shaking incubator (37 °C, 200 rpm) until an OD₆₀₀ of 0.6 was reached.

2.2.3 Induction of Protein Expression

Bacterial cultures of OD₆₀₀ = 0.6 were placed in a shaking incubator at 18 °C for one hour. Following this IPTG was added to a final concentration of 0.5 mM, and induction of protein expression was allowed to continue for 16 hours prior to lysis.

2.3 General Molecular Biology

2.3.1 Isolation of Plasmid DNA

2.3.1.1 Plasmid Isolation from *E. coli*

Plasmid DNA was isolated from overnight *E. coli* cultures in LB media using the New England Biolabs Monarch® Plasmid Miniprep Kit, following the manufacturers protocol.⁹²

2.3.1.2 Plasmid Isolation from Filter Paper (PBS-Based Soaking Extraction)

A portion of filter paper bearing the relevant plasmid DNA was soaked in PBS buffer for 30 minutes. Filter paper was then removed from the buffer solution and discarded prior to further use of the extract.

2.3.1.3 Plasmid Isolation from Filter Paper (TAE-Based Soaking Extraction)

A portion of filter paper bearing the relevant plasmid DNA was soaked in TAE buffer for 10 minutes. Filter paper was then removed from the buffer solution and discarded prior to further use of the extract.

2.3.1.4 Plasmid Isolation from Filter Paper (TAE-Based Shredded Paper Extraction)

A portion of filter paper bearing the relevant plasmid DNA was shredded prior to soaking in TAE buffer for 10 minutes. Shredded filter paper was not removed from buffer solution prior to further use of the extract.

2.3.2 DNA Analysis

2.3.2.1 Agarose Gel Electrophoresis

All agarose gels used for DNA analysis were made in TAE buffer with 1% agarose (w/v) and 0.01% SYBR™ Safe DNA Gel Stain. Into each well was loaded 15 µL of sample and 10 µL of New England Biolabs® Gel Loading Dye, Purple (6X). Gels were run submerged in TAE buffer, with a running voltage of 100 V. Running times varied depending on the speed of DNA transit down the gel, with electrophoresis halted when DNA was observed to be approximately 80% towards the anode. Most run times were approximately 60 minutes.

10 µL of New England Biolabs® 1 kb DNA Ladder was loaded in each gel to provide a comparative ladder with which to compare DNA fragment size.

2.3.2.2 Nanodrop Measurement of DNA Concentration

The concentration of extracted DNA was assessed using an IMPLEN NanoPhotometer® NP80.

2.3.2.3 DNA Sequencing

Sequencing of DNA extracts was outsourced to Macrogen Inc., extracts were prepared and shipped as per the organisation specifications.

2.3.3 Transformation of Competent Cells

2.3.3.1 Transformation of BL21 Cells

The transformation of in-house produced chemically competent BL21 cells was achieved according to a modified version of a protocol derived from Merck.⁹³ Protocol modifications are described herein.

DNA extract, in varying volume, was added to 40 µL of cells in a chilled 15 mL polypropylene centrifuge tube. After brief stirring the mixture was incubated on ice for 30 minutes. Cells were then heat-shocked using a heating block at 42 °C for 60 seconds, before being cooled on ice for 2 minutes. SOC media was then added to bring the total volume of the tube to 2 mL, before the tubes were incubated at 37 °C and 200 rpm for 90 minutes. A sample of each culture, in varying volume, was then plated onto an agar plate bearing solid LB media using the quadrant streaking method. Plates were incubated at 37 °C overnight, following which single colonies were isolated from each plate and used to inoculate liquid cultures to be processed for long term maintenance.

2.3.3.2 Transformation of Stellar™ Cells

The transformation of chemically competent Stellar™ cells was achieved according to the manufacturer's protocol.⁹⁴

2.3.4 Lysis of Bacterial Cultures

2.3.4.1 Chemical Lysis

Chemical lysis of bacterial cultures was achieved using BugBuster® 10X Protein Extraction Reagent, according to a modified version of the manufacturers protocol.⁹⁵ Protocol modifications are described herein. Cell harvest from *E. coli* culture was achieved through centrifugation at 6000 x g for 20 minutes. BugBuster® 10X was diluted with the relevant lysis buffer in a 1:9 ratio. cComplete™ EDTA-free

Protease Inhibitor Cocktail, sourced from Roche, was used to provide protease inhibition. Pierce™ Universal Nuclease was used in place of Benzonase. Removal of insoluble cell debris from lysate was achieved through centrifugation at 30,000 x g for 30 minutes. Supernatants were clarified through filtration with 0.22 µm filters.

2.3.4.2 Sonication Lysis

Sonication lysis of bacterial cultures was achieved using an Omni-Ruptor 4000 system. Cell harvest from *E. coli* culture was achieved through centrifugation at 6000 x g for 20 minutes. Following discard of the supernatant, the cell pellet was resuspended in the relevant lysis buffer at a ratio of 5 mL per g wet cell paste. The resulting mixture was then placed on ice and subject to sonication (70% power, 50% pulse) for 15 minutes. Following this insoluble cell debris was removed through centrifugation at 30,000 x g for 30 minutes and the resulting supernatant was clarified through filtration with 0.22 µm filters.

2.4 Protein Purification

2.4.1 Spin Column Purification

His-tagged recombinant proteins were purified from clarified *E. coli* lysate using His SpinTrap™ microcentrifuge columns according to the manufacturers protocol.⁹⁶ The specific equilibration and elution buffers used varied dependant on the target protein.

2.4.2 Immobilised Metal Affinity Chromatography (IMAC) Purification

Purification of larger volumes of His-tagged recombinant proteins was achieved using an AKTA pure 25 version 1.8.0.6 chromatography system, equipped with a HisTrap™ HP (5 mL) column and either a 50 mL or 200 mL Superloop™ dependant on the volume of sample to be loaded. Fraction collection was achieved in a 96-well plate in 1.6 mL fractions. The specific equilibration and elution buffers used varied dependant on the target protein (*Section 2.1.6*). Equilibration buffer was assigned to pump A and elution buffer was assigned to pump B. Prior to each use the system was first washed into dH₂O then the relevant buffer. Following each use the system was washed into dH₂O then 20% ethanol.

Following IMAC purification relevant fractions were identified and consolidated before washing and concentration as described in *Section 2.4.5*.

Componentry of the AKTA pure 25 system was as follows; sample pump S9, inlet A V9-IAB part A, inlet B V9-IAB part B, sample inlet V9-IS, column valve V9-Cs, outlet valve V9-Os, UV monitor U9-

M, conductivity monitor C9, external air sensor L9, fraction collector F9-C, system pump A P9 A, system pump B P9 B, system pressure monitor R9, mixer M9, injection valve V9-Inj.

The purification method is described in *Table 2.3*.

Method Section	Volume	% B	Flow rate	Elution Outlet
Column Wash	5 CV	0	5 mL/min	Waste
Equilibration	5 CV	0	5 mL/min	Waste
Sample Application	Variable	0	2 mL/min	Fraction Collector
Column Wash	5 CV	0	5 mL/min	Waste
Elution	8 CV	0-100	5 mL/min	Fraction Collector

Table 2.3: Description of method program for IMAC protein purification via AKTA pure 25.

2.4.3 Anion Ion Exchange Chromatography (IEC) Purification

Purification of recombinant target proteins through IEC was achieved using an AKTA pure 25 version 1.8.0.6 chromatography system, equipped with a HiTrap™ Q FF (5 mL) column and a 50 mL Superloop™. Fraction collection was achieved in a 96-well plate in 1.6 mL fractions. The specific equilibration and elution buffers used varied dependant on the target protein. Equilibration buffer was assigned to pump A and elution buffer was assigned to pump B. Prior to each use the system was first washed into dH₂O then the relevant buffer. Following each use the system was washed into dH₂O then 20% ethanol.

Following IEC purification relevant fractions were identified and consolidated before washing and concentration as described in *Section 2.4.5*.

Componentry of the AKTA pure 25 system was as described in *Section 2.4.2*.

The purification method is described in *Table 2.4*.

Method Section	Volume	% B	Flow rate	Elution Outlet
Column Wash	5 CV	0	5 mL/min	Waste
Equilibration	5 CV	0	5 mL/min	Waste
Sample Application	Variable	0	2 mL/min	Fraction Collector
Column Wash	5 CV	0	5 mL/min	Waste
Elution	8 CV	0-100	5 mL/min	Fraction Collector
Column Wash	5 CV	0	5 mL/min	Waste

Table 2.4: Description of method program for IEC protein purification via AKTA pure 25.

2.4.4 Protein Dialysis

Elution fractions containing target protein were dialysed against 20 mM Tris buffer (pH 7.5) overnight using a Slide-A-Lyzer® 30 mL dialysis cassette as per manufacturer's instructions.⁹⁷

2.4.5 Protein Concentration

Elution fractions containing target protein were placed in a Vivaspin® Turbo 10K MWCO centrifugal concentrator and centrifuged at 4500 x g until concentrated to approximately 1 mL volume. The concentrator was then filled to 15 mL with 20 mM Tris (pH 7.5) and centrifuged at 4500 x g until concentrated to approximately 1 mL volume. This process was repeated until three washes with 20 mM Tris (pH 7.5) had been completed. Protein solution was then concentrated to a final concentration capable of being diluted to the 10 mg/mL final concentration described in *Section 2.4.6*.

2.4.6 Protein Storage

Solution containing target protein was diluted with 20 mM Tris buffer (pH 7.5) to a final concentration of 10 mg/mL protein, 10 mM DTT, 10% glycerol. This solution was then split into 50 µL aliquots, which were flash frozen using liquid nitrogen prior to storage at -80 °C.

2.4.7 Production of Pyruvate Kinase

PK used in the experiments of the present study was produced through expression and purification from in-house generated genetically modified BL21 *E. coli* cells transformed with a plasmid encoding the enzyme. 50 mL of liquid LB media was inoculated with frozen BL21 glycerol stocks and placed in a shaking incubator (37 °C, 200 rpm) overnight. To three 2500 mL Erlenmeyer flasks were each added 1 L of liquid LB media, to each of these 15 mL of overnight BL21 culture was added. These 1L bacterial cultures were grown in a shaking incubator (37 °C, 200 rpm) to an OD₆₀₀ of 0.6, following which they were placed in a cooled shaking incubator (18 °C, 200 rpm) for one hour prior to the induction of protein expression via IPTG addition to a final concentration of 0.5 mM. Flasks remained in the cooled shaking incubator (18 °C, 200 rpm) for approximately 16 hours following this, after which they were lysed via sonication as per *Section 2.3.5.1*. Following lysis PK was extracted from lysate through IMAC purification as described in *Section 2.4.2*. UV spectroscopic analysis was used to identify protein elution and relevant elution fractions were concentrated and prepared for long-term storage as described in *Section 2.4.5* and *Section 2.4.6* respectively.

2.5 Protein Analysis

2.5.1 Polyacrylamide Gel Electrophoresis

All polyacrylamide gel electrophoresis (PAGE) was conducted using Invitrogen Bolt™ 4 to 12%, Bis-Tris, 1.0 mm Mini Protein Gels. Samples were prepared using 4X Bolt™ LDS Sample Buffer and 50 mM DTT, prior to gel loading samples were denatured through heating to 70 °C for 10 minutes. 25 µL of sample was loaded per well. 10 µL of Novex™ Sharp Pre-stained Protein Standard was loaded in each gel to provide a comparative ladder for assessing protein fragment size. PAGE was conducted in NuPAGE™ MOPS SDS Running Buffer (20X) and dH₂O in a ratio of 1:19. PAGE was run at a constant voltage of 200 V, until dye was observed to be nearing the bottom of the gel. Most run times were approximately 35 minutes.

Following electrophoresis gels were placed in a staining tray with dH₂O and gently agitated for 4 minutes, after which dH₂O was drained from the tray. This process was repeated 3 times for each gel. Following this staining agent was added to the tray. Both Coomassie Brilliant Blue stain and SimplyBlue™ SafeStain were used as staining agents' dependant on availability.

In the case of Coomassie Brilliant Blue stain, following overnight staining with gentle agitation any remaining stain was drained from the tray prior to the addition of methanol. After soaking for enough time for protein bands to be clearly visible in the gel, the gel was photographed and discarded.

In the case of SimplyBlue™ SafeStain, following overnight staining with gentle agitation any remaining stain was drained from the tray prior to the addition of dH₂O. After soaking for enough time for protein bands to be clearly visible in the gel, the gel was photographed and discarded.

2.5.2 Measurement of Protein Concentration

The protein concentration of purified protein samples was assessed using an IMPLEN NanoPhotometer® NP80. Where relevant, the molecular weight and extinction coefficient of the target protein were input to the NanoPhotometer® to allow calculation of UV absorbance parameters.

2.6 Enzyme Bioactivity Assays

2.6.1 General Reaction Process

All enzymatic reactions were conducted in 1.7 mL Eppendorf tubes at 1 mL volume, in rNK reaction buffer (*Section 2.1.6*) with the addition of 5% D₂O. Ingredient compounds and buffer were added as 100 µL of 10× solution. ATP was used as phosphate donor for all relevant reactions. Enzyme aliquots

were defrosted on ice prior to addition to reaction mixtures. Following enzyme addition tubes were heated via heating block to 37 °C for the duration of reaction, after which heating was increased to 70 °C for 15 minutes to halt activity. Reaction tubes were then allowed to cool, prior to 0.22 µM filtration and the transfer of approximately 600 µL of filtered solution to a 5 mm Deuterotube™ for analysis.

2.7 Analysis of Catalytic Activity

2.7.1 Small Molecule Analysis

2.7.1.1 Liquid Chromatography-Mass Spectrometry

Liquid chromatography-mass spectrometry (LCMS) was performed on an Agilent 1260 Infinity II machine equipped with and Agilent Poroshell 120 HILIC-Z 21.x1500mm 2.7 micron column. Mobile phase A: 200mM ammonium acetate : MeCN 95:5, B: MeCN 0.1% F.A.. Method: 0.200 mL/min 10% A: 90% B 0 to 0.5 min isocratic, 70% A: 30% B over 30 min gradient, 70% A: 30% B 3 min isocratic. 5 min post run at 10% A: 90% B. Detection by UV DAD at 210 nm, 230 nm, 260 nm, 280 nm. Mass spectroscopy carried out with an Agilent Infinity Lab LC/MSD API-ES positive detection mode.

2.7.1.2 Nuclear Magnetic Resonance Spectroscopy

NMR spectroscopic analysis was carried out using either a JEOL 2-Channel 500MHz Nuclear Magnetic Resonance Spectrometer (type JNM-ECZ500S) equipped with an inverse detection proton sensitive auto tuneable HC probe, or a JEOL 3-Channel 500MHz Nuclear Magnetic Resonance Spectrometer type (JNM-ECZ500S) equipped with a 500MHz Royal Probe.

³¹P NMR spectra were gathered using the ‘single_pulse_dec’ pulse sequence, at 202.47 MHz spectrometer frequency. All spectra were gathered at 48 scans unless stated otherwise.

MestReNova version 14.1.2-25024 software was used for NMR data analysis.

2.7.2 Enzyme Turnover Quantification

To quantify conversion of uridine to UMP by rNK enzymes using the relevant peak intensities observed in ³¹P NMR spectra, a quantification curve was generated. A series of samples representing 5% increments of uridine to UMP conversion were generated in triplicate, based on 0% conversion component concentrations of 12.5 mM uridine, 13.75 mM PEP, 2.5 mM ATP. All samples were generated in rNK reaction buffer and 5% D₂O. Total sample volume was 1 mL.

To mimic the conditions of the *in vitro* enzymatic reaction uridine was assumed to be converted to UMP in a 1:1 molar ratio, with a corresponding 1:1 decrease in PEP concentration to account for ATP regeneration by PK. This equated to a 0.625 mM increase in UMP concentration and a 0.625 mM decrease in uridine and PEP concentration per 5% increment. ATP concentration was kept steady for each sample.

Each sample was analysed via ^{31}P NMR spectroscopy as described in *Section 2.7.1.2*.

3.0 Results: Protein Production

3.1 Selection of Kinases

Initial selection of rNK enzymes for use in the present study was determined by both predicted utility and availability. Plasmid encoding AgAK was received as a gift from Vern Schramm. Online plasmid catalogues were searched for each of the enzymes identified in *Section 1.5* and plasmids encoding human UCK1, human UCK2, PfGUK, *E. coli* ADK (*EcADK*), and human CMPK were identified and sourced as per *Section 2.1.2*. Of these plasmids, all encode enzymes bearing a terminal His-tag with the exception of the plasmids encoding human UCK2 and CMPK. These plasmids instead encode enzymes with terminal FLAG-tags.

Due to the likelihood of difficulty in purifying enzymes lacking a His-tag given the equipment available, it was decided to also source plasmids encoding those enzymes bearing a terminal His-tag. DNA constructs were designed through incorporation of the relevant genes into pET-28(+) vectors and sourced as per *Section 2.1.2*.

3.2 Adenosine Kinase (*Anopheles gambiae*)

3.2.1 Transformation of BL21

Plasmid encoding AgAK, as described in *Section 2.1.2*, was stored on filter paper at -20 °C. To maximise the chances of a successful transformation three different methodologies were employed to extract plasmid DNA from this filter paper, as described in *Section 2.3.1*. Analysis of the resulting extracts via gel electrophoresis, as described in *Section 2.3.2.1*, indicated that both of the TAE-based methods had been effective with the observation of a DNA fragment at approximately 4500 base pairs in length (*Figure 3.1*).

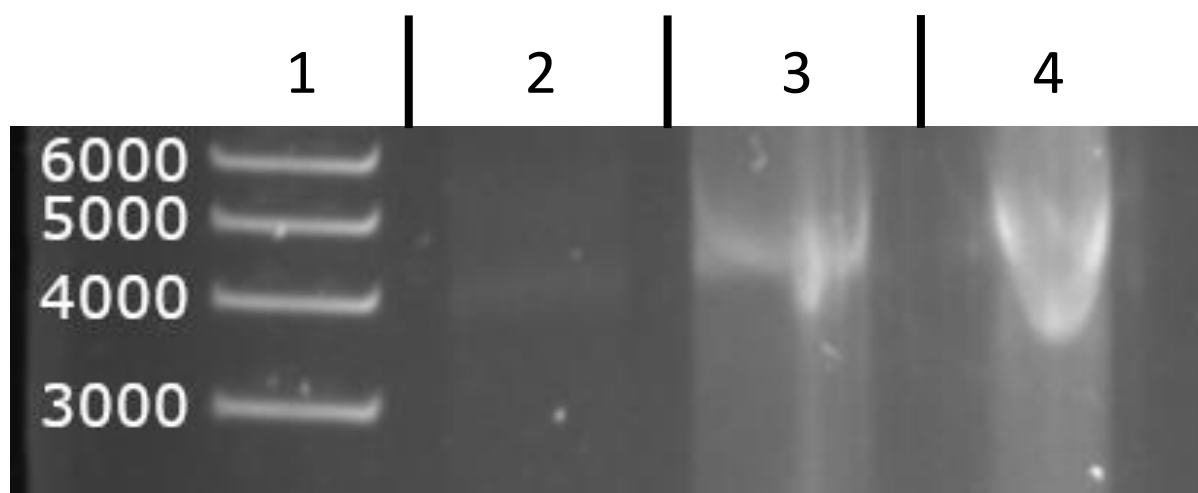


Figure 3.1: Comparison of gel electrophoresis results of different AgAK plasmid extraction methods. Lanes described from left to right: 1 - Invitrogen™ 1 Kb Plus DNA ladder; 2 - PBS-based soaking extract; 3 - TAE-based soaking extract; 4 - TAE-based shredded paper extract. DNA ladder has been annotated with size of each band in base pairs. Only relevant areas of gel depicted. Imaged via UV exposure. Gel electrophoresis performed as per Section 2.3.2.1.

Initial transformation of chemically competent BL21 cells using these extracts failed, conducted as per Section 2.3.3.1. Each of the previously described TAE-based AgAK plasmid extracts were then successfully used to transform Stellar™ cells (Figure 3.2), as described in Section 2.3.3.2.

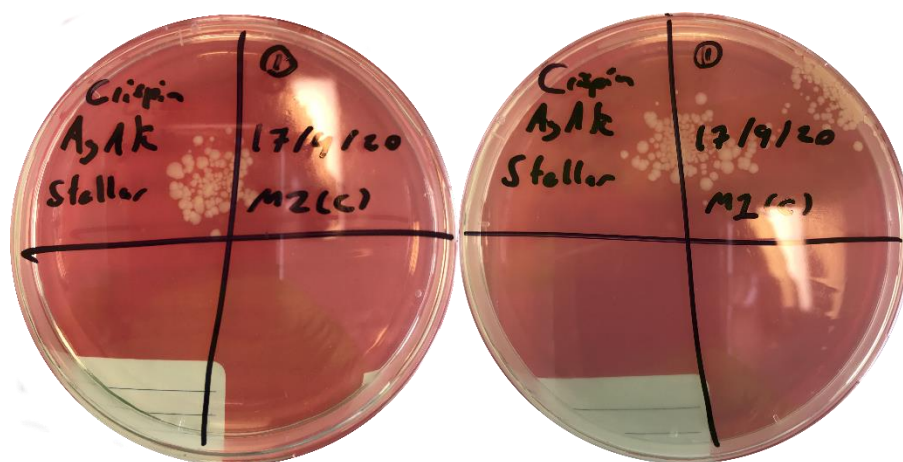


Figure 3.2: Picture of representative agar plates produced from transformation of Stellar™ cells with TAE-based AgAK plasmid extracts. Plates are pictured following 16 hours of growth. Left: TAE-based soaking extract. Right: TAE-based shredded paper extract. Transformation conducted as described in Section 2.3.3.2.

Plasmid extraction was conducted as per Section 2.3.1.1 on 50 mL of overnight liquid LB media that had been inoculated with a single colony of Stellar™ transformant, resulting in 30 µL of DNA extract at 153.6 ng/µL. Sequencing of the extract, as per Section 2.3.2.3, confirmed the integrity of the target gene. Successful transformation of BL21 cells with AgAK plasmid was achieved, as per Section 2.3.3.1, using the previously described DNA extract (Figure 3.3).



Figure 3.3: Picture of representative agar plate produced from transformation of BL21 cells with AgAK plasmid extract from Stellar™ cells. Plate is pictured following 16 hours of growth. Transformation conducted as described in Section 2.3.3.1.

3.2.2 Protein Purification

AgAK BL21 cells were grown in 150 mL of liquid LB media and protein expression was induced as per methods described by Cassera et al.⁶³ Bacterial cultures were chemically lysed as per Section 2.3.4.1 using AgAK lysis buffer as described in Section 2.1.6, resulting in 15 mL of lysate. Lysate was loaded onto a 50 mL Superloop™ and protein purification was performed via IMAC as per Section 2.4.2. UV spectroscopic analysis indicated that no protein had been eluted (Figure 3.4), this was confirmed via PAGE analysis, as described in Section 2.5.1.

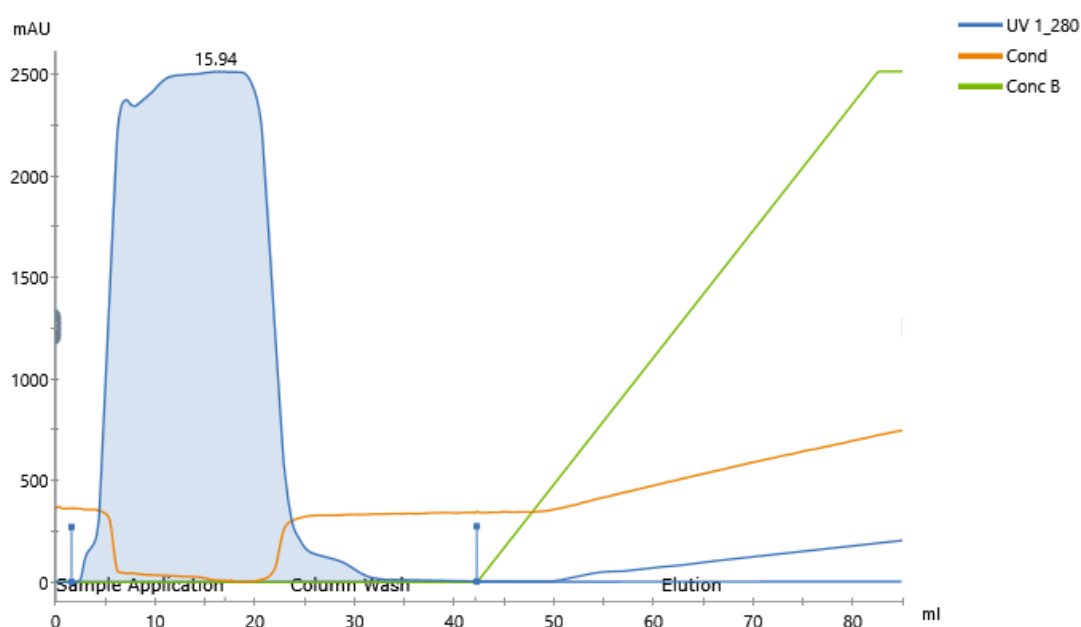


Figure 3.4: IMAC purification of cell lysate derived from AgAK BL21 liquid culture. UV absorbance monitored at 280 nm. Methodology as described in Section 2.4.2.

In order to determine whether the mode of lysis was affecting the success of protein purification, the effect of sonication lysis was examined. AgAK BL21 cells were grown in 50 mL of liquid LB media and protein expression was induced as previously described.⁶³ Cells were lysed via sonication and protein purification attempted using a His SpinTrap™ column, as described in *Section 2.3.4.2* and *Section 2.4.1* respectively. Analysis of the eluent via PAGE (*Section 2.5.1*) did not indicate that any significant amount of the target protein has been successfully purified (*Figure 3.5*).

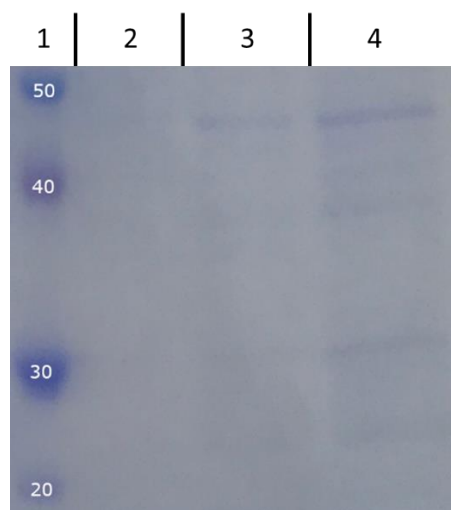


Figure 3.5: PAGE of eluent from His SpinTrap™ purification of AgAK BL21 cell lysate. Molecular weight of AgAK is approximately 40 kDa.⁶³ Lanes described from left to right: 1 - Novex Sharp Pre-Stained Protein Standard; 2 - 25% AgAK BL21 eluent in dH₂O; 3 - 50% AgAK BL21 eluent in dH₂O; 4 - 100% AgAK BL21 eluent. Protein ladder has been annotated by molecular weight of bands in kDa. Only relevant areas of gel depicted. PAGE conducted as per *Section 2.5.1*.

Further attempts at expression and purification of AgAK from 1 L liquid LB AgAK BL21 cultures, prepared as per *Section 2.2.2*, utilising 0.1% (w/v) and 0.4% (w/v) arabinose induction concentrations and methods as previously described were also unsuccessful.

A final attempt at the isolation of AgAK from BL21 cells was conducted using IEC. 1 L of AgAK BL21 liquid LB culture was prepared, as described in *Section 2.2.2*, and protein expression was induced as described previously.⁶³ Cells were chemically lysed and the resulting lysate was processed via IEC according to *Section 2.3.4.1* and *Section 2.4.3* respectively. UV spectroscopic analysis indicated the elution of protein with two UV maxima occurring at 57.88 and 72.44 mL of elution volume respectively (*Figure 3.6*). Analysis of the relevant fractions via PAGE, as described in *Section 2.5.1*, resulted in the detection of a protein fragment the approximate size of AgAK in the eluent relating to the UV maximum at 57.88 mL of elution volume (*Figure 3.7*). Significant contamination by non-target proteins in the purified sample rendered said sample unsuitable for synthetic use, however.

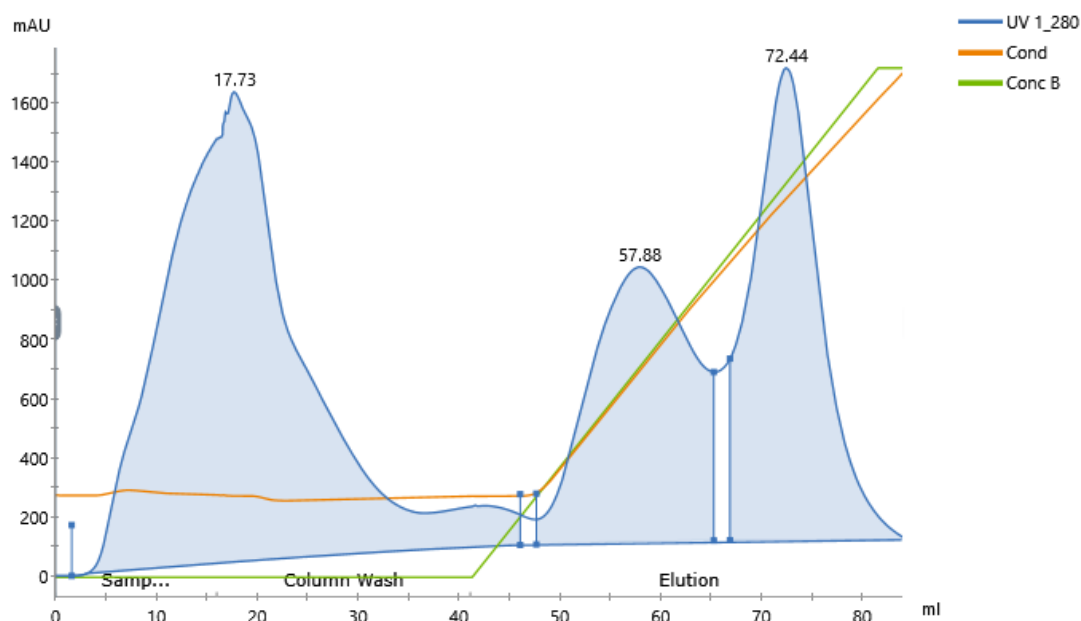


Figure 3.6: IEC purification of cell lysate derived from AgAK BL21 liquid culture. UV absorbance monitored at 280 nm. Methodology as described in Section 2.4.3.

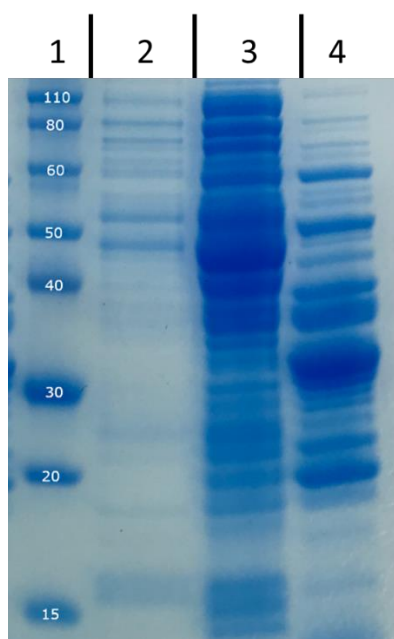


Figure 3.7: PAGE of fractions collected from IEC of AgAK BL21 cell lysate. Molecular weight of AgAK is approximately 40 kDa.⁶³ Lanes described from left to right: 1 - Novex Sharp Pre-Stained Protein Standard; 2 - sample covering 20 to 40 mL of elution volume; 3 - sample covering 67 to 77 mL of elution volume; 4 - sample covering 53 to 63 mL of elution volume. Protein ladder has been annotated by molecular weight of bands in kDa. Only relevant areas of gel depicted. PAGE conducted as per Section 2.5.1.

3.3 Uridine Cytidine Kinase 1 (human)

3.3.1 Transformation of BL21

Plasmid encoding UCK1, as described in *Section 2.1.2*, was sourced as a bacterial stab of Mach1 *E. coli* cells bearing the target plasmid. A single colony of the previously described bacterial stab was isolated and used to inoculate 50 mL of liquid LB media. This liquid media was incubated overnight following which plasmid extraction was performed, as per *Section 2.3.1.1*, resulting in approximately 50 μ L of DNA extract at a concentration of 133.75 ng/mL. Transformation of BL21 cells was then successfully conducted as described in *Section 2.3.3.1* (*Figure 3.8*).



Figure 3.8: Picture of representative agar plate produced from transformation of BL21 cells with UCK1 plasmid extract from Mach1 cells. Plate is pictured following 16 hours of growth. Transformation conducted as described in Section 2.3.3.1.

3.3.2 Protein Purification

UCK1 BL21 cells were grown in 50 mL of liquid LB media to OD₆₀₀ of 0.6 and protein expression was induced as per *Section 2.2.3*. Cell culture was then chemically lysed and protein purification was conducted using a His SpinTrap™ column as described in *Section 2.3.4.1* and *Section 2.4.1* respectively. Spin column purification resulted in a sample containing approximately 0.95 ng of protein which was analysed via PAGE, as described in *Section 2.5.1*. A protein fragment approximately 28 kDa in size was observed (*Figure 3.9*), indicating the presence of human UCK1.⁵⁹

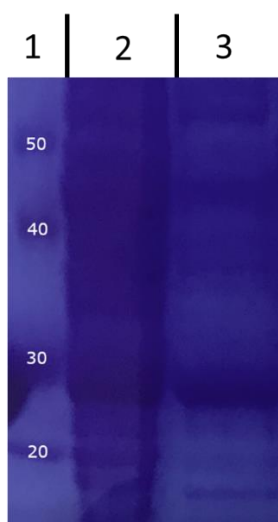


Figure 3.9: PAGE of UCK1 BL21 cell lysate and His SpinTrap™ eluent. Molecular weight of human UCK1 is 28.2 kDa.⁵⁹ Lanes described from left to right: 1 - Novex Sharp Pre-Stained Protein Standard; 2 - human UCK1 BL21 lysate; 3 - His SpinTrap™ eluent . Protein ladder has been annotated by molecular weight of bands in kDa. Only relevant areas of gel depicted. Picture has been colour-altered to increase readability. PAGE conducted as per Section 2.5.1.

Next, the initial production of human UCK1 for synthetic use occurred through extraction from 150 mL of LB liquid culture. Liquid LB media was inoculated with UCK1 BL21 cells, grown to OD₆₀₀ of 0.6, and had recombinant protein expression induced as per Section 2.2.3. Cell culture was then chemically lysed (Section 2.3.4.1) and protein purification was conducted via IMAC as described in Section 2.4.2. UV spectroscopy indicated the successful elution of protein with a UV maximum at an elution volume of 70.32 mL (Figure 3.10). PAGE analysis, conducted as per Section 2.5.1, supported the presence of human UCK1 within the eluent with the observation of a protein fragment approximately 28 kDa in size (Figure 3.11). Approximately 2.74 mg of human UCK1 was purified, the relevant fractions were concentrated and prepared for long-term storage as per Section 2.4.5 and Section 2.4.6 respectively.

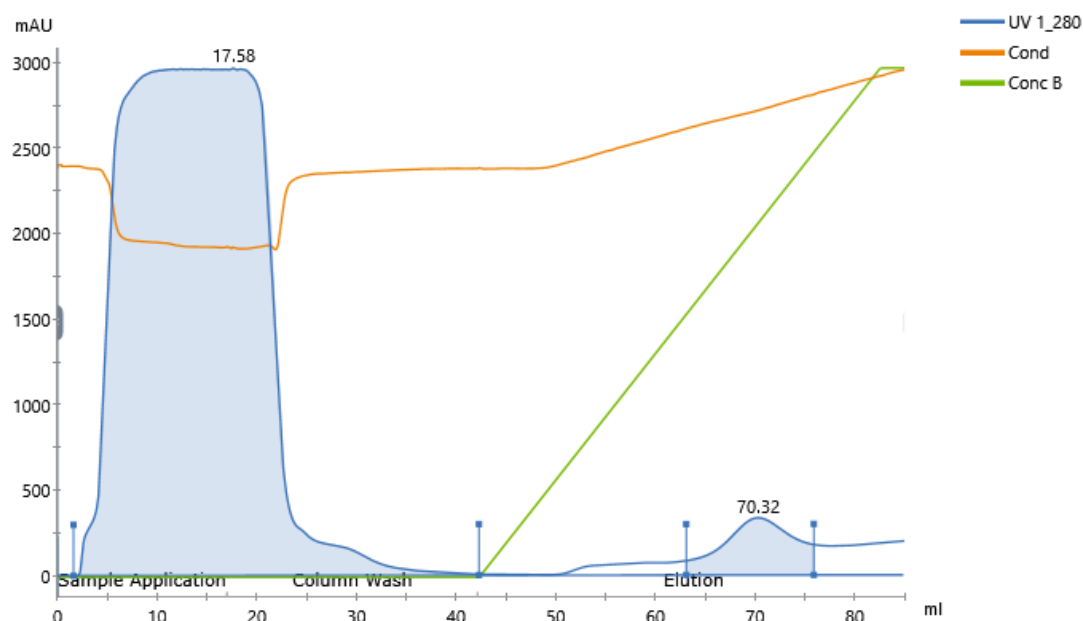


Figure 3.10: IMAC purification of cell lysate derived from 150 mL UCK1 BL21 liquid culture. UV absorbance monitored at 280 nm. Methodology as described in Section 2.4.2.

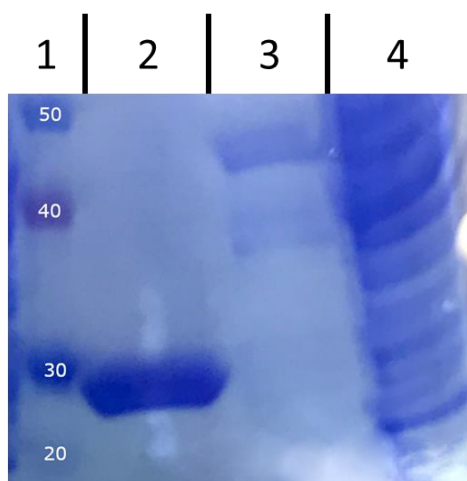


Figure 3.11: PAGE of eluent from IMAC purification of UCK1 BL21 cell lysate. Molecular weight of human UCK1 is 28.2 kDa.⁵⁹ Lanes described from left to right: 1 - Novex Sharp Pre-Stained Protein Standard; 2 - sample covering 65 to 75 mL elution volume; 3 - sample taken at approximately 50 mL elution volume; 4 - sample taken at approximately 20 mL elution volume. Protein ladder has been annotated by molecular weight of bands in kDa. Only relevant areas of gel depicted. PAGE conducted as per Section 2.5.1.

Due to the poor yields from the previously described human UCK1 purification, a larger scale process was needed. This was achieved using larger volumes of liquid culture. Three 1 L cultures of UCK1 BL21 were prepared, protein expression was induced, and sonication lysis was conducted as per *Section 2.2.2*, *Section 2.2.3*, and *Section 2.3.4.2* respectively. IMAC purification was conducted as per *Section 2.4.2*. UV spectroscopic analysis indicated the successful elution of protein with a UV maximum at 98.88 mL of elution volume (*Figure 3.12*), collection of the relevant fractions and subsequent concentration as per *Section 2.4.5* resulted in the purification of 58.5 mg of protein. PAGE analysis of

IMAC eluent, conducted as per *Section 2.5.1*, confirmed the presence of UCK1 (*Figure 3.13*). This process was repeated as required to maintain enzyme stocks for further experiments.

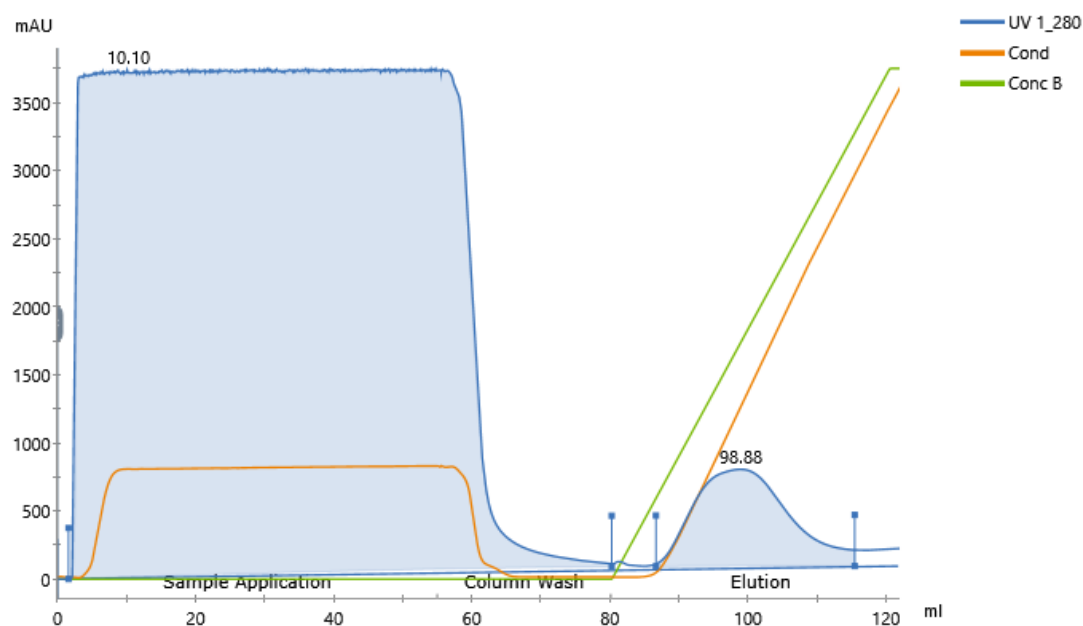


Figure 3.12: IMAC purification of cell lysate derived from 3 L UCK1 BL21 liquid culture. UV absorbance monitored at 280 nm. Methodology as described in *Section 2.4.2*.

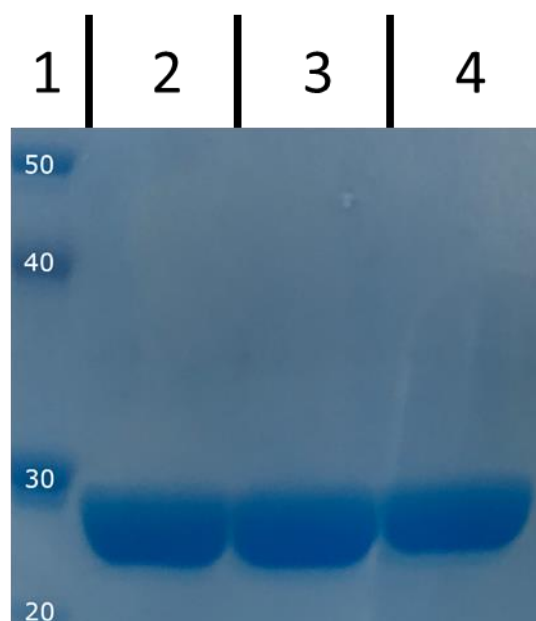


Figure 3.13: PAGE of eluent from large scale IMAC purification of UCK1 BL21 cell lysate. Molecular weight of human UCK1 is 28.2 kDa.⁵⁹ Lanes described from left to right: 1 - Novex Sharp Pre-Stained Protein Standard; 2 - sample taken at approximately 90 mL elution volume; 3 - sample taken at approximately 100 mL elution volume; 4 - sample taken at approximately 110 mL elution volume. Protein ladder has been annotated by molecular weight of bands in kDa. Only relevant areas of gel depicted. PAGE conducted as per *Section 2.5.1*.

3.4 Uridine Cytidine Kinase 2 (human)

3.4.1 FLAG-tagged UCK2

3.4.1.1 Transformation

Plasmid encoding UCK2 (FLAG-tag), as described in *Section 2.1.2*, was sourced as a bacterial stab of Stbl3 *E. coli* cells bearing the target plasmid. A single colony of the previously described bacterial stab was isolated and used to inoculate 50 mL of liquid LB media. This liquid media was incubated overnight and following this plasmid extraction was performed, as per *Section 2.3.1.1*, resulting in approximately 50 μ L of DNA extract at a concentration of 324.75 ng/mL. Transformation of BL21 cells was then successfully conducted as described on *Section 2.3.3.1* (*Figure 3.14*).

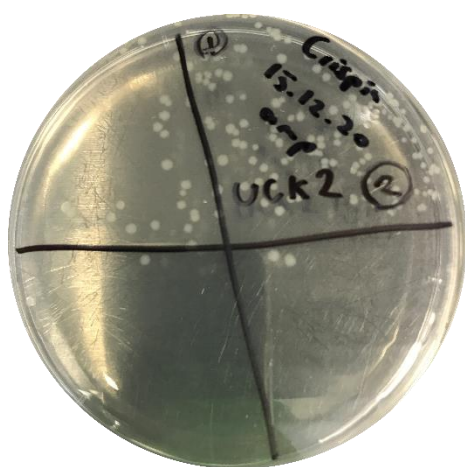


Figure 3.14: Picture of representative agar plate produced from transformation of BL21 cells with UCK2 (FLAG-tag) plasmid extract from Stbl3 cells. Plate is pictured following 16 hours of growth. Transformation conducted as described in *Section 2.3.3.1*.

3.4.1.2 Purification

1 L of UCK2 BL21 (FLAG-tag) liquid LB culture was prepared, protein expression was induced, and cells were chemically lysed as per *Section 2.2.2*, *Section 2.2.3*, and *Section 2.3.4.1* respectively. IEC purification was conducted as described in *Section 2.4.3*. UV spectroscopic analysis indicated the elution of protein with two UV maxima at elution volumes of 53.19 and 67.22 mL (*Figure 3.15*). Approximately 7.35 mg of protein was eluted. Eluted protein was analysed via PAGE, as described in *Section 2.5.1*, and a protein approximately 28 kDa in size was observed indicating that UCK2 may be present in the collected elution fractions (*Figure 3.16*). It was also observed that many other polypeptide fragments were present in the elution sample, rendering it unsuitable for synthetic use.

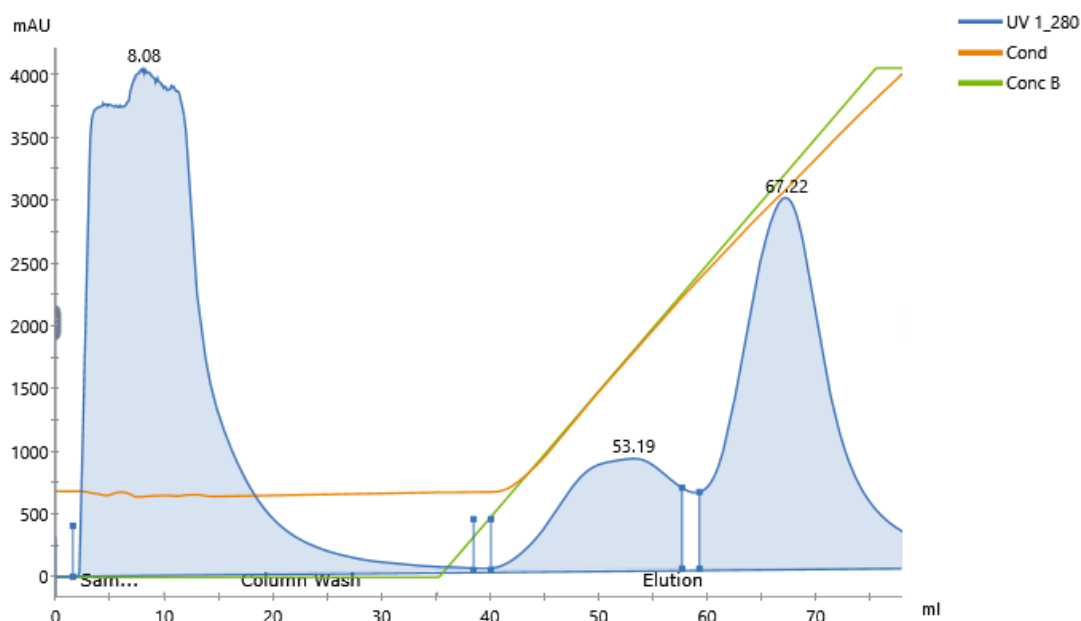


Figure 3.15: IEC purification of cell lysate derived from UCK2 (FLAG-tag) BL21 liquid culture. UV absorbance monitored at 280 nm. Methodology as described in Section 2.4.3.

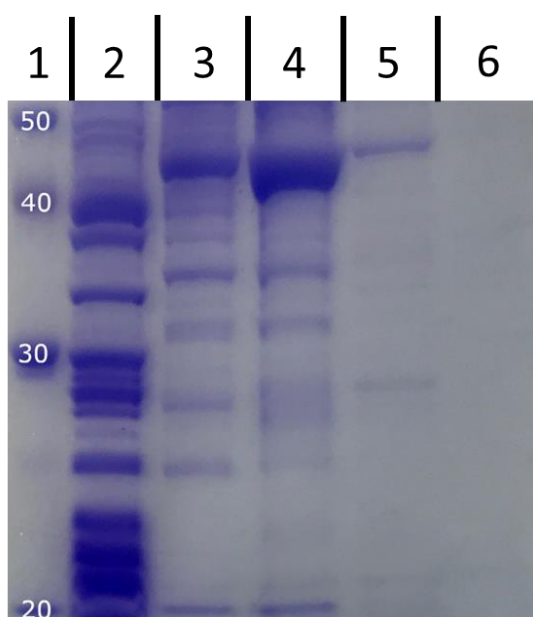


Figure 3.16: PAGE of fractions collected from IEC of UCK2 (FLAG-tag) BL21 cell lysate. Molecular weight of UCK2 monomer is 28.3 kDa.⁹⁸ Lanes described from left to right: 1 - Novex Sharp Pre-Stained Protein Standard; 2 - sample covering 0 to 20 mL of elution volume; 3 - sample covering 48 to 53 mL of elution volume; 4 - sample covering 53 to 58 mL of elution volume; 5 - sample covering 62 to 67 mL of elution volume; 6 - sample covering 67 to 72 mL of elution volume. Protein ladder has been annotated by molecular weight of bands in kDa. Only relevant areas of gel depicted. PAGE conducted as per Section 2.5.1.

To address the issue of elution sample contamination with unwanted polypeptides during IEC of UCK2 (FLAG-tag), it was theorised that a purification process involving two successive runs of IEC purification may provide a more pure sample. The preparation of 1 L liquid culture, induction of protein expression, chemical lysis, and initial IEC purification was conducted as previously described.

Fractions relating to the peak observed at 47.99 mL elution volume (*Figure 3.17*) were collected and run through the IEC process again using the previously described methodology, although in this case the elution gradient was run from 0% to 60% elution buffer. UV spectroscopic analysis indicated the elution of protein with a UV maximum at 71.82 mL of elution volume (*Figure 3.18*). Analysis of the relevant elution fractions with PAGE, as per *Section 2.5.1*, indicated that no protein of relevant size was present in the double purification eluent although a small amount of such protein was observed in samples taken from the initial run (*Figure 3.19*).

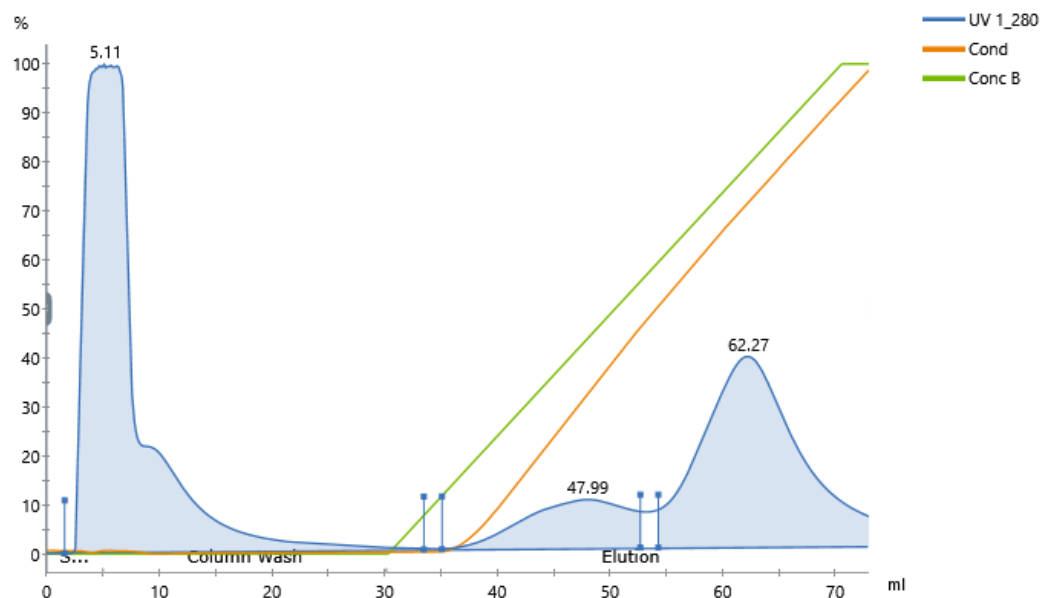


Figure 3.17: Double-purification IEC of cell lysate derived from UCK2 (FLAG-tag) BL21 liquid culture. UV absorbance monitored at 280 nm. Methodology as described in Section 2.4.3. Run 1 of 2.

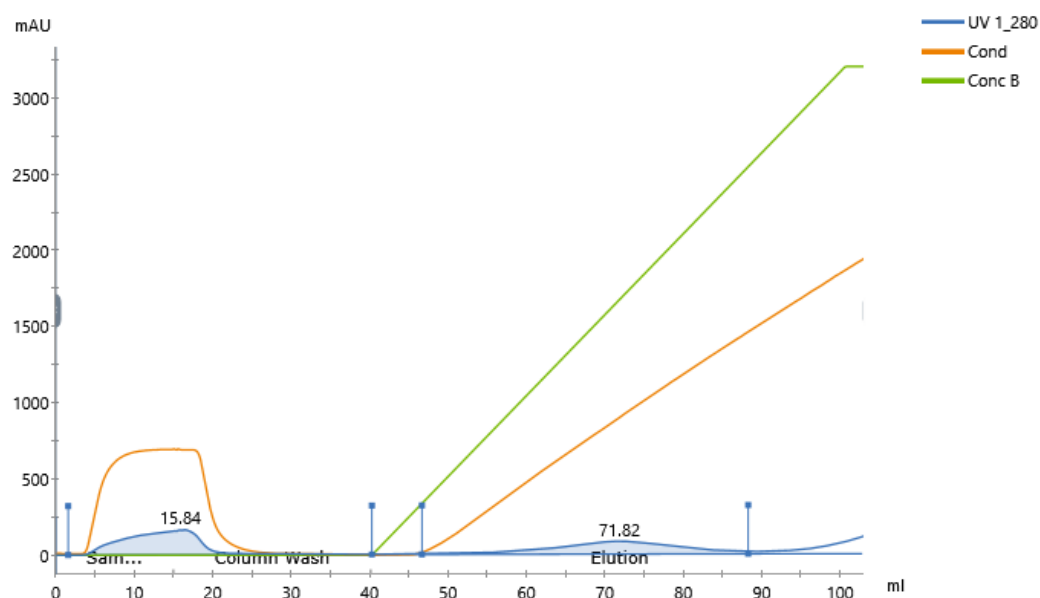


Figure 3.18: Double-purification IEC of cell lysate derived from UCK2 (FLAG-tag) BL21 liquid culture. UV absorbance monitored at 280 nm. Methodology as described in Section 2.4.3. Run 2 of 2.

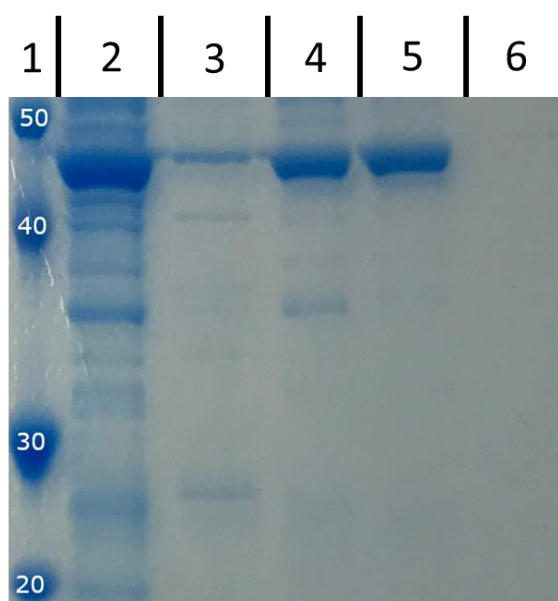


Figure 3.19: PAGE of fractions collected from double-purification IEC of UCK2 (FLAG-tag) BL21 cell lysate. Molecular weight of UCK2 monomer is 28.3 kDa.⁹⁸ Lanes described from left to right: 1 - Novex Sharp Pre-Stained Protein Standard; 2 - sample covering 40 to 52 mL of elution volume from run 1; 3 - sample covering 58 to 68 mL of elution volume of run 1; 4 - sample covering 62 to 72 mL of elution volume of run 2; 5 - sample covering 72 to 82 mL of elution volume of run 2; 6 - sample covering 90 to 100 mL of elution volume of run 2. Protein ladder has been annotated by molecular weight of bands in kDa. Only relevant areas of gel depicted. PAGE conducted as per Section 2.5.1.

3.4.2 His-tagged UCK2

3.4.2.1 Transformation

Plasmid encoding UCK2 (His-tag), as described in Section 2.1.2, was used to successfully transform BL21 cells as per Section 2.3.3.1 (Figure 3.20).

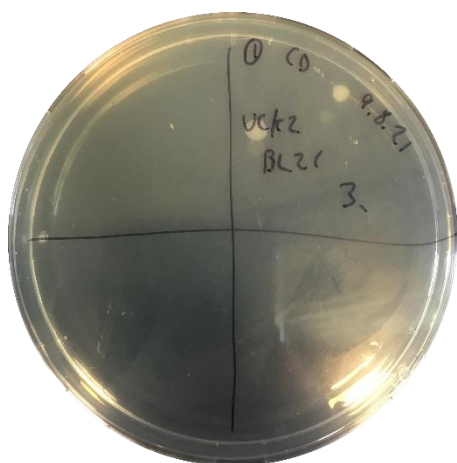


Figure 3.20: Picture of representative agar plates produced from transformation of BL21 cells with pure UCK2 (His-tag) plasmid. Plate is pictured following 16 hours of growth. Transformation conducted as described in Section 2.3.3.1.

3.4.2.2 Purification

Initial confirmation of UCK2 (His-tag) production by transformed BL21 cells was achieved using His SpinTrap™ purification. UCK2 (His-tag) BL21 cells were grown in 50 mL of liquid LB media to an OD₆₀₀ of 0.6 and protein expression was induced as described in *Section 2.2.3*. Cell culture was then chemically lysed and protein purification conducted using a His SpinTrap™ column as described in *Section 2.3.4.1* and *Section 2.4.1* respectively. Spin column purification resulted in a sample of 400 µL of 0.4 ng/mL protein which was analysed via PAGE, as described in *Section 2.5.1*. The results of this analysis did not support the presence of UCK2 in the His SpinTrap™ eluent (*Figure 3.21*).

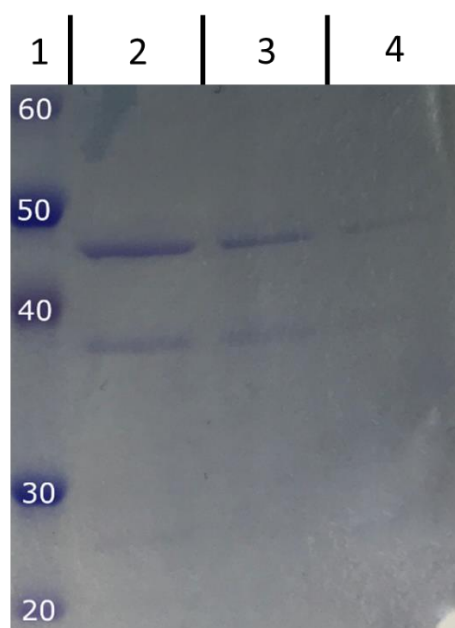


Figure 3.21: PAGE of eluent from His SpinTrap™ purification of UCK2 (His-tag) BL21 cell lysate. Molecular weight of UCK2 monomer is 28.3 kDa.⁹⁸ Lanes described from left to right: 1 - Novex Sharp Pre-Stained Protein Standard; 2 - 100% UCK2 (His-tag) BL21 eluent; 3 - 50% UCK2 (His-tag) BL21 eluent in dH₂O; 4 - 25% UCK2 (His-tag) BL21 eluent in dH₂O. Protein ladder has been annotated by molecular weight of bands in kDa. Only relevant areas of gel depicted. PAGE conducted as per *Section 2.5.1*.

It was theorised that larger culture volumes may lead to the production of observable amounts of UCK2. Three 1 L liquid LB cultures of UCK2 BL21 (His-tag) cells were prepared, protein expression was induced, and sonication lysis was conducted as per *Section 2.2.2*, *Section 2.2.3*, and *Section 2.3.4.2* respectively. IMAC purification was conducted as per *Section 2.4.2*. A slight UV maximum was observed at an elution volume of 90.27 mL indicating that protein had been successfully purified (*Figure 3.22*). Concentration of relevant fractions, as per *Section 2.4.5*, revealed that 24 mg of UCK2 was purified. Analysis of concentrated protein via PAGE indicated that human UCK2 was present in solution with the observation of a protein fragment approximately 28 kDa in size (*Figure 3.23*). Concentrated protein was processed for long term storage as per *Section 2.4.6*. This process was repeated as required to maintain enzyme stocks for further experiments.

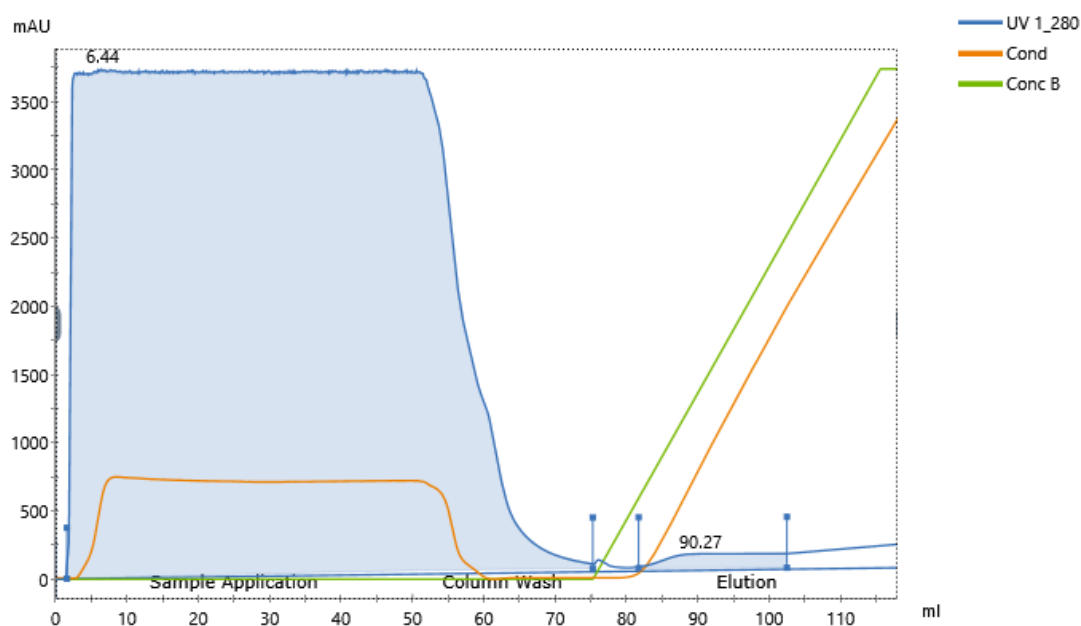


Figure 3.22: IMAC purification of cell lysate derived from 3 L UCK2 (His-tag) BL21 liquid culture. UV absorbance monitored at 280 nm. Methodology as described in Section 2.4.2.

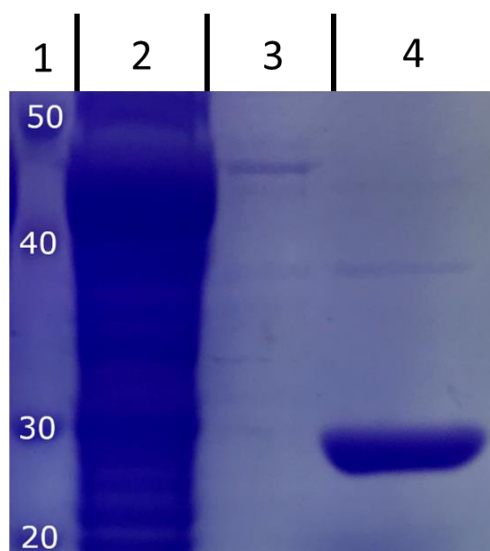


Figure 3.23: PAGE of eluent from large scale IMAC purification of UCK2 (His-tag) BL21 cell lysate. Molecular weight of human UCK2 is 28.3 kDa.⁹⁸ Lanes described from left to right: 1 - Novex Sharp Pre-Stained Protein Standard; 2 - sample taken at approximately 50 mL elution volume; 3 - sample taken at approximately 80 mL elution volume; 4 - concentrated sample covering 85 to 95 mL elution volume. Protein ladder has been annotated by molecular weight of bands in kDa. Only relevant areas of gel depicted. PAGE conducted as per Section 2.5.1.

3.5 Adenylate Kinase (*Escherichia coli*)

3.5.1 Transformation

Plasmid encoding *EcADK*, as described in *Section 2.1.2*, was sourced as a bacterial stab of DH5-Alpha *E. coli* cells bearing the target plasmid. A single colony of the previously described bacterial stab was isolated and used to inoculate 50 mL of liquid LB media. This liquid media was incubated overnight following plasmid extraction was performed, as per *Section 2.3.1.1*, resulting in approximately 50 μ L of DNA extract at a concentration of 123.95 ng/mL. Transformation of BL21 cells was then successfully conducted as described on *Section 2.3.3.1* (*Figure 3.24*).

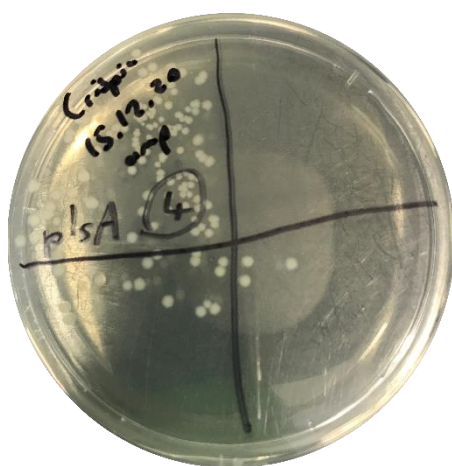


Figure 3.24: Picture of representative agar plate produced from transformation of BL21 cells with EcADK plasmid extract from DH5-Alpha cells. Plate is pictured following 16 hours of growth. Transformation conducted as described in Section 2.3.3.1.

3.5.2 Protein Expression

EcADK BL21 cells were grown in 50 mL of liquid LB media to OD₆₀₀ of 0.6 and protein expression was induced as per *Section 2.2.3*. Cell culture was then chemically lysed and protein purification was conducted using a His SpinTrap™ column as described in *Section 2.3.4.1* and *Section 2.4.1* respectively. Spin column purification resulted in a sample containing approximately 1.23 ng of protein which was analysed via PAGE, as described in *Section 2.5.1*. A protein fragment between 20 and 30 kDa in size was observed (*Figure 3.25*), indicating the presence of *EcADK*.⁹⁹

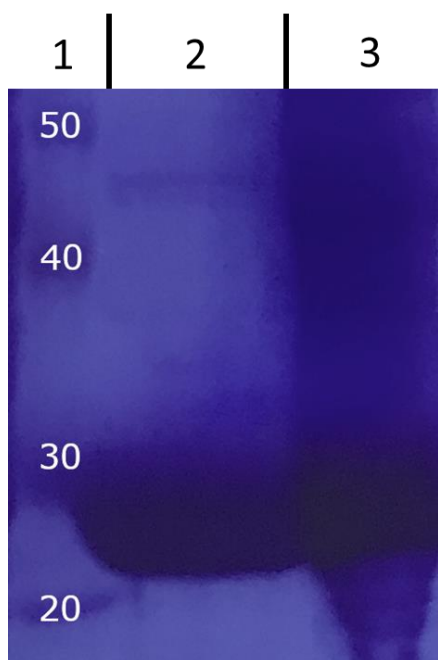


Figure 3.25: PAGE of EcADK BL21 cell lysate and His SpinTrap™ eluent. Molecular weight of EcADK is 23.6 kDa.¹⁰⁰ Lanes described from left to right: 1 - Novex Sharp Pre-Stained Protein Standard; 2 - His SpinTrap™ eluent; 3 - EcADK BL21 lysate. Protein ladder has been annotated by molecular weight of bands in kDa. Only relevant areas of gel depicted. Picture has been colour-altered to increase readability. PAGE conducted as per Section 2.5.1.

Production of EcADK for synthetic use was achieved through extraction from 150 mL of LB media which had been inoculated with EcADK BL21 cells, grown to OD₆₀₀ of 0.6, and had recombinant protein expression induced as per Section 2.2.3. Cell culture was then chemically lysed (Section 2.3.4.1) and protein purification was conducted via IMAC as described in Section 2.4.2. UV spectroscopy indicated the successful elution of protein with the UV maximum at 44.76 mL of elution volume (Figure 3.26) and PAGE analysis, conducted as per Section 2.5.1, supported the presence of EcADK within the eluent with the observation of a protein fragment approximately between 20 and 30 kDa in size (Figure 3.27). Approximately 39.36 mg of EcADK was purified, the relevant fractions were concentrated and prepared for long-term storage as per Section 2.4.5 and Section 2.4.6 respectively. This process was repeated as required to maintain enzyme stocks for further experiments.

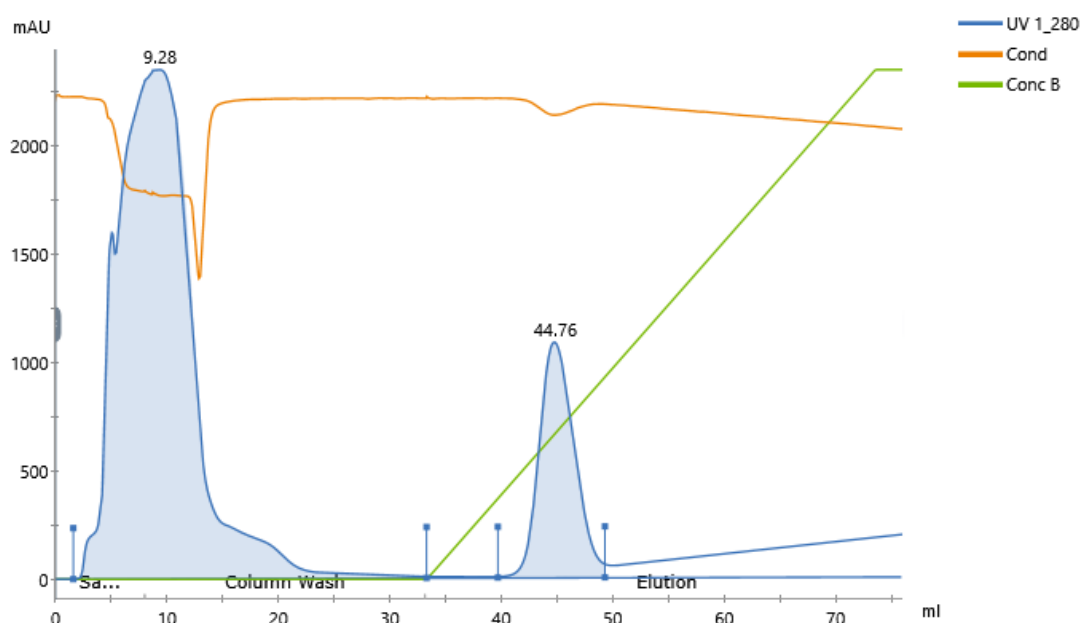


Figure 3.26: IMAC purification of cell lysate derived from 150 mL EcADK BL21 liquid culture. UV absorbance monitored at 280 nm. Methodology as described in Section 2.4.2.

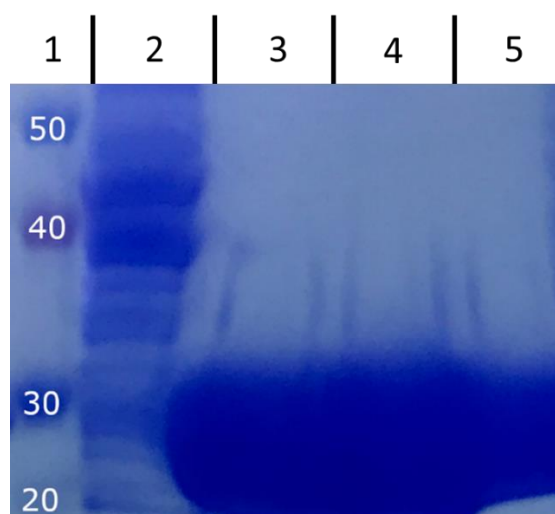


Figure 3.27: PAGE of eluent from IMAC purification of EcADK BL21 cell lysate. Molecular weight of EcADK is 23.6 kDa.¹⁰⁰ Lanes described from left to right: Novex Sharp Pre-Stained Protein Standard; Sample covering 15 to 25 mL elution volume; Sample taken at approximately 43 mL elution volume; Sample taken at approximately 44.5 mL elution volume; Sample taken at approximately 46 mL elution volume. Protein ladder has been annotated by molecular weight of bands in kDa. Only relevant areas of gel depicted. PAGE conducted as per Section 2.5.1.

3.6 Guanylate Kinase (*Plasmodium falciparum*)

3.6.1 Transformation

Plasmid encoding *PfGUK*, as described in Section 2.1.2, was sourced as a bacterial stab of Stbl3 *E. coli* cells bearing the target plasmid. A single colony of the previously described bacterial stab was isolated

and used to inoculate 50 mL of liquid LB media. This liquid media was incubated overnight following which plasmid extraction was performed, as per *Section 2.3.1*, resulting in approximately 50 μ L of DNA extract at a concentration of 147.9 ng/mL. Transformation of BL21 cells was then successfully conducted as described on *Section 2.3.3.1* (*Figure 3.28*).

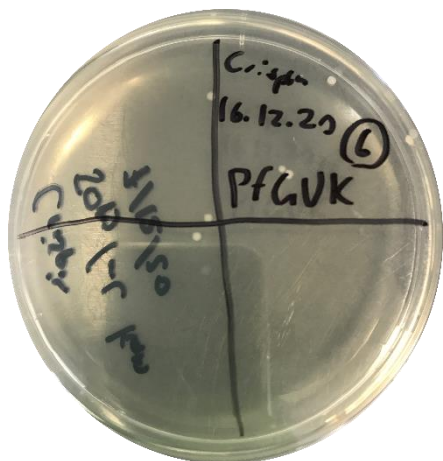


Figure 3.28: Picture of representative agar plate produced from transformation of BL21 cells with PFGUK plasmid extract from Stbl3 cells. Plate is pictured following 16 hours of growth. Transformation conducted as described in Section 2.3.3.1.

3.6.2 Protein Expression

PfGUK BL21 cells were grown in 50 mL of liquid LB media to an OD₆₀₀ of 0.6 and protein expression was induced as per *Section 2.2.3*. Cell culture was then chemically lysed and protein purification was conducted using a His SpinTrap™ column as described in *Section 2.3.4.1* and *Section 2.4.1* respectively. Spin column purification resulted in a sample containing approximately 0.07 ng of protein which was analysed via PAGE, as described in *Section 2.5.1*. A protein fragment at approximately 24 kDa was observed (*Figure 3.29*), indicating the presence of PfGUK.¹⁰¹

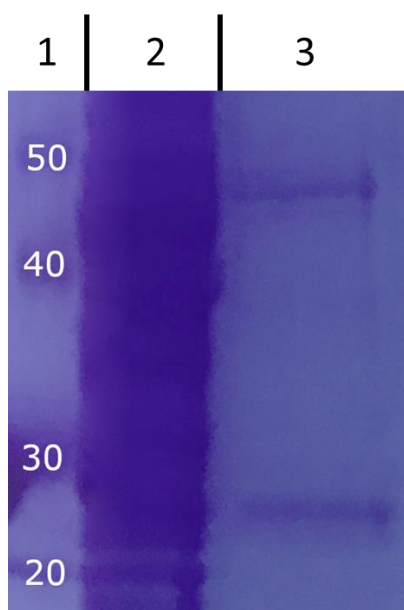


Figure 3.29: PAGE of *PfGUK* BL21 cell lysate and His SpinTrap™ eluent. Molecular weight of *PfGUK* is 24 kDa.¹⁰¹ Lanes described from left to right: 1 - Novex Sharp Pre-Stained Protein Standard; 2 - *PfGUK* BL21 lysate; 3 - His SpinTrap™ eluent. Protein ladder has been annotated by molecular weight of bands in kDa. Only relevant areas of gel depicted. Picture has been colour-altered to increase readability. PAGE conducted as per Section 2.5.1.

Initial attempts at production of *PfGUK* for synthetic use occurred through extraction from 150 mL of LB media inoculated with *PfGUK* BL21 cells, grown to OD₆₀₀ of 0.6, and the induction of protein expression as per Section 2.2.3. Cell culture was then chemically lysed (Section 2.3.4.1) and protein purification was conducted via IMAC as described in Section 2.4.2. No peaks were observed in UV spectroscopic analysis of collected fractions, indicating that protein was not eluted in any significant amount (Figure 3.30). Analysis of samples across the elution gradient by PAGE, as described in Section 2.5.1, supported these results however the observation of a very slight protein fragment approximately 24 kDa in size indicated that *PfGUK* was present albeit in insufficient quantity to have utility (Figure 3.31).

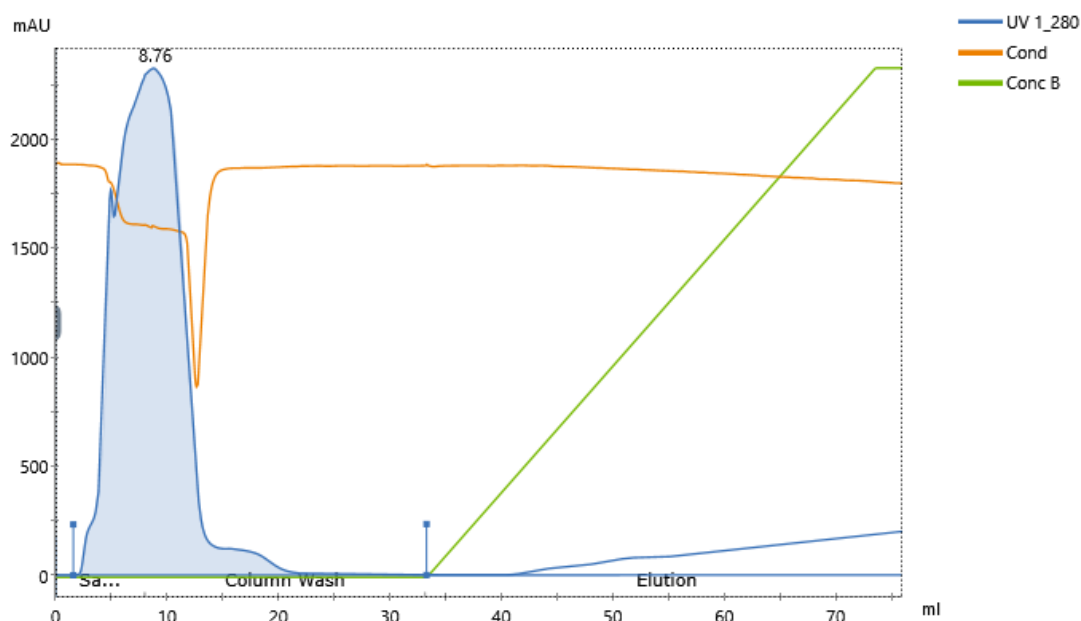


Figure 3.30: IMAC purification of cell lysate derived from *PfGUK BL21* liquid culture. UV absorbance monitored at 280 nm. Methodology as described in Section 2.4.2.

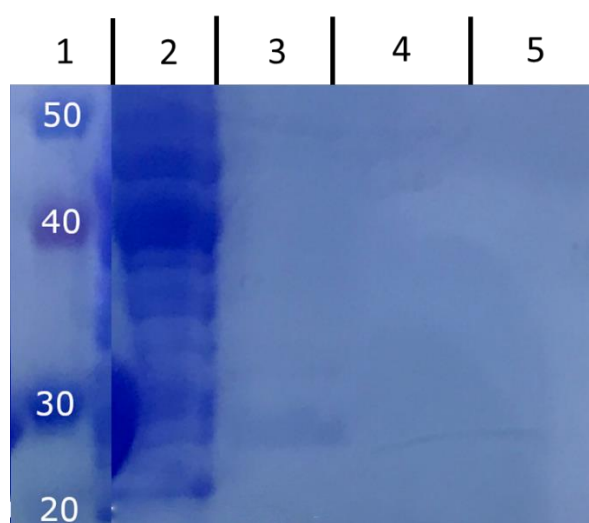


Figure 3.31: PAGE of eluent from IMAC purification of *PfGUK BL21* cell lysate. Molecular weight of *PfGUK* is 24 kDa.¹⁰¹ Lanes described from left to right: 1 - Novex Sharp Pre-Stained Protein Standard; 2 - sample covering 15 to 25 mL elution volume; 3 - sample covering 40 to 50 mL elution volume; 4 - sample covering 50 to 60 mL elution volume; 5 - sample covering 60 to 70 mL elution volume. Protein ladder has been annotated by molecular weight of bands in kDa. Only relevant areas of gel depicted. PAGE conducted as per Section 2.5.1.

To determine if an alternate mode of lysis would improve purification efficiency, the effect of lysis via sonication was assessed. *PfGUK BL21* cells were grown in 50 mL of liquid LB media and protein expression was induced as described in Section 2.3.3. Cells were lysed via sonication and protein purification attempted using a His SpinTrap™, as described in Section 2.3.4.2 and Section 2.4.1 respectively. Analysis of the eluent via PAGE (Section 2.5.1) indicated that a protein approximately 24

kDa in size was present in solution, suggesting that *PfGUK* had been successfully purified (*Figure 3.32*).¹⁰¹ Amounts of protein within the eluent were too low to warrant preparation for long term storage.

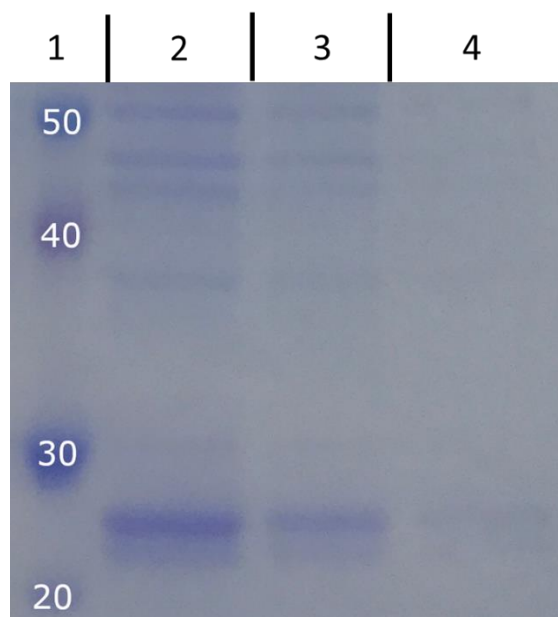


Figure 3.32: PAGE of eluent from His SpinTrap™ purification of *PfGUK* BL21 cell lysate. Molecular weight of *PfGUK* is 24 kDa.¹⁰¹ Lanes described from left to right: 1 - Novex Sharp Pre-Stained Protein Standard; 2 - 100% *PfGUK* BL21 eluent; 3 - 50% *PfGUK* BL21 eluent in dH₂O; 4 - 25% *PfGUK* BL21 eluent in dH₂O. Protein ladder has been annotated by molecular weight of bands in kDa. Only relevant areas of gel depicted. PAGE conducted as per Section 2.5.1.

A final attempt at the isolation of *PfGUK* from the previously transformed BL21 cells was conducted using IEC. 1 L of *PfGUK* BL21 liquid LB culture was prepared, and protein expression was induced as described in Section 2.2.2 and Section 2.2.3 respectively. Cells were chemically lysed, and IEC was performed according to Section 2.3.4.1 and Section 2.4.3 respectively. UV spectroscopic analysis indicated the elution of protein with two UV maxima occurring at 65.02 and 78.61 mL of elution volume (*Figure 3.33*). Analysis of the relevant fractions via PAGE, conducted as per Section 2.5.1, indicated that *PfGUK* was eluted in the maxima at 65.02 mL elution volume with the presence of a protein fragment approximately 24 kDa in size (*Figure 3.34*). Elution fractions relevant to this UV maxima were concentrated and processed for long term storage, as per Section 2.4.5 and Section 2.4.6. Approximately 23.7 mg of protein were purified in total.

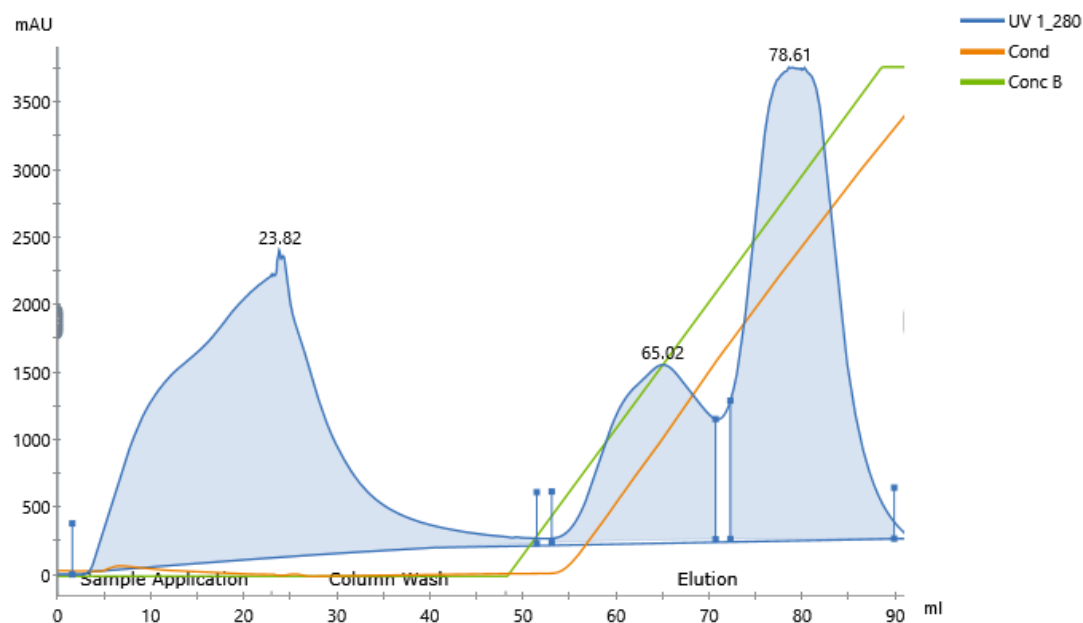


Figure 3.33: IEC purification of cell lysate derived from PfGUK BL21 liquid culture. UV absorbance monitored at 280 nm. Methodology as described in Section 2.4.3.

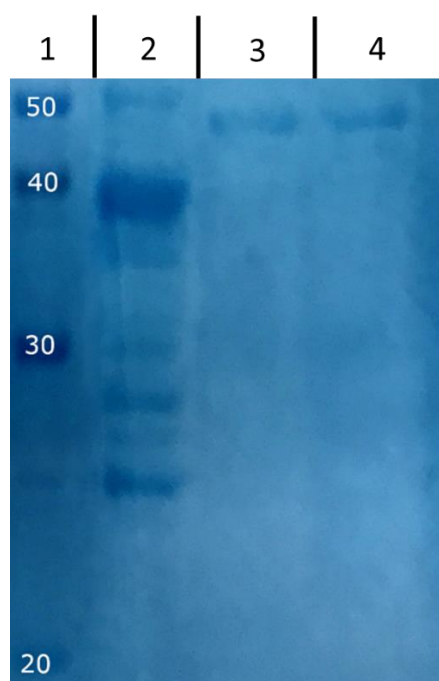


Figure 3.34: PAGE of fractions collected from IEC of PfGUK BL21 cell lysate. Molecular weight of PfGUK is 24 kDa.¹⁰¹ Lanes described from left to right: 1 - Novex Sharp Pre-Stained Protein Standard; 2 - sample covering 20 to 40 mL of elution volume; 3 - sample covering 60 to 70 mL of elution volume; 4 - sample covering 75 to 85 mL of elution volume. Protein ladder has been annotated by molecular weight of bands in kDa. Only relevant areas of gel depicted. PAGE conducted as per Section 2.5.1.

3.7 Uridine Monophosphate-Cytidine Monophosphate Kinase (human)

3.7.1 FLAG-tagged CMPK

3.7.1.1 Transformation

Plasmid encoding CMPK, as described in *Section 2.1.2*, was sourced as a bacterial stab of Stbl3 *E. coli* cells bearing the target plasmid. A single colony of the previously described bacterial stab was isolated and used to inoculate 50 mL of liquid LB media. This liquid media was incubated overnight following plasmid extraction was performed, as per *Section 2.3.1.1*, resulting in approximately 50 μ L of DNA extract at a concentration of 341.25 ng/mL. Transformation of BL21 cells was then successfully conducted as described in *Section 2.3.3.1* (*Figure 3.35*).



Figure 3.35: Picture of representative agar plate produced from transformation of BL21 cells with CMPK (FLAG-tag) plasmid extract from Stbl3 cells. Plate is pictured following 16 hours of growth. Transformation conducted as described in Section 2.3.3.1.

3.7.1.2 Purification

1 L of CMPK BL21 (FLAG-tag) liquid LB culture was prepared, protein expression was induced, and cells were chemically lysed as per *Section 2.2.2*, *Section 2.2.3*, and *Section 2.3.4.1* respectively. IEC purification was conducted as described in *Section 2.4.3*. UV spectroscopic analysis revealed that protein was successfully eluted with the observation of UV maxima at 54.94 and 74.01 mL of elution volume (*Figure 3.36*). Approximately 35.85 mg of protein was eluted. Eluted protein was analysed via PAGE, as described in *Section 2.5.1*, and a protein approximately 22 kDa in size was observed as having eluted between 50 and 60 mL elution volume indicating that CMPK may have been successfully eluted (*Figure 3.37*). It was also observed that many other polypeptides were present in the elution sample, rendering it unsuitable for synthetic use.

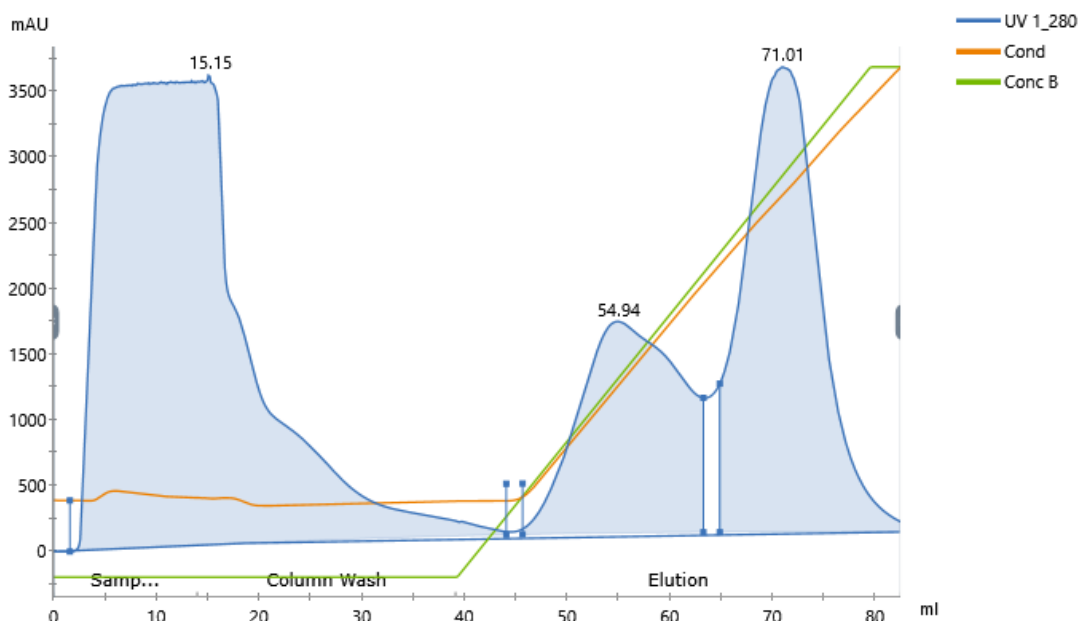


Figure 3.36: IEC purification of cell lysate derived from CMPK (FLAG-tag) BL21 liquid culture. UV absorbance monitored at 280 nm. Methodology as described in Section 2.4.3.

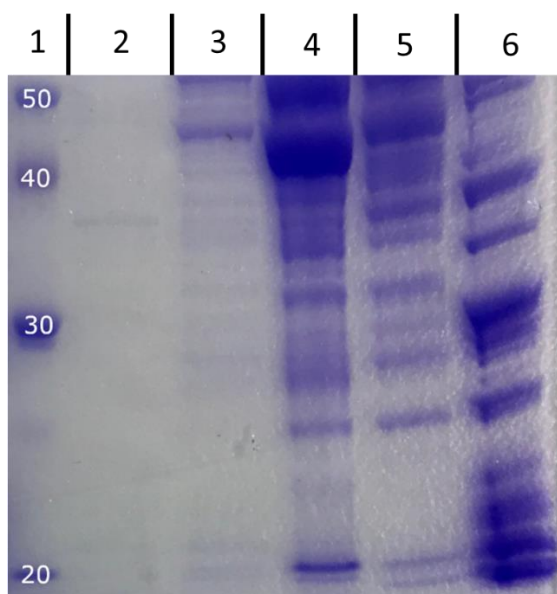


Figure 3.37: PAGE of fractions collected from IEC of CMPK (FLAG-tag) BL21 cell lysate. Molecular weight of CMPK is 22.3 kDa.¹⁰² Lanes described from left to right: 1 - Novex Sharp Pre-Stained Protein Standard; 2 - sample covering 72 to 76 mL of elution volume; 3 - sample covering 66 to 71 mL of elution volume; 4 - sample covering 55 to 60 mL of elution volume; 5 - sample covering 55 to 67 mL of elution volume; 6 - sample covering 20 to 30 mL of elution volume. Protein ladder has been annotated by molecular weight of bands in kDa. Only relevant areas of gel depicted. PAGE conducted as per Section 2.5.1.

To address the issue of elution sample contamination with unwanted polypeptides during IEC purification of CMPK (FLAG-tagged) from BL21 cell lysate, it was theorised that a purification process involving two successive runs of IEC purification may provide a more pure sample. Preparation of 1 L liquid culture, induction of protein expression, chemical lysis, and initial IEC purification was

conducted as previously described. Fractions relating to the UV maxima observed at 60.77 mL of elution volume in run 1 (*Figure 3.38*) were collected and run through the IEC process again using the previously described methodology, although in this case the elution gradient was run from 0% to 60% elution buffer. UV spectroscopic analysis indicated the elution of protein with a UV maximum at 72.94 mL of elution volume (*Figure 3.39*). Analysis of the relevant elution fractions via PAGE, as per *Section 2.5.1*, indicated the presence of CMPK (FLAG-tag) in the fractions relating to the previously described peak (*Figure 3.40*). Eluted protein was concentrated and prepared for long term storage for later activity testing, as per *Section 2.4.5* and *Section 2.4.6* respectively.

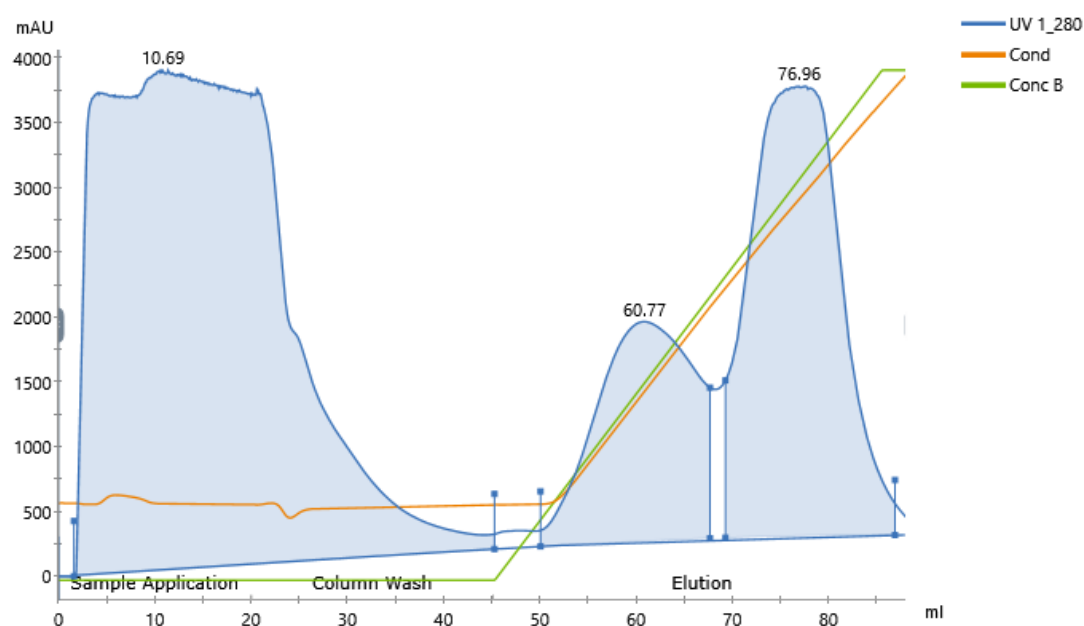


Figure 3.38: Double-purification IEC of cell lysate derived from CMPK (FLAG-tag) BL21 liquid culture. UV absorbance monitored at 280 nm. Methodology as described in Section 2.4.3. Run 1 of 2.

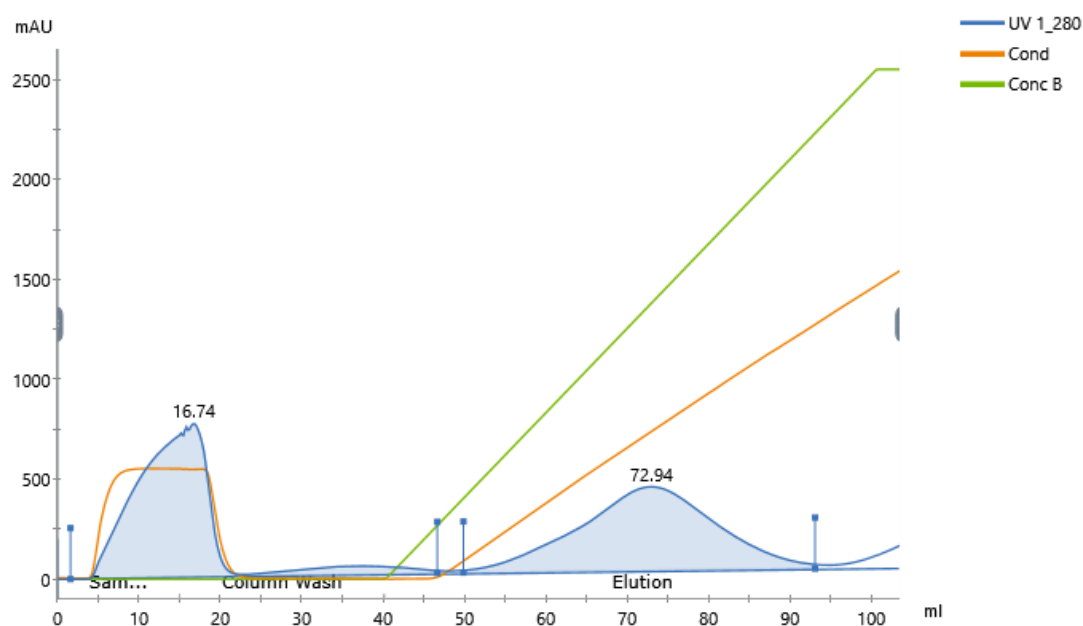


Figure 3.39: Double-purification IEC of cell lysate derived from CMPK (FLAG-tag) BL21 liquid culture. UV absorbance monitored at 280 nm. Methodology as described in Section 2.4.3. Run 2 of 2.

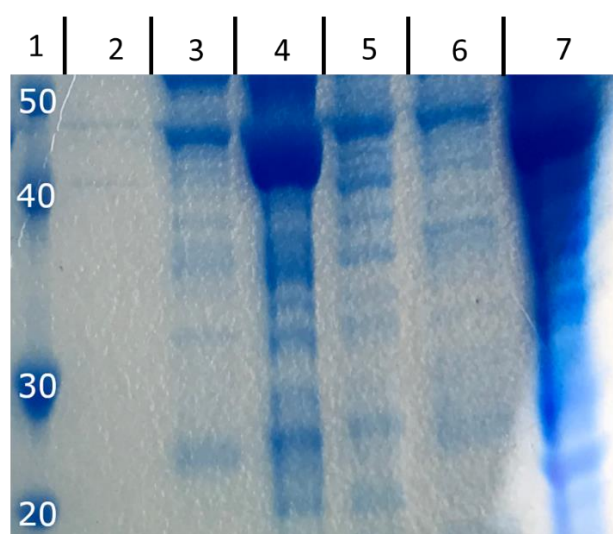


Figure 3.40: PAGE of fractions collected from double-purification IEC of CMPK (FLAG-tag) BL21 cell lysate. Molecular weight of CMPK is 22.3 kDa.¹⁰² Lanes described from left to right: 1 - Novex Sharp Pre-Stained Protein Standard; 2 - sample covering 94 to 104 mL of elution volume from run 2; 3 - sample covering 80 to 90 mL of elution volume of run 2; 4 - sample covering 70 to 80 mL of elution volume of run 2; 5 - sample covering 60 to 70 mL of elution volume of run 2; 6 - sample covering 72 to 82 mL of elution volume of run 1; 7 - sample covering 56 to 66 mL of elution volume of run 1. Protein ladder has been annotated by molecular weight of bands in kDa. Only relevant areas of gel depicted. PAGE conducted as per Section 2.5.1.

3.7.2 His-tagged CMPK

3.7.2.1 Transformation

Plasmid encoding CMPK (His-tag), as described in Section 2.1.2, was used to successfully transform BL21 cells as per Section 2.3.3.1 (Figure 3.41).



Figure 3.41: Picture of representative agar plates produced from transformation of BL21 cells with pure CMPK (His-tag) plasmid. Plate is pictured following 16 hours of growth. Transformation conducted as described in Section 2.3.3.1.

3.7.2.2 Purification

Initial confirmation of CMPK (His-tag) production by transformed BL21 cells was achieved using His SpinTrap™ purification. CMPK (His-tag) BL21 cells were grown in 50 mL of liquid LB media to an OD₆₀₀ of 0.6 and protein expression was induced as described in Section 2.2.3. Cell culture was then chemically lysed and protein purification conducted using a His SpinTrap™ column as described in Section 2.3.4.1 and Section 2.4.1 respectively. Spin column purification resulted in a sample containing approximately 0.28 ng of protein which was analysed via PAGE, as described in Section 2.5.1. The results of this analysis did not support the presence of CMPK in the eluent (Figure 3.42).

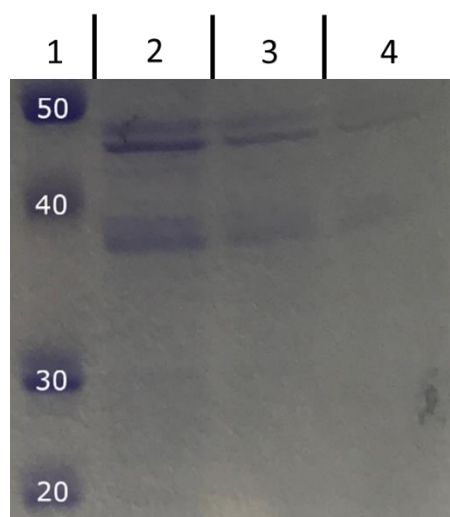


Figure 3.42: PAGE of eluent from His SpinTrap™ purification of CMPK (His-tag) BL21 cell lysate. Molecular weight of CMPK is 22.3 kDa.¹⁰² Lanes described from left to right: 1 - Novex Sharp Pre-Stained Protein Standard; 2 - 100% CMPK (His-tag) BL21 eluent; 3 - 50% CMPK (His-tag) BL21 eluent in dH₂O; 4 - 25% CMPK (His-tag) BL21 eluent in dH₂O. Protein ladder has been annotated by molecular weight of bands in kDa. Only relevant areas of gel depicted. PAGE conducted as per Section 2.5.1.

It was theorised that larger culture volumes may lead to the production of observable amounts of CMPK. Three 1 L liquid LB CMPK BL21 cell cultures were prepared, protein expression was induced, and sonication lysis was conducted as per *Section 2.2.2*, *Section 2.2.3*, and *Section 2.3.4.2* respectively. IMAC purification was conducted as per *Section 2.4.2*.

UV spectroscopy revealed a slight UV maximum at 60.52 mL elution volume (*Figure 3.43*). Analysis of elution fractions relating to this peak via PAGE, conducted as per *Section 2.5.1*, indicated the presence of CMPK within the sample with the observation of a protein fragment between 20 and 30 kDa in size (*Figure 3.*). The relevant elution fractions were concentrated and prepared for long-term storage as per *Section 2.4.5* and *Section 2.4.6* respectively.

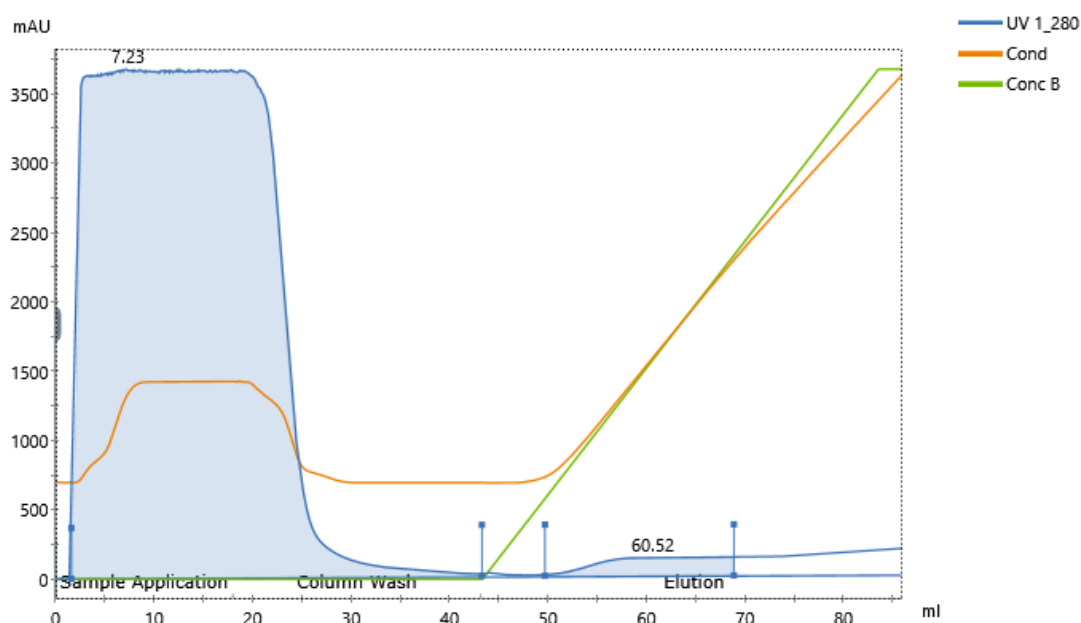


Figure 3.43: IMAC purification of cell lysate derived from 3 L CMPK (His-tag) BL21 liquid culture. UV absorbance monitored at 280 nm. Methodology as described in *Section 2.4.2*.

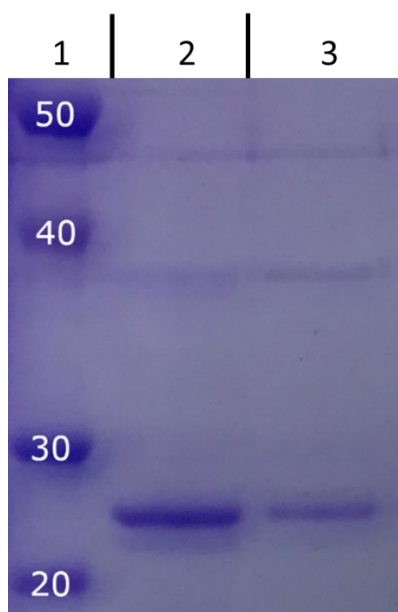


Figure 3.44: PAGE of eluent from large scale IMAC purification of CMPK (His-tag) BL21 cell lysate. Molecular weight of human CMPK is 22.3 kDa.¹⁰² Lanes described from left to right: 1 - Novex Sharp Pre-Stained Protein Standard; 2 - sample covering 55 to 65 mL elution volume; 3 - 50% sample covering 55 to 65 mL elution volume in dH₂O. Protein ladder has been annotated by molecular weight of bands in kDa. Only relevant areas of gel depicted. PAGE conducted as per Section 2.5.1.

4.0 Reaction Optimisation

4.1 Introduction

It was decided that activity tests for all enzymes of the present study should be conducted in identical conditions, as the ultimate goal of providing a ‘one-pot’ system would require this manner of function. This decision also provided a means to limit the scope of the project to one suitable for the timeframe provided. For each protein for which the purification was described in *Section 3.0*, relevant literature was analysed to determine a starting point from which the optimisation of reaction could proceed (*Table 4.1*). A reaction buffer composition of 50 mM Tris-HCl, 5 mM MgCl₂, 100 mM KCl, at pH 7.5 was selected. A reaction temperature of 37 °C was selected for a reaction duration of 30 minutes, to maintain the feasibility of processing the large volume of samples required for reaction optimisation.

All buffers used are described in *Section 2.1.6*.

Reference	Enzyme	Buffer	Buffer Conc.	pH	MgCl ₂ Conc.	KCl Conc.	Temperature
Van Rompay et al., 2001 ⁶⁰	UCK	Tris-HCl	50 mM	7.6	5 mM	N/A	37 °C
Lossani et al., 2009 ¹⁰³	UCK	Tris-HCl	50 mM	7.5	2.4 mM	N/A	37 °C
Saint Girons et al., 1987 ¹⁰⁴	ADK	Tris-HCl	50 mM	7.4	2 mM	100 mM	27 °C
Huss & Glaser, 1983 ¹⁰⁵	ADK	Tris-HCl	100 mM	7.5	10 mM	100 mM	25 °C
Xu et al., 2008 ¹⁰⁶	CMPK	Tris-HCl	50 mM	8	0.5 mM	N/A	37 °C
Hsu et al., 2005 ¹⁰⁷	CMPK	Tris-HCl	50 mM	7.5	0 - 8 mM	N/A	37 °C
Agarwal et al., 1978 ⁶⁷	GUK	Tris-HCl	100 mM	7.5	10 mM	100 mM	30 °C
Hall & Kühn., 1986 ¹⁰⁸	GUK	Tris-HCl	50 mM	8	10 mM	250 mM	30 °C

Table 4.1: Literature analysis of reaction conditions for nucleoside kinase catalytic activity.

4.2 Standards

Individual standards of the various components of the rNK-catalysed reactions to be described in the present section were analysed via ³¹P NMR to facilitate the attribution of peaks to these components in an NMR spectrum of the reaction. Standards containing various relevant combinations of these components were also analysed in this manner, to further facilitate peak attribution.

4.2.1 Adenosine Triphosphate

A 25 mM ATP solution in rNK reaction buffer, 5% D₂O, was analysed (*Figure 4.*). There are three significant peaks that exist in a ³¹P NMR spectrum of ATP alone. The triplet that occurs at a chemical shift of approximately -22.0 ppm can be attributed to the phosphorus of the β-phosphate of ATP. The two doublet peaks, with chemical shifts of approximately -11.0 and -10.0 ppm can be attributed to the phosphorus atoms of the α- and γ-phosphate groups respectively. A very small peak can be observed at a chemical shift of approximately 0.5 ppm, this can be attributed to free phosphate in solution as a result of degradation due to the inherent instability of aqueous ATP. The ³¹P NMR signals of the α- and β-phosphate groups of ADP are known to closely mimic those of the α- and γ-phosphate groups of ATP, thus any ADP formed via this degradation would likely be indistinguishable from ATP in solution.¹⁰⁹

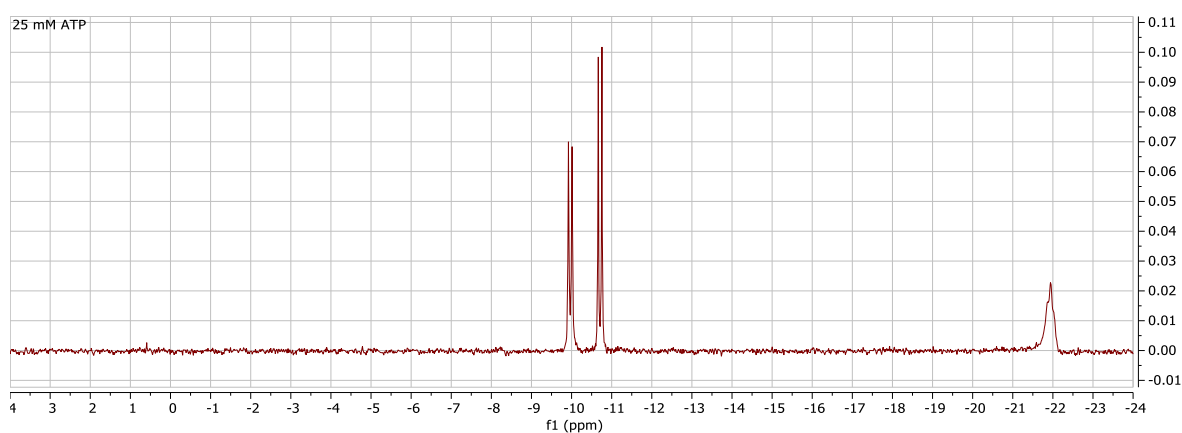


Figure 4.1: ³¹P NMR spectrum derived from 25 mM ATP in rNK reaction buffer, 5% D₂O. NMR analysis conducted as described in Section 2.7.1.2.

4.2.2 Uridine

A 25 mM uridine solution in rNK reaction buffer, 5% D₂O, was analysed (*Figure 4.*). As expected, due to the lack of phosphorus atoms in solution, the ³¹P NMR spectrum contains no observable peaks.

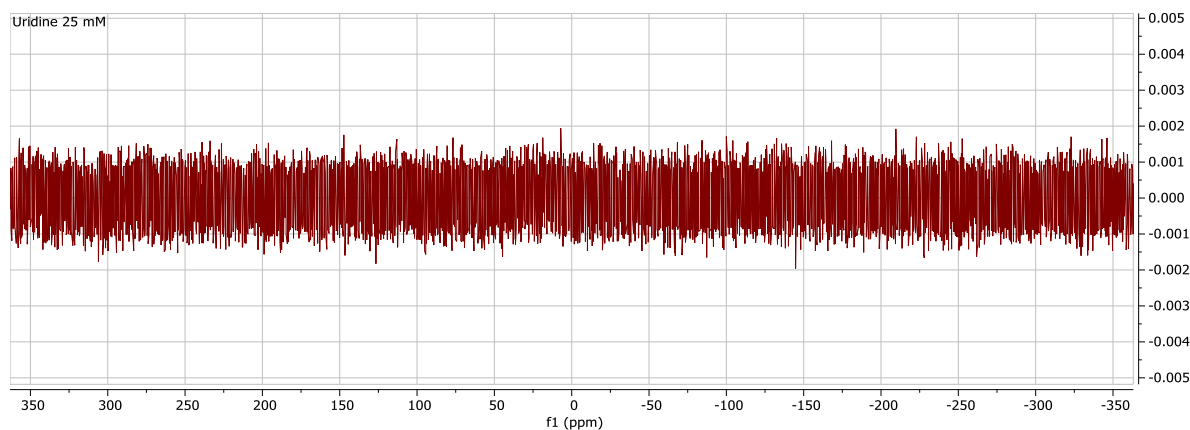


Figure 4.2: ³¹P NMR spectrum derived from 25 mM uridine solution, 5% D₂O. NMR analysis conducted as described in Section 2.7.1.2.

4.2.3 Uridine Monophosphate

A 25 mM UMP solution in rNK reaction buffer, 5% D₂O, was analysed (*Figure 4.3*). The sole observable peak, a singlet at a chemical shift of approximately 4.0 ppm can be attributed to the phosphorus atom in the α -phosphate of UMP.

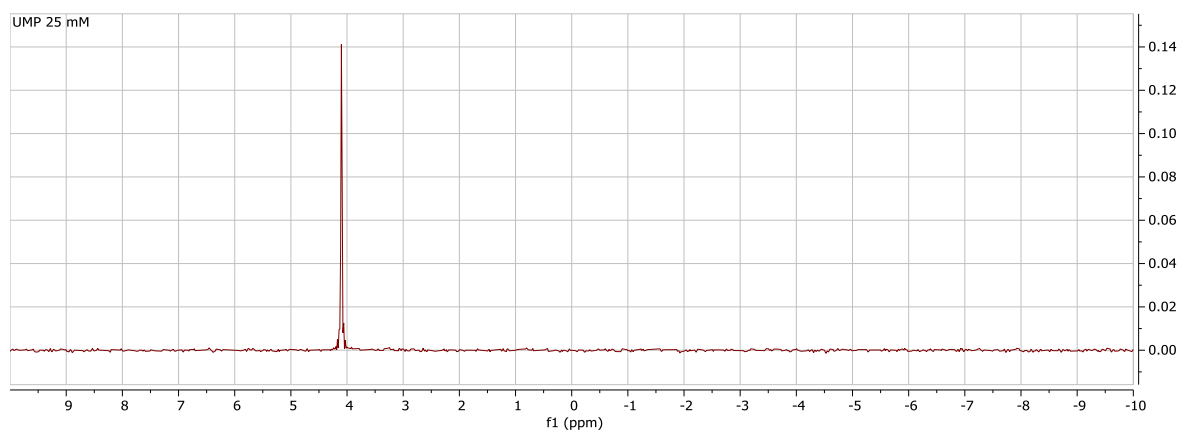


Figure 4.3: ³¹P NMR spectrum derived from 25 mM UMP in rNK reaction buffer, 5% D₂O. NMR analysis conducted as described in Section 2.7.1.2.

4.2.4 Adenosine Monophosphate

A 25 mM AMP solution in rNK reaction buffer, 5% D₂O, was analysed (*Figure 4.4*). The sole observable peak, a singlet at a chemical shift of approximately 1.2 ppm can be attributed to the phosphorus atom within the 5'-phosphate group of AMP.

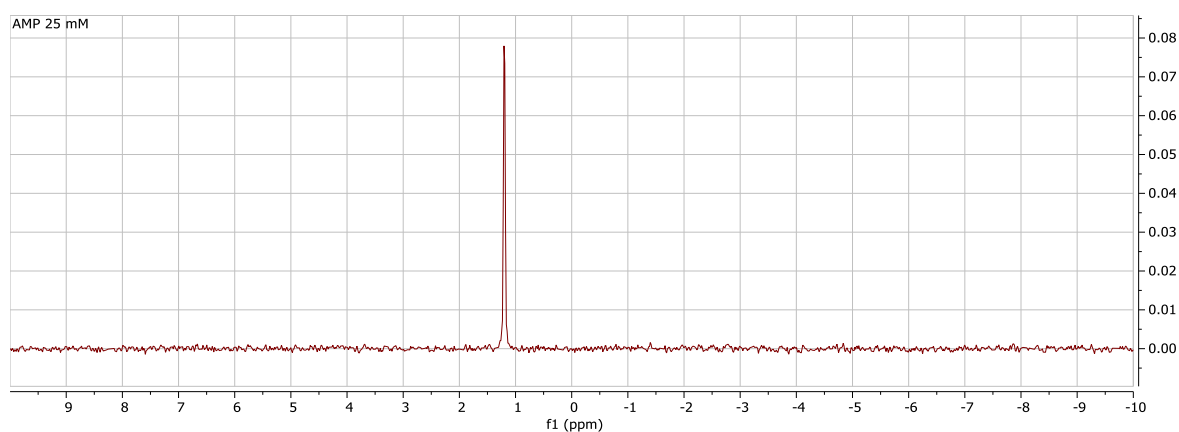


Figure 4.4: ³¹P NMR spectrum derived from 25 mM AMP in rNK reaction buffer, 5% D₂O. NMR analysis conducted as described in Section 2.7.1.2.

4.2.5 Adenosine Diphosphate

A 25 mM ADP solution in rNK reaction buffer, 5% D₂O, was analysed (*Figure 4.5*). Two doublet peaks can be observed, occurring at chemical shifts of -10.7 ppm and -10.1 ppm. These peaks can be attributed to the phosphorus atoms of the α - and β - phosphates of ADP respectively.

The peaks observed at chemical shifts of approximately 0.6 and 0.8 ppm can likely be attributed to free phosphate and AMP respectively, both produced as a result of ADP degradation.

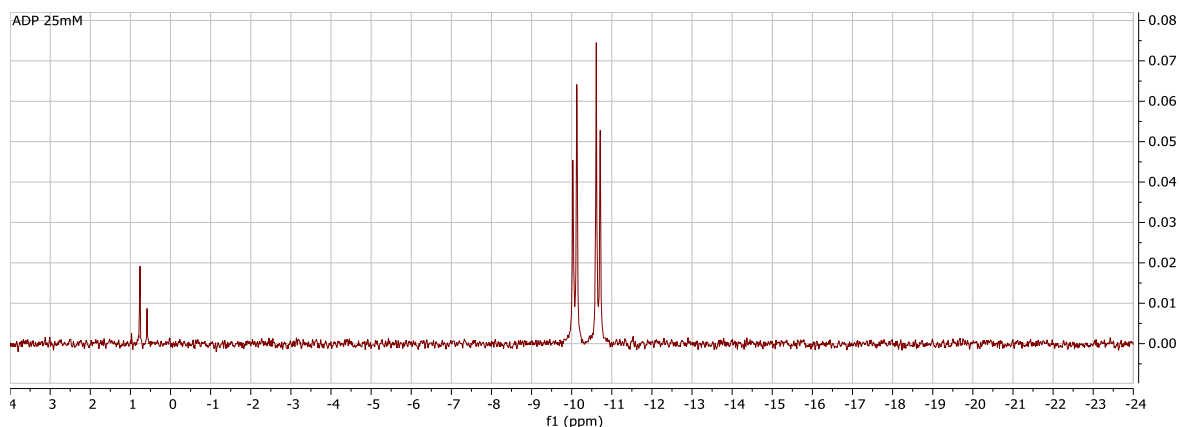


Figure 4.5: ³¹P NMR spectrum derived from 25 mM ADP in rNK reaction buffer, 5% D₂O. NMR analysis conducted as described in Section 2.7.1.2.

4.2.6 Phosphoenolpyruvate

A 137.5 mM PEP solution in rNK reaction buffer, 5% D₂O, was analysed (*Figure 4.6*). The sole observable peak, a singlet at a chemical shift of approximately -4.0 ppm can be attributed to the phosphorus atom within the phosphate group of PEP.

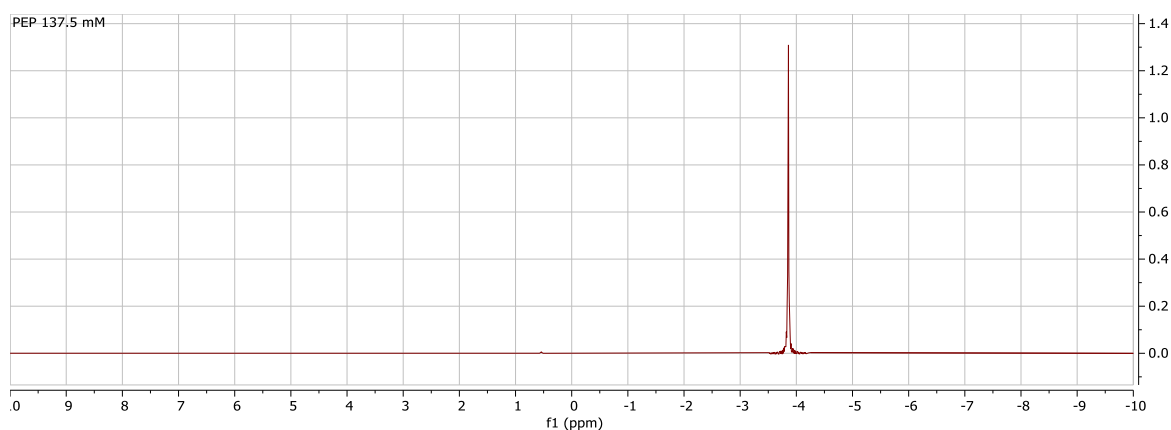


Figure 4.6: ³¹P NMR spectrum derived from 137.5 mM PEP in rNK reaction buffer, 5% D₂O. NMR analysis conducted as described in Section 2.7.1.2.

4.2.7 Mixed Standards

A standard containing all non-protein components of a typical reaction mixture in rNK reaction buffer, 5% D₂O, was analysed (*Figure 4.7*). This included uridine (12.5 mM), PEP (13.75 mM), and ATP (2.5 mM). The presence of PEP in solution is detected through the peak at a chemical shift of approximately -4.0 ppm. The doublet peaks observed at chemical shifts of approximately -11.0 and -10.0 ppm can be attributed to the α - and γ -phosphate groups of ATP respectively, while the small peak observed at a chemical shift of approximately -22.0 ppm can be attributed to the β -phosphate of ATP. These peak attributions are supported by those observed in *Section 4.2.1* and *Section 4.2.6*.

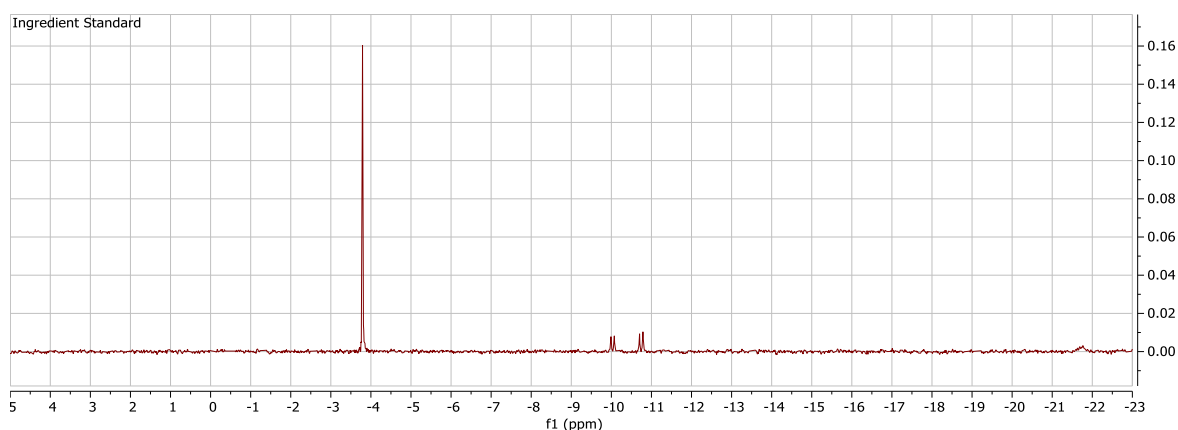


Figure 4.7: ³¹P NMR spectrum derived from 12.5 mM uridine, 13.75 mM PEP, 2.5 mM ATP in rNK reaction buffer, 5% D₂O. NMR analysis conducted as described in *Section 2.7.1.2*.

To simulate conversion of uridine to UMP, a standard containing uridine (25 mM), UMP (25 mM), PEP (25 mM), and ATP (25 mM) in rNK reaction buffer, 5% D₂O, was analysed (*Figure 4.8*). The peaks at chemical shifts of -10.7, -21.9, and -9.9 ppm can be attributed to the α -, β -, and γ -phosphate groups of ATP respectively. The peak observed at a chemical shift of -3.7 ppm can be attributed to the phosphate group of PEP. The peak observed at a chemical shift of 0.7 ppm can be attributed to the phosphate group of UMP. These peak attributions are supported by those observed in *Section 4.2.1*, *Section 4.2.3*, and *Section 4.2.6*.

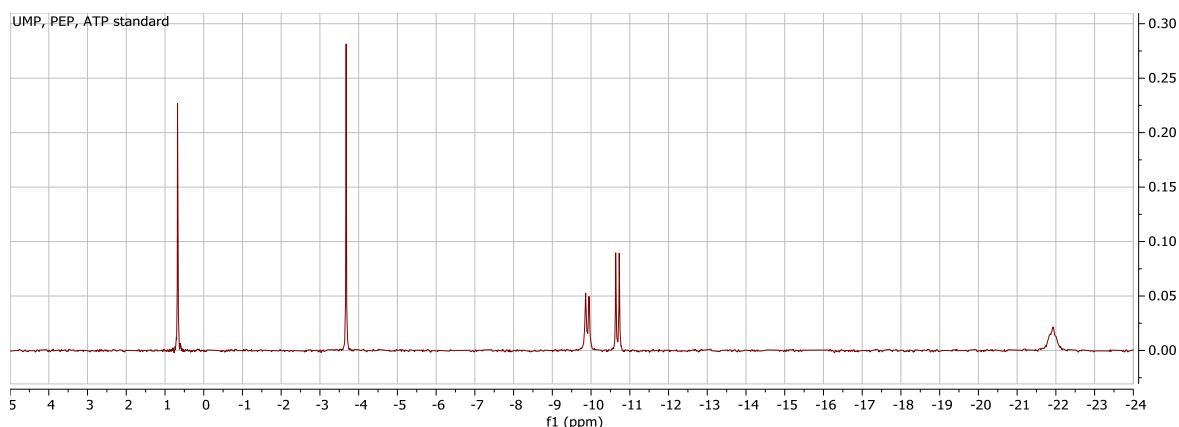


Figure 4.8: ^{31}P NMR spectrum derived from 25 mM UMP, 25 mM PEP, 25 mM ATP in rNK reaction buffer, 5% D_2O . NMR analysis conducted as described in Section 2.7.1.2.

4.2.8 Heat Study

In order to assess whether the heating process involved in the presently discussed reaction process would affect the observable peaks in ^{31}P NMR spectra, equivalent standards to those previously described were subject to 30 minutes at 37 °C followed by 15 minutes at 70 °C prior to analysis. As can be seen in *Figures 4.9-4.15* the observable peaks in these spectra remained largely similar to those of the samples not exposed to heat, with the exception of the presence of small peak at a chemical shift of approximately 0.6 ppm that existed in all heated samples aside from that of UMP. This peak can be attributed to free phosphate in solution, produced as a result of the heat-mediated degradation of phosphate-containing compounds. This free phosphate peak often exists very close to that of UMP when both compounds exist in solution together, as can be seen in *Figure 4.15*.

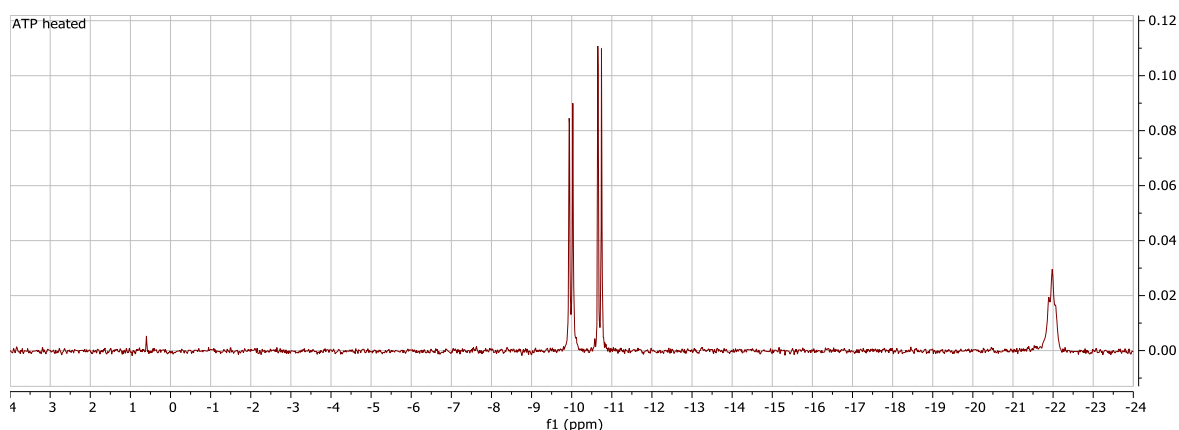


Figure 4.9: ^{31}P NMR spectrum derived from 25 mM ATP in rNK reaction buffer, 5% D_2O . Sample heated as described in Section 4.2.8. NMR analysis conducted as described in Section 2.7.1.2.

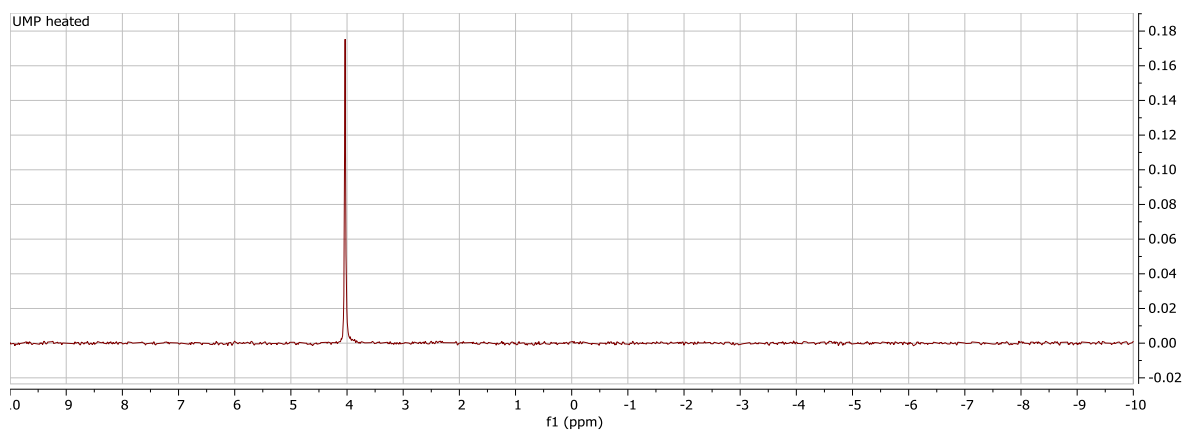


Figure 4.10: ^{31}P NMR spectrum derived from 25 mM UMP in rNK reaction buffer, 5% D_2O . Sample heated as described in Section 4.2.8. NMR analysis conducted as described in Section 2.7.1.2.

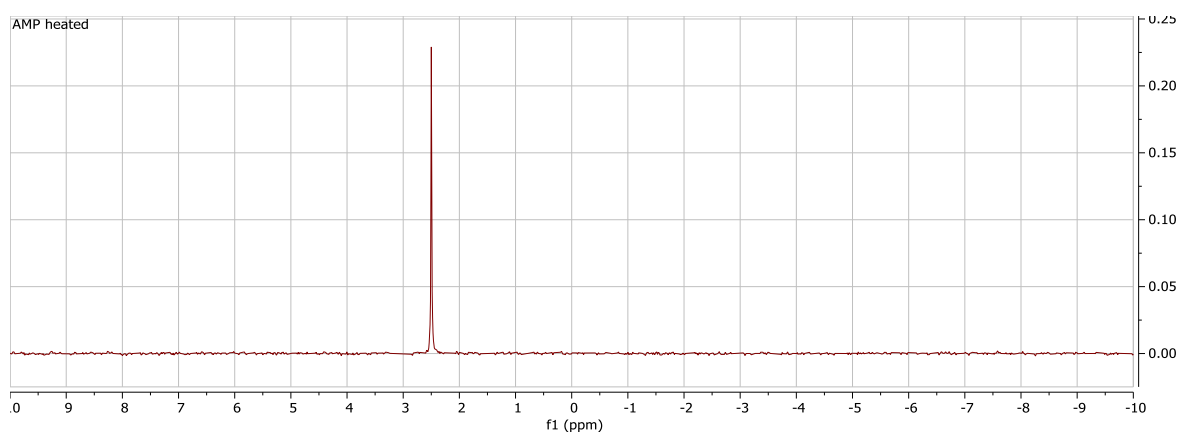


Figure 4.11: ^{31}P NMR spectrum derived from 25 mM AMP in rNK reaction buffer, 5% D_2O . Sample heated as described in Section 4.2.8. NMR analysis conducted as described in Section 2.7.1.2.

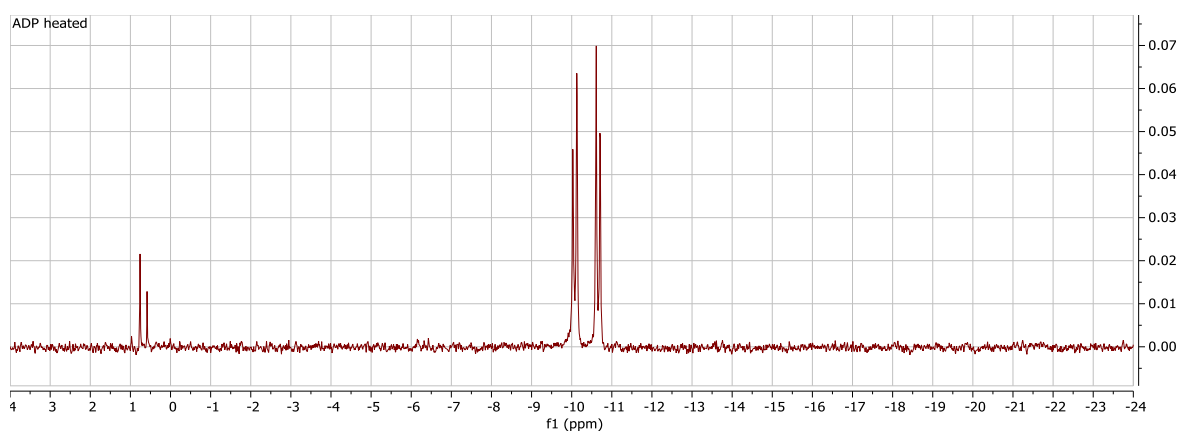


Figure 4.12: ^{31}P NMR spectrum derived from 25 mM ADP in rNK reaction buffer, 5% D_2O . Sample heated as described in Section 4.2.8. NMR analysis conducted as described in Section 2.7.1.2.

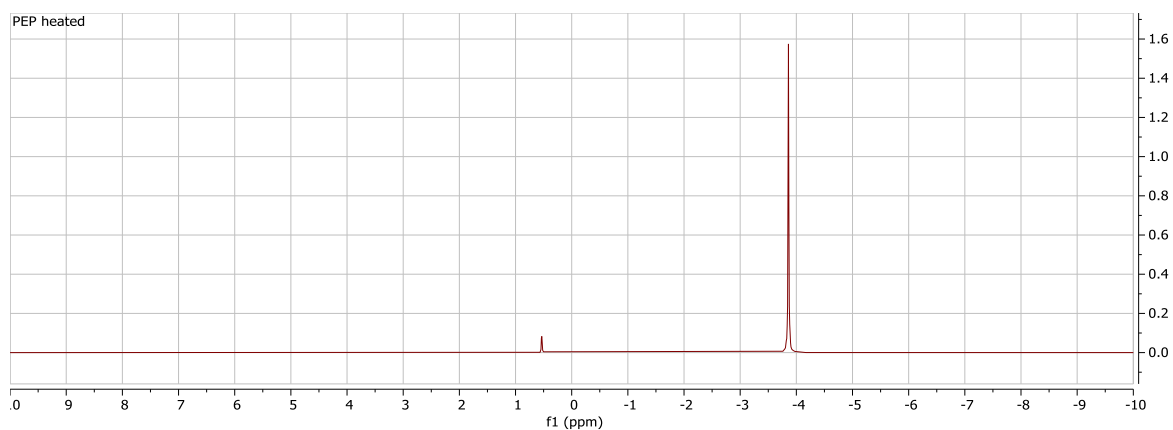


Figure 4.13: ^{31}P NMR spectrum derived from 137.5 mM PEP in rNK reaction buffer, 5% D_2O . Sample heated as described in Section 4.2.8. NMR analysis conducted as described in Section 2.7.1.2.

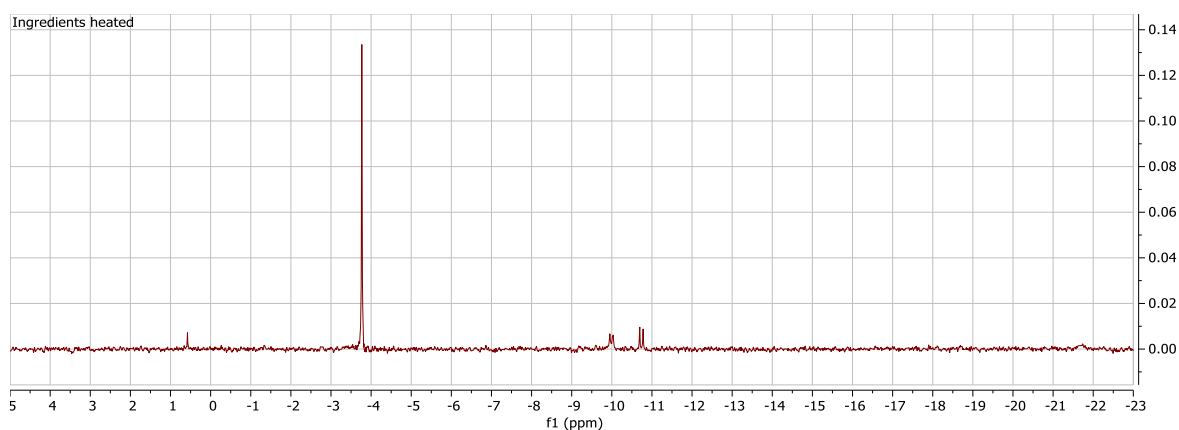


Figure 4.14: ^{31}P NMR spectrum derived from 12.5 mM uridine, 13.75 mM PEP, 2.5 mM ATP in rNK reaction buffer, 5% D_2O . Sample heated as described in Section 4.2.8. NMR analysis conducted as described in Section 2.7.1.2.

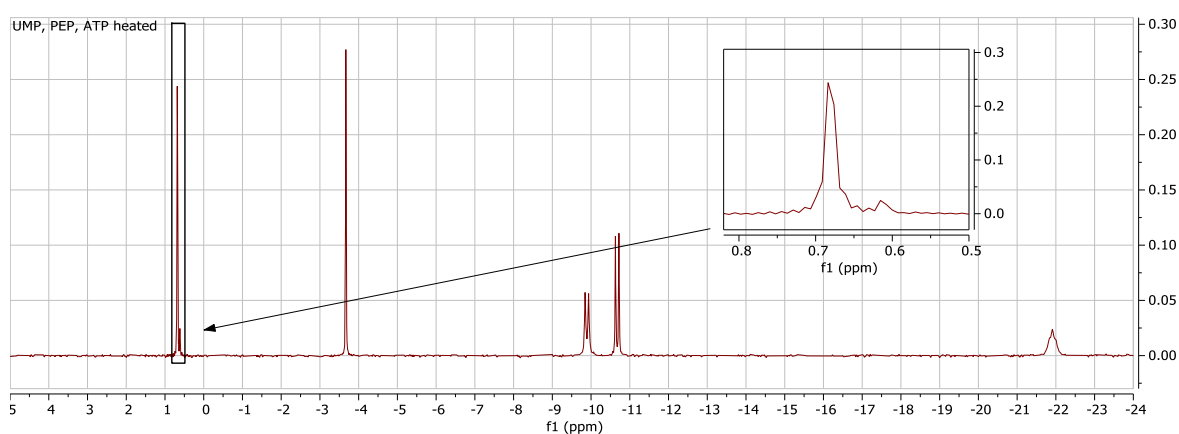


Figure 4.15: ^{31}P NMR spectrum derived from 25 mM UMP, 25 mM PEP, 25 mM ATP in rNK reaction buffer, 5% D_2O . Sample heated as described in Section 4.2.8. NMR analysis conducted as described in Section 2.7.1.2. Zoom region depicts UMP peak and adjacent peak attributed to free phosphate.

4.2.9 pH study

In order to assess how changes in solution pH would affect the appearance of the previously described peaks on a ^{31}P NMR spectrum, a series of standard solutions were produced (UMP 25 mM, PEP 25 mM, ATP 25 mM) with buffer pH ranging from 6.5 to 8.5. These samples were analysed via ^{31}P NMR as described in *Section 2.7.1.2*.

As can be seen in *Figures 4.16-4.18*, decreasing pH results in a reduction in size of the peak attributed to the γ -phosphate of ATP. The peak attributed to the β -phosphate of ATP is more clearly defined as a triplet at pH 6.5 than pH values above this.

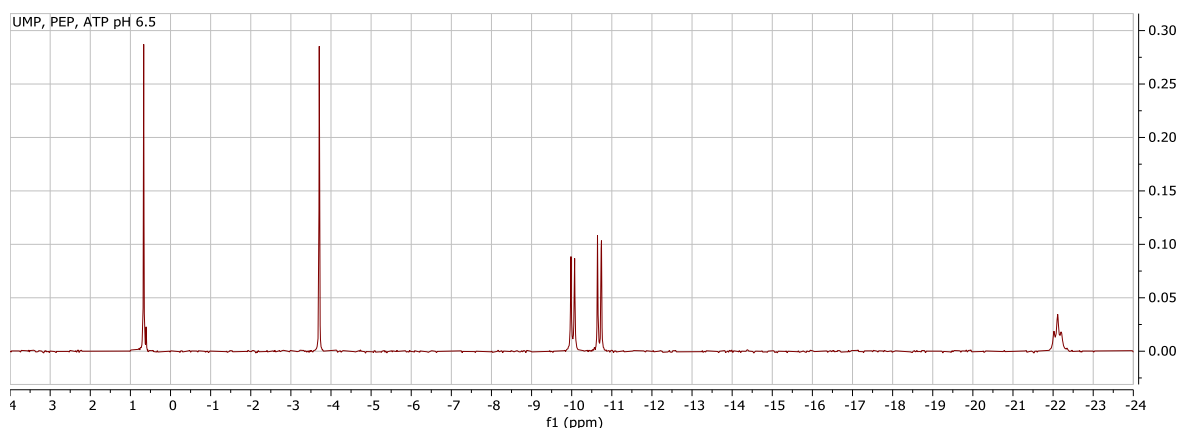


Figure 4.16: ^{31}P NMR spectrum derived from 25 mM UMP, 25 mM PEP, 25 mM ATP in rNK reaction buffer (pH 6.5), 5% D_2O . Sample heated as described in *Section 4.2.8*. NMR analysis conducted as described in *Section 2.7.1.2*.

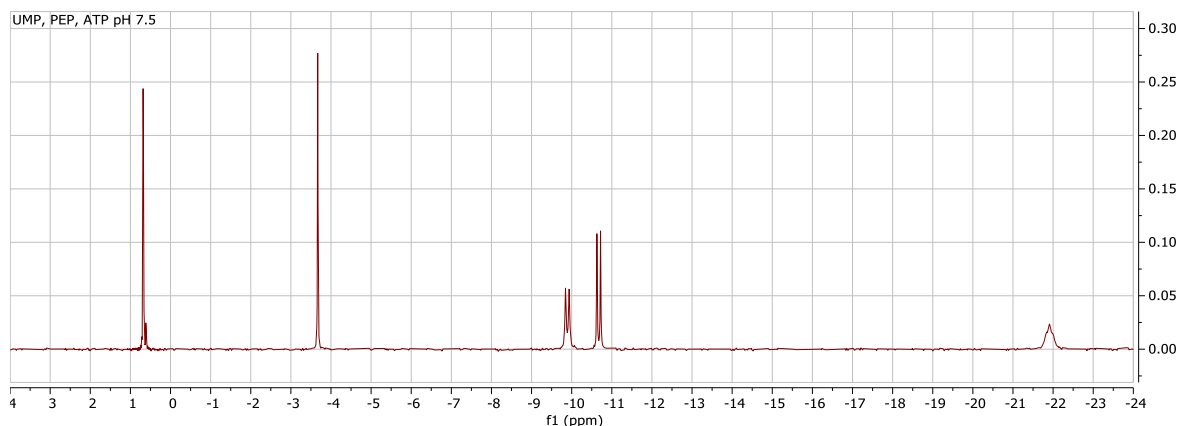


Figure 4.17: ^{31}P NMR spectrum derived from 25 mM UMP, 25 mM PEP, 25 mM ATP in rNK reaction buffer (pH 7.5), 5% D_2O . Sample heated as described in *Section 4.2.8*. NMR analysis conducted as described in *Section 2.7.1.2*.

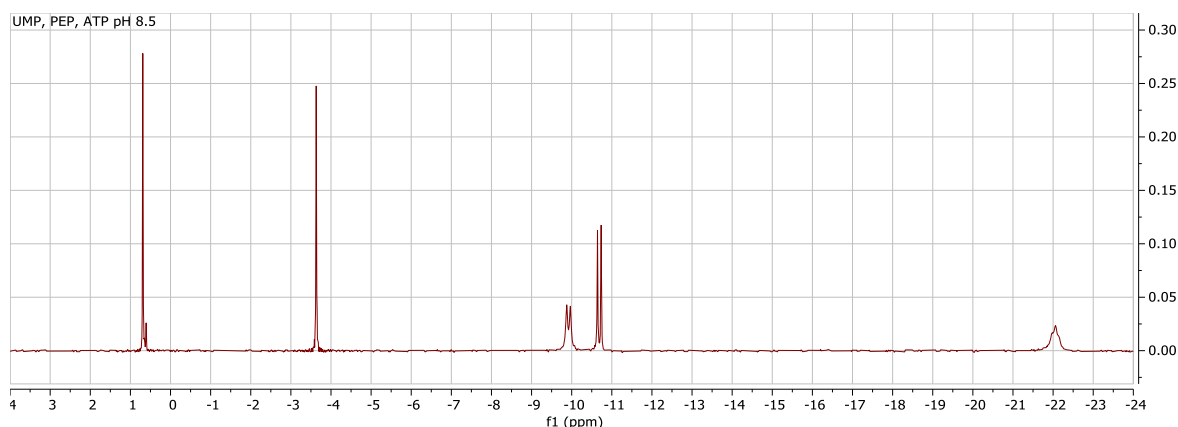


Figure 4.18: ^{31}P NMR spectrum derived from 25 mM UMP, 25 mM PEP, 25 mM ATP in rNK reaction buffer (pH 8.5), 5% D_2O . Sample heated as described in Section 4.2.8. NMR analysis conducted as described in Section 2.7.1.2.

4.3 Confirmation of Enzymatic Activity

The identification of phosphorylative activity from the purified enzyme samples described in Section 3.0 was achieved using ^{31}P NMR analysis of reaction mixtures. For each enzyme both a reaction and negative control sample were generated, visual assessment of these spectra was used with significant differences between reaction and control samples being considered indicative of activity.

As previously described in Section 1.6.2 the inclusion of PK in a nucleoside kinase reaction mixture provides ATP regeneration, allowing the reduction of initial ATP concentration thus mitigating the interference of ATP-derived ^{31}P peaks with detection of enzymatic activity.⁸³ Due to supply chain issues caused by the Covid-19 pandemic, access to PK for the purposes of the present study was significantly delayed. Due to this, initial attempts at confirming enzymatic activity did not involve PK.

4.3.1 ADK

The assessment of *EcADK* activity, as purified in Section 3.5.2, was attempted using a reaction mixture comprising 25 mM AMP, 25 mM ATP, and 1 mg *EcADK* which had catalytic activity induced and was processed for ^{31}P NMR analysis as described in Section 2.6.1 and Section 2.7.1.2 respectively. A negative control identical except lacking *EcADK* addition was also generated in the same manner.

As can be seen in Figure 4.19 and Figure 4.20 the reaction sample features a novel doublet peak at an approximate chemical shift of -10 ppm, this can likely be attributed to the β -phosphate of ADP produced as a result of *EcADK* catalytic activity. There also seems to be a novel doublet peak occurring at an approximate chemical shift of -10.6 ppm that is overlapping with the doublet at that position observed in the control sample, depicted in a clearer manner in *Error! Reference source not found.*. This novel peak can likely be attributed to the α -phosphate of ADP.

The presence of these novel peaks indicates that ADP is present in the reaction sample, consistent with catalytic activity of *Ec*ADK. The overlap of ATP and ADP-related peaks and strong ATP signal make drawing firm conclusions as to this difficult, however.

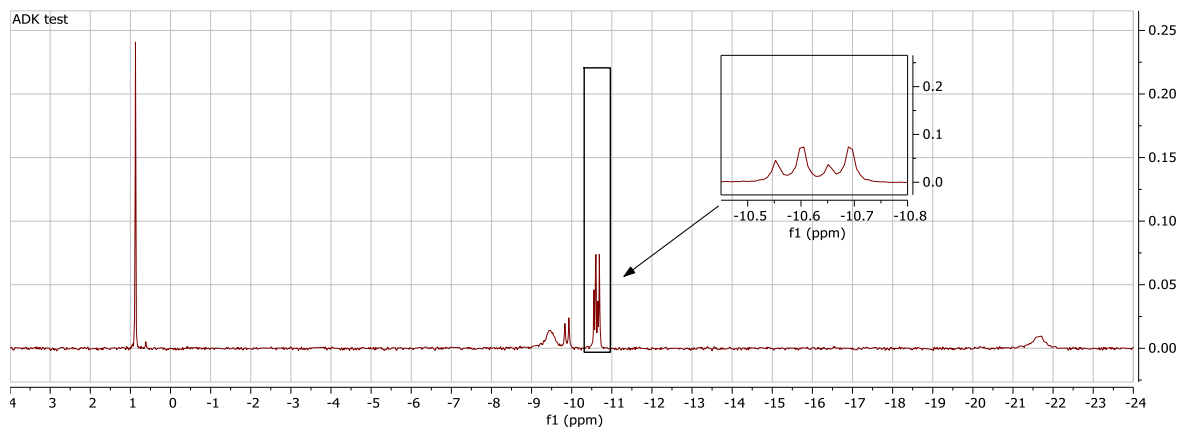


Figure 4.19: ^{31}P NMR spectrum derived from ADK activity test reaction sample. Reaction conducted as described in Section 2.6.1. NMR analysis conducted as described in Section 2.7.1.2. Zoom region depicts overlapping doublet peaks at -10.6 ppm.

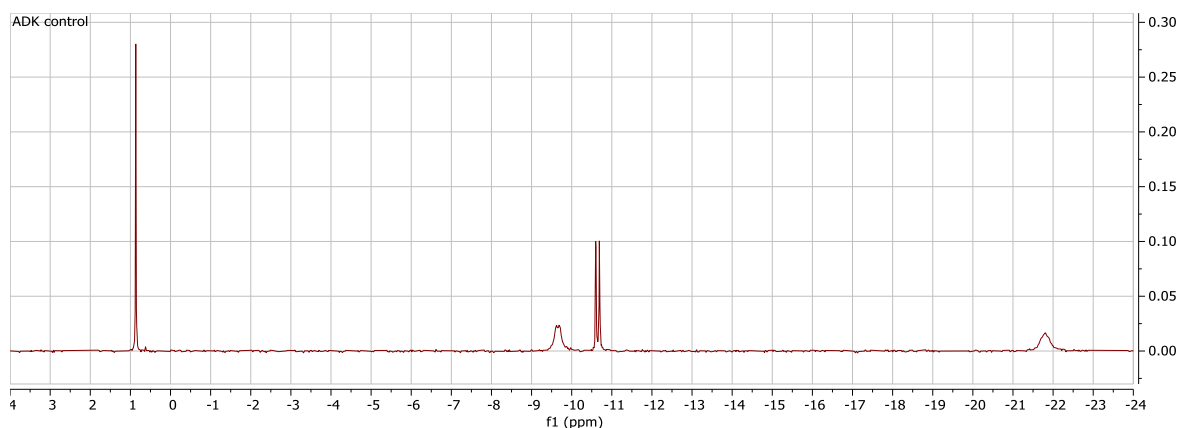


Figure 4.20: ^{31}P NMR spectrum derived from ADK activity test negative control sample. Sample heated as described in Section 4.2.8. NMR analysis conducted as described in Section 2.7.1.2.

4.3.2 GUK

Initial attempts at the assessment of *Pf*GUK activity used GMP as substrate, given the much greater affinity that the enzyme possesses for GMP over AMP.¹⁰¹ However addition of $10 \times$ GMP stock solution to the reaction mixture resulted in the formation of a gel-like substance (Figure 4.21) which prevented ^{31}P NMR analysis of the mixture. The self-assembly of guanosine nucleotides into gels has, in the presence of K^+ ions, been previously reported in the literature.^{110, 111} Given this it was decided to utilise AMP as substrate for these experiments.



Figure 4.21: Image of *Pf*GUK reaction mixture approximately two minutes following the addition of GMP. Gel-like substance can be seen having settled just below the solution meniscus.

The assessment of *Pf*GUK activity, as purified in *Section 3.6.2*, was attempted using a reaction mixture comprising 25 mM AMP, 25 mM ATP, and 1 mg *Pf*GUK which had catalytic activity induced and was processed for ^{31}P NMR analysis as described in *Section 2.6.1* and *Section 2.7.1.2* respectively. A negative control identical except lacking *Pf*GUK addition was also generated in the same manner.

As can be seen in *Figure 4.22* and *Figure 4.23* there is no significant visual difference between the spectra of the reaction and control samples. As the expected product compound is ADP, this may be due to overlap of the signals derived from the α - and γ -phosphate groups of ATP with those of the phosphate groups of ADP. ATP is at equal concentration to substrate in solution, as necessary for it to be a non-limiting factor in the reaction, thus the interfering effect of any potential overlap is magnified. Due to this potential overlap the lack of difference here cannot be used to infer a lack of catalytic activity by *Pf*GUK.

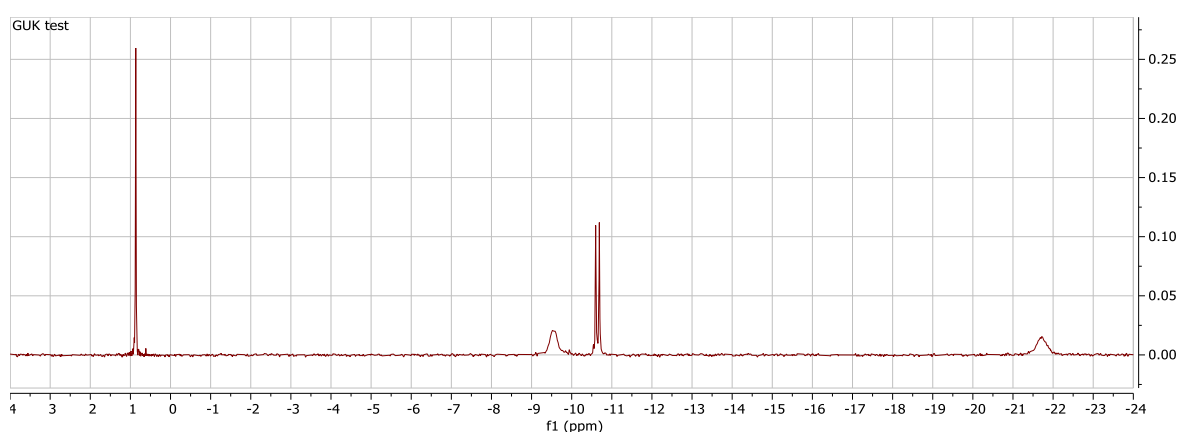


Figure 4.22: ^{31}P NMR spectrum derived from GUK activity test reaction sample. Reaction conducted as described in *Section 2.6.1*. NMR analysis conducted as described in *Section 2.7.1.2*.

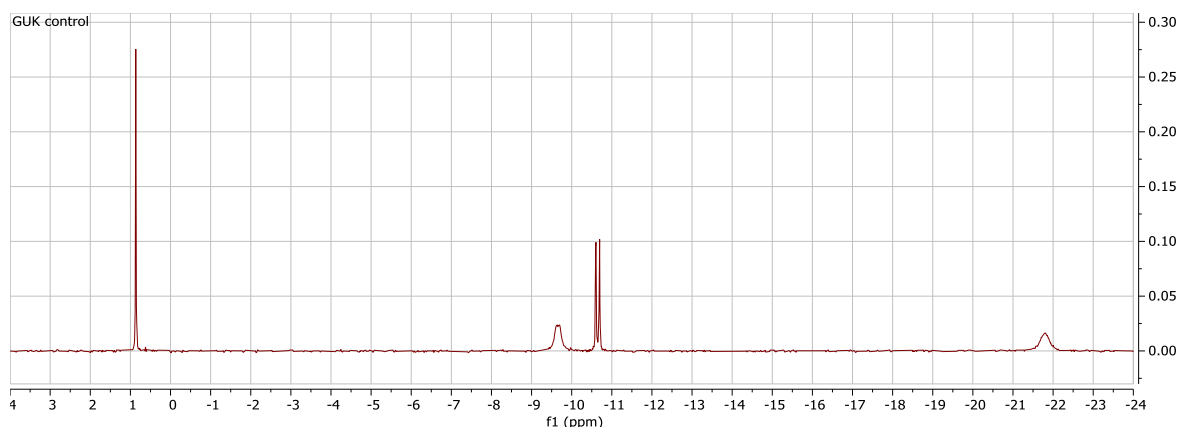


Figure 4.23: ^{31}P NMR spectrum derived from GUK activity test negative control sample. Sample heated as described in Section 4.2.8. NMR analysis conducted as described in Section 2.7.1.2.

4.3.3 UCK1

The assessment of human UCK1 activity, as purified in Section 3.3.2, was attempted using a reaction mixture comprising 25 mM uridine, 25 mM ATP, and 1 mg UCK1 which had catalytic activity induced and was processed for ^{31}P NMR analysis as described in Section 2.6.1 and Section 2.7.1.2 respectively. A negative control identical except lacking UCK1 addition was also generated in the same manner.

As can be seen in Figure 4.24 and Figure 4.25 there is no significant visual difference between the spectra of the reaction and control samples. Although the expected product compound is UMP thus the ^{31}P NMR peak derived from this would be distinct from those of the phosphate groups of ATP, the strong signals derived from the phosphate groups of ATP may still be interfering with the ability to detect lower levels of UMP production. Due to this potential interference the lack of difference here cannot be used to infer a lack of catalytic activity by UCK1.

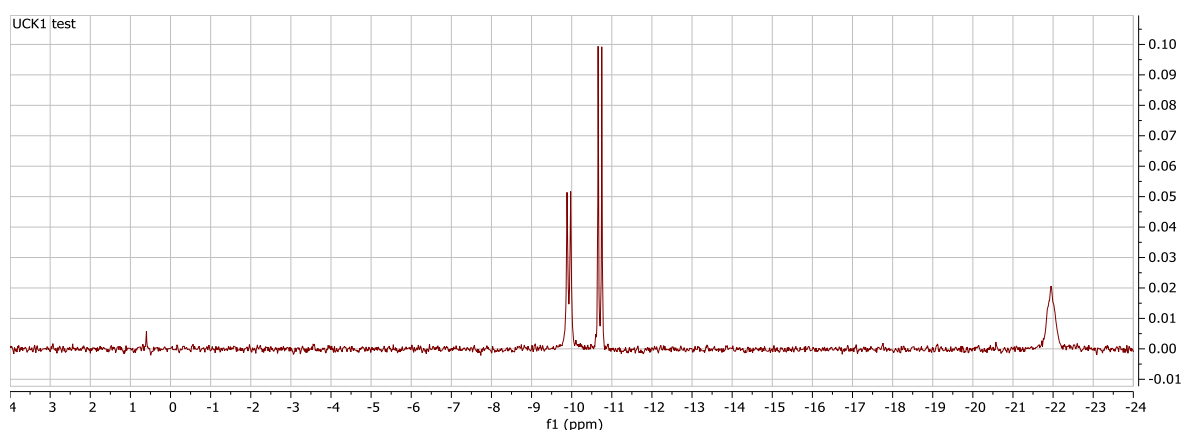


Figure 4.24: ^{31}P NMR spectrum derived from UCK1 activity test reaction sample. Reaction conducted as described in Section 2.6.1. NMR analysis conducted as described in Section 2.7.1.2.

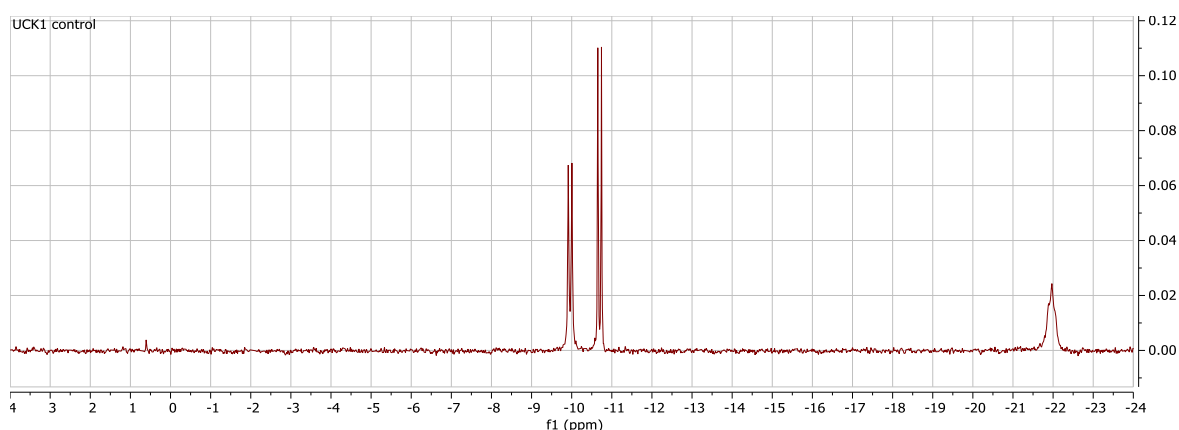


Figure 4.25: ^{31}P NMR spectrum derived from UCK1 activity test negative control sample. Sample heated as described in Section 4.2.8. NMR analysis conducted as described in Section 2.7.1.2.

4.3.4 UCK2 (FLAG-tag)

The assessment of human UCK2 (FLAG-tag) activity, as purified in Section 3.4.1.2, was attempted using a reaction mixture comprising 25 mM uridine, 25 mM ATP, and 1 mg UCK2 which had catalytic activity induced and was processed for ^{31}P NMR analysis as described in Section 2.6.1 and Section 2.7.1.2 respectively. A negative control identical except lacking UCK2 addition was also generated in the same manner.

As can be seen in Figure 4.26 and Figure 4.27 there is no significant visual difference between the spectra of the reaction and control samples. Although the expected product compound is UMP thus the ^{31}P NMR peak derived from this would be distinct from those of the phosphate groups of ATP, the strong signals derived from the phosphate groups of ATP may still be interfering with the ability to detect lower levels of UMP production. Due to this potential interference the lack of difference here cannot be used to infer a lack of catalytic activity by UCK2.

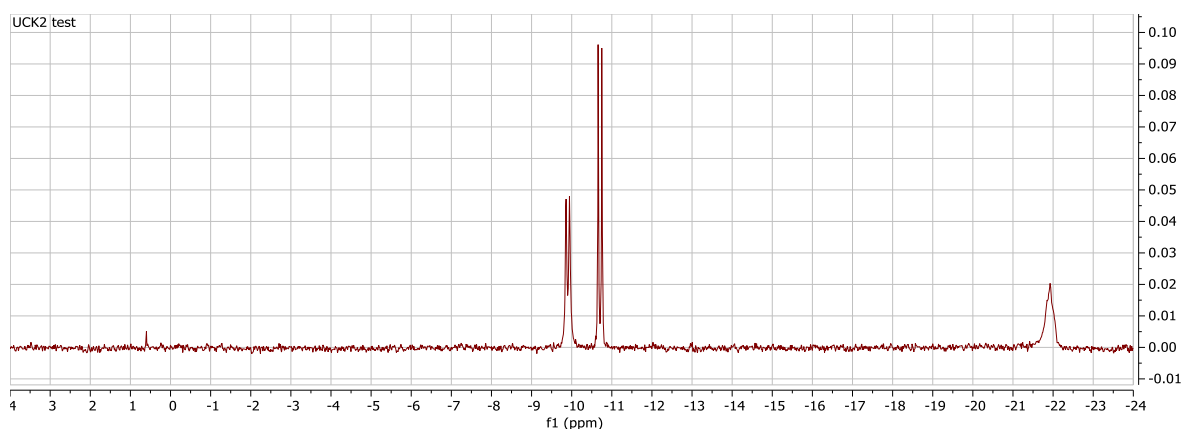


Figure 4.26: ^{31}P NMR spectrum derived from UCK2 (FLAG-tag) activity test reaction sample. Reaction conducted as described in Section 2.6.1. NMR analysis conducted as described in Section 2.7.1.2.

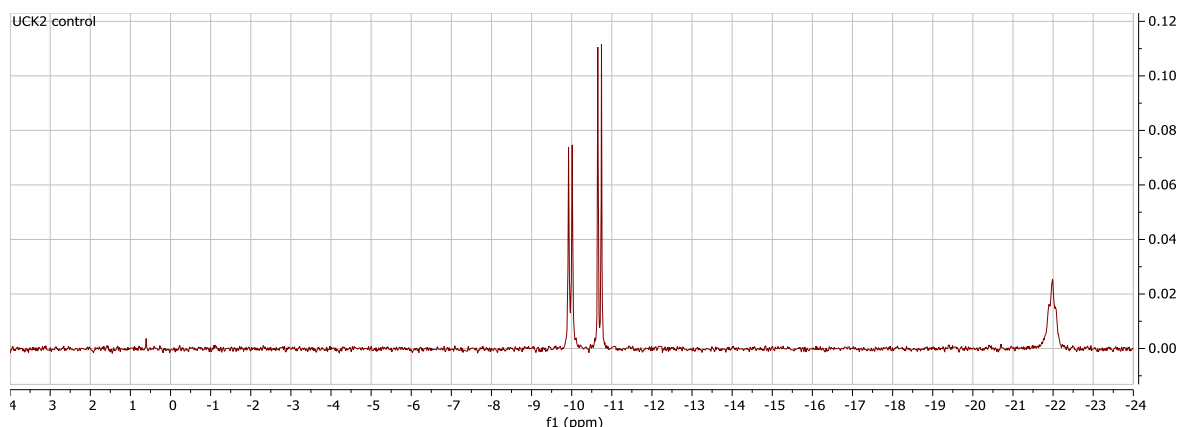


Figure 4.27: ^{31}P NMR spectrum derived from UCK2 (FLAG-tag) activity test negative control sample. Sample heated as described in Section 4.2.8. NMR analysis conducted as described in Section 2.7.1.2.

4.3.5 CMPK (FLAG-tag)

The assessment of human CMPK (FLAG-tag) activity, as purified in Section 3.7.1.2, was attempted using a reaction mixture comprising 25 mM UMP, 25 mM ATP, and 1 mg CMPK which had catalytic activity induced and was processed for ^{31}P NMR analysis as described in Section 2.6.1 and Section 2.7.1.2 respectively. A negative control identical except lacking CMPK addition was also generated in the same manner.

As can be seen in Figure 4.28 and Figure 4.29 the only significant difference in the spectra of the reaction and control samples is the presence of a novel peak at an approximate chemical shift of 1.5 ppm in the reaction sample. Based on the various nucleoside diphosphate spectra studied in Section 4.2 this peak does not seem to relate to the presence of the target product compound uridine diphosphate (UDP).

As the expected product compound is UDP, the lack of observation of product-related peaks is likely due to overlap of the signals derived from the α - and γ -phosphate groups of ATP with those of the phosphate groups of UDP. ATP is at equal concentration to substrate in solution, as necessary for it to be a non-limiting factor in the reaction, thus the interfering effect of any potential overlap is magnified. Due to this potential overlap the lack of difference here cannot be used to infer a lack of catalytic activity by CMPK.

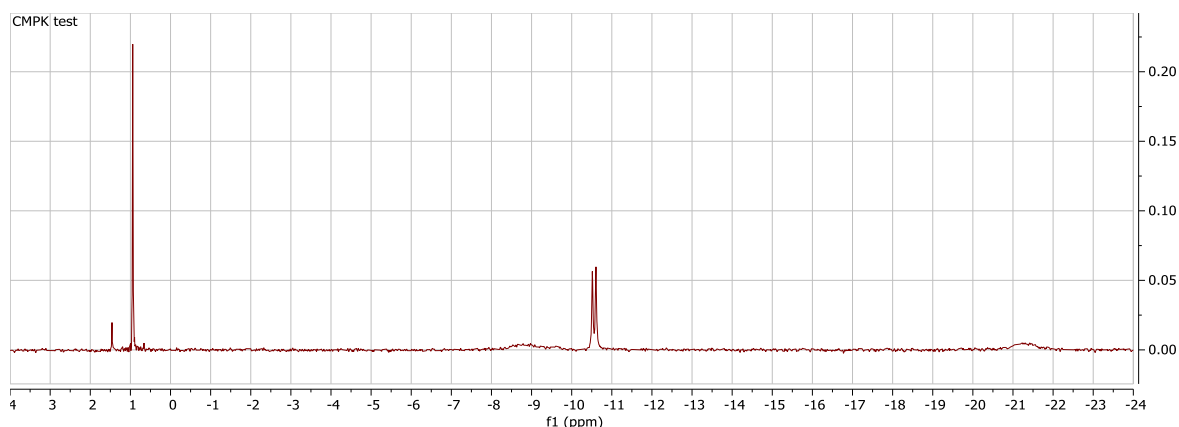


Figure 4.28: ^{31}P NMR spectrum derived from CMPK (FLAG-tag) activity test reaction sample. Reaction conducted as described in Section 2.6.1. NMR analysis conducted as described in Section 2.7.1.2.

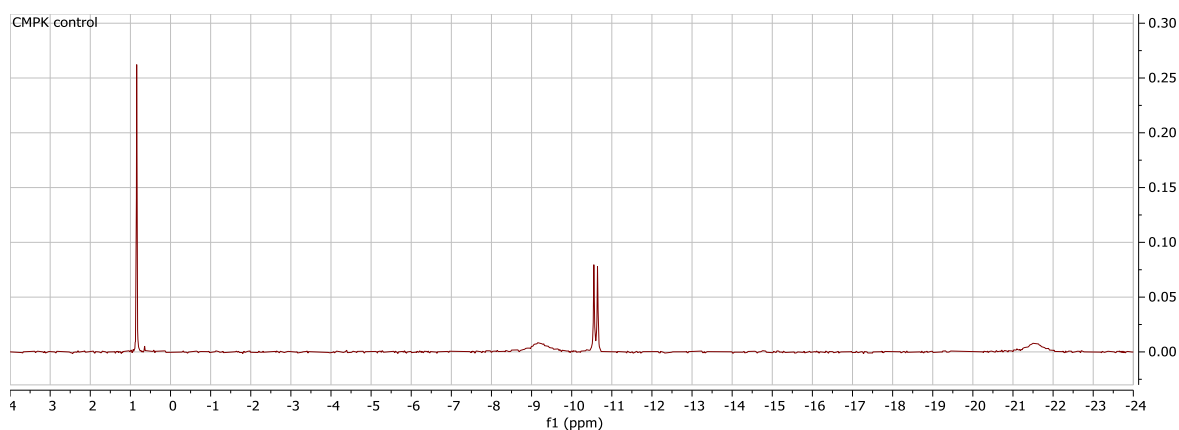


Figure 4.29: ^{31}P NMR spectrum derived from CMPK (FLAG-tag) activity test negative control sample. Sample heated as described in Section 4.2.8. NMR analysis conducted as described in Section 2.7.1.2.

4.4 Optimisation of Component Concentration

Given the lack of access to PK and the failure to identify enzymatic activity in the previously described experiments, further studies focused on the development of a reaction system that would allow the identification of rNK activity via ^{31}P NMR spectroscopy. As the intended eventual target substrates for activity testing were largely pyrimidine nucleosides, a methodology for the purification of UCK1 with good yields had been established, and uridine was accessible in plentiful amounts, the UCK1-catalysed uridine to UMP reaction was chosen as the basis for this reaction system.

In order to assess whether the concentration of substrate and phosphate donor in solution was a limiting factor in the identification of UCK1 phosphorylative activity in the absence of PK, a series of reactions at a range of component concentrations were conducted. For each reaction the concentration of substrate

(uridine) and phosphate donor (ATP) in solution was stoichiometrically equivalent, ranging from 5 mM to 50 mM. 0.125 mg of UCK1 was used in each sample. These reactions were compared to control reactions, which lacked substrate.

In order to comparatively assess the ^{31}P spectra the integrals of each peak were normalised to the peak attributed to β -phosphate of ATP, as visual observation indicated that this peak was the most consistent in size across the spectra.

As can be seen in *Table 4.2* in all samples of the present experiment no peak was identified that could be attributed to UMP, implying a lack of detectable enzymatic action at all component concentration levels. A consistent trend can be seen in that the size of the peak attributed to the α -phosphate of ATP is proportionally larger compared to other ATP-associated peaks at lower component concentrations. Data from the reaction and control samples with 5 mM component concentrations is not included in *Table 4.2* as the baseline noise of those spectra was too great for reasonable analysis to occur.

The lack of observable UMP production indicates that the concentration of reaction components in solution is not a significant limiting factor in the detection of UCK1 phosphorylative activity via ^{31}P NMR in the absence of PK.

Component Conc.	Sample	Peak No.	Attribution	Range	Integral (Normalised)
12.5 mM	Reaction	1	Free phosphate	0.64 ... 0.59	0.043
		2	ATP (γ)	-9.58 ... -9.82	0.960
		3	ATP (α)	-10.56 ... -10.80	1.449
		4	ATP (β)	-21.63 ... -22.03	1.000
	Control	1	Free phosphate	0.64 ... 0.59	0.037
		2	ATP (γ)	-9.61 ... -9.85	1.043
		3	ATP (α)	-10.56 ... -10.80	1.484
		4	ATP (β)	-21.62 ... -22.02	1.000
25 mM	Reaction	1	Free phosphate	0.64 ... 0.59	0.022
		2	ATP (γ)	-9.85 ... -10.09	1.034
		3	ATP (α)	-10.58 ... -10.82	1.136
		4	ATP (β)	-21.85 ... -22.25	1.000
	Control	1	Free phosphate	0.64 ... 0.59	0.029
		2	ATP (γ)	-9.88 ... -10.12	1.042
		3	ATP (α)	-10.58 ... -10.82	1.056
		4	ATP (β)	-21.90 ... -22.30	1.000
50 mM	Reaction	1	Free phosphate	0.65 ... 0.59	0.045
		2	ATP (γ)	-9.90 ... -10.14	0.990
		3	ATP (α)	-10.56 ... -10.80	1.019
		4	ATP (β)	-21.90 ... -22.30	1.000
	Control	1	Free phosphate	0.64 ... 0.59	0.032
		2	ATP (γ)	-9.90 ... -10.14	0.989
		3	ATP (α)	-10.54 ... -10.78	0.978
		4	ATP (β)	-21.90 ... -22.30	1.000

Table 4.2: Data from ^{31}P NMR spectra of samples from component concentration study. Peak attributions made as per observations described in Section 4.2. Relevant spectra can be seen in Appendix I.1.

4.5 Reaction Duration Study

In order to assess whether the duration of reaction was a limiting factor in detecting UCK1 activity a series of reactions with durations of heating at 37 °C between 30 and 120 minutes were conducted and analysed via ^{31}P NMR (Table 4.3). These experiments were conducted in rNK reaction buffer, with 15 mM uridine, 15 mM ATP, and 0.125 mg human UCK1. Negative controls consisted of equivalent reaction mixtures with no substrate compound present.

In order to comparatively assess the ^{31}P spectra the integrals of each peak were normalised to the peak attributed to β -phosphate of ATP, as visual observation indicated that this peak was the most consistent in size across the spectra.

As can be seen in Table 4.3, there are no peaks on any spectra that have been attributed to UMP indicating that catalytic activity of UCK1 was not observed. The normalised integral values of all peaks are relatively stable across all samples aside from peak 1, attributed to free phosphate. The normalised integral of this peak appears to vary in a non-consistent nature between reaction and control samples.

The results of this study indicate that the duration of reaction was not a significant limiting factor in the detection of human UCK1 activity via ^{31}P NMR in the absence of PK.

Reaction Duration	Sample	Peak No.	Attribution	Range	Integral (Normalised)
30	Reaction	1	Free phosphate	0.65 ... 0.59	0.031
		2	ATP (γ)	-9.74 ... -10.00	1.039
		3	ATP (α)	-10.56 ... -10.80	1.217
		4	ATP (β)	-21.74 ... -22.14	1.000
	Control	1	Free phosphate	0.65 ... 0.59	0.023
		2	ATP (γ)	-9.74 ... -10.00	1.087
		3	ATP (α)	-10.56 ... -10.80	1.203
		4	ATP (β)	-21.74 ... -22.14	1.000
60	Reaction	1	Free phosphate	0.65 ... 0.59	0.025
		2	ATP (γ)	-9.74 ... -10.00	1.132
		3	ATP (α)	-10.56 ... -10.80	1.292
		4	ATP (β)	-21.74 ... -22.14	1.000
	Control	1	Free phosphate	0.65 ... 0.59	0.037
		2	ATP (γ)	-9.74 ... -10.00	1.073
		3	ATP (α)	-10.56 ... -10.80	1.306
		4	ATP (β)	-21.74 ... -22.14	1.000
90	Reaction	1	Free phosphate	0.65 ... 0.59	0.042
		2	ATP (γ)	-9.74 ... -10.00	1.107
		3	ATP (α)	-10.56 ... -10.80	1.279
		4	ATP (β)	-21.74 ... -22.14	1.000
	Control	1	Free phosphate	0.65 ... 0.59	0.055
		2	ATP (γ)	-9.74 ... -10.00	1.139
		3	ATP (α)	-10.56 ... -10.80	1.301
		4	ATP (β)	-21.74 ... -22.14	1.000
120	Reaction	1	Free phosphate	0.65 ... 0.59	0.042
		2	ATP (γ)	-9.74 ... -10.00	1.128
		3	ATP (α)	-10.56 ... -10.80	1.233
		4	ATP (β)	-21.74 ... -22.14	1.000
	Control	1	Free phosphate	0.62 ... 0.56	0.007
		2	ATP (γ)	-9.64 ... -9.90	1.184
		3	ATP (α)	-10.58 ... -10.82	1.312
		4	ATP (β)	-21.54 ... -21.94	1.000

Table 4.3: Data from ^{31}P NMR spectra of samples from reaction duration study. Peak attributions made as per observations described in Section 4.2. Relevant spectra can be seen in Appendix I.2.

4.6 Substrate Excess Study

In order to assess whether decreasing concentration of ATP relative to that of the substrate donor would facilitate the detection of human UCK1 activity, a series of reactions with increasing ratio of uridine to ATP concentration were conducted and analysed via ^{31}P NMR (Table 4.4). These reactions were conducted in rNK reaction buffer with uridine concentration of 25 mM and 0.125 mg of human UCK1.

ATP concentrations ranged from 10 to 20 mM. Negative controls consisted of equivalent reaction mixtures with no substrate compound present.

In order to comparatively assess the ^{31}P spectra the integrals of each peak were normalised to the peak attributed to β -phosphate of ATP, as visual observation indicated that this peak was the most consistent in size across the spectra.

As can be seen in *Appendix I.3* there were no significant differences in the spectra of the control samples and those with uridine as the substrate across all uridine:ATP concentration ratios. These results indicate that the lowering of phosphate donor concentration relative to substrate concentration does not facilitate the identification of nucleotide kinase enzymatic activity, and that alternate means of mitigating the inhibitory effect of high ATP concentration relative to substrate on detecting such activity via ^{31}P NMR spectra must be sought.

As can be seen in *Table 4.4* in all samples of the present experiment no peak was identified that could be attributed to UMP, implying a lack of visible enzymatic action at all component concentrations. A trend can be seen in that the normalised integral of the peak attributed to the α -phosphate of ATP becomes proportionally larger than those other ATP-associated peaks at lower ATP concentrations, in similarity to what was observed in *Section 4.2*. These results indicate that the ratio of phosphate donor concentration relative to substrate concentration was not a significant limiting factor in the detection of human UCK1 activity via ^{31}P NMR in the absence of PK.

ATP Conc.	Sample	Peak No.	Attribution	Range	Integral (Normalised)
10 mM	Reaction	1	Free phosphate	0.65 ... 0.59	0.056
		2	ATP (γ)	-9.35 ... -9.65	0.866
		3	ATP (α)	-10.55 ... -10.77	1.343
		4	ATP (β)	-21.35 ... -21.95	1.000
	Control	1	Free phosphate	0.65 ... 0.59	0.023
		2	ATP (γ)	-9.45 ... -9.75	0.850
		3	ATP (α)	-10.55 ... -10.77	1.149
		4	ATP (β)	-21.45 ... -22.05	1.000
15 mM	Reaction	1	Free phosphate	0.65 ... 0.59	0.033
		2	ATP (γ)	-9.72 ... -10.02	0.976
		3	ATP (α)	-10.58 ... -10.80	1.097
		4	ATP (β)	-21.65 ... -22.25	1.000
	Control	1	Free phosphate	0.65 ... 0.59	0.037
		2	ATP (γ)	-9.72 ... -10.02	1.024
		3	ATP (α)	-10.59 ... -10.81	1.116
		4	ATP (β)	-21.65 ... -22.25	1.000
20 mM	Reaction	1	Free phosphate	0.65 ... 0.59	0.025
		2	ATP (γ)	-9.80 ... -10.10	1.002
		3	ATP (α)	-10.58 ... -10.80	0.980
		4	ATP (β)	-21.75 ... -22.35	1.000
	Control	1	Free phosphate	0.65 ... 0.59	0.030
		2	ATP (γ)	-9.80 ... -10.10	1.020
		3	ATP (α)	-10.58 ... -10.80	1.029
		4	ATP (β)	-21.75 ... -22.35	1.000

Table 4.4: Data from ^{31}P NMR spectra of samples from substrate excess study. Peak attributions made as per observations described in Section 4.2. Relevant spectra can be seen in Appendix I.3.

4.7 Use of Pyruvate Kinase

Upon the eventual sourcing of PK, the activity of the enzyme and its effect on the rNK reaction mixtures of the present study were assessed. In order to confirm the activity of PK, purified as described in Section 2.4.7, a reaction mixture comprising 13.75 mM ADP, 13.75 mM PEP and 2 mg PK was generated, had catalytic activity induced, and was processed for ^{31}P NMR analysis as described in Section 2.7.1.2. In concert to this, a negative control sample with identical components but lacking PK addition was also processed in this manner.

In order to comparatively assess the ^{31}P spectra of the reaction and control samples the integrals of each peak were normalised to the peak attributed to free phosphate in solution, as visual observation indicated that this peak was the most consistent in size across the spectra.

As can be seen in Figure 4.30, the ^{31}P NMR peak attributed to the phosphate group of PEP is larger in the spectrum relating to the control sample than that of the reaction sample, with normalised integrals of 11.38 and 12.32 respectively. The peaks attributed to the α - and β -phosphates of ADP are also

observed to be larger in the control sample than the reaction sample. In this case the normalised integrals of the α - and β peaks are 11.29 and 10.91 respectively for the control sample and 10.48 and 10.51 respectively for the reaction sample.

The decrease in PEP peak integral size between the control and reaction samples is consistent with conversion of PEP and ADP to ATP and pyruvate, indicating that catalytic action of PK is in fact taking place. The decrease in ADP peak size may also be explainable in this manner, however the similarity in these peaks and those arising from the γ - and α -phosphate groups of ATP means that any ATP produced due to enzymatic activity would contribute to the observed integrals. Without further experiments inference as to how one would expect these peaks to change as ADP levels decrease and ATP levels rise cannot be made.

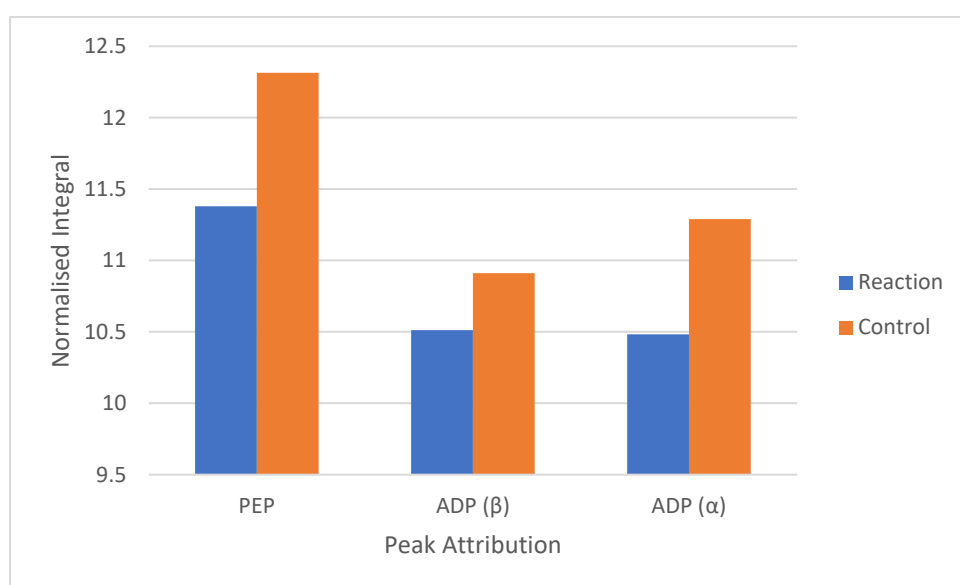


Figure 4.30: Comparative bar graph depicting difference in integrals of relevant peaks between reaction and control sample of PK activity study. Full data described in Table 4.5.

Sample	Peak No.	Attribution	Range	Integral (Normalised)
Reaction	1	AMP	0.77 ... 0.71	0.714
	2	Phosphate	0.61 ... 0.55	1.000
	3	PEP	-3.73 ... -3.82	11.379
	4	ADP (β)	-10.03 ... -10.22	10.512
	5	ADP (α)	-10.60 ... -10.79	10.483
Control	1	AMP	0.76 ... 0.70	0.975
	2	Phosphate	0.61 ... 0.55	1.000
	3	PEP	-3.75 ... -3.84	12.315
	4	ADP (β)	-10.04 ... -10.23	10.912
	5	ADP (α)	-10.60 ... -10.79	11.290

Table 4.5: Data from ^{31}P NMR spectra of samples from PK activity study. Peak attributions made as per observations described in Section 4.2. Relevant spectra can be seen in Appendix I.4.

In order for PK to regenerate ATP in the reaction mixture, its substrate PEP must also be present.⁸³ To ensure that uridine to UMP conversion was not limited by PEP depletion causing a lack of ATP regeneration it was decided to use a uridine to PEP ratio of 10:11 in the reaction mixture. As PK would be present in the reaction mixture, and thus able to regenerate ATP levels the initial ATP concentration was reduced to a uridine to ATP ratio of 5:1.

4.8 Confirmation of Enzymatic Activity

With the confirmation of PK activity, further attempts were made to confirm the activity of the various purified ribonucleotide kinases described in *Section 3.0*.

4.8.1 ADK

In order to assess whether the *EcADK* samples purified in *Section 3.5.2* exhibited ribonucleotide monophosphate kinase activity, a reaction mixture comprising 12.5 mM AMP, 13.75 mM PEP, 5 mM ATP, 1.5 mg *EcADK*, and 3 mg PK was generated, had catalytic activity induced, and was processed for ³¹P NMR analysis as described in *Section 2.6.1* and *Section 2.7.1.2* respectively. A negative control sample identical except lacking *EcADK* and PK addition was also generated in the same manner. ³¹P spectra derived from these samples can be found in *Appendix I.5*.

As can be seen in *Figure 4.31*, when normalised from the peak attributed to the α -phosphate of ADP/ α -phosphate of ATP a clear decrease in integral value can be seen for both the AMP and PEP peaks from the control to reaction sample spectra. This indicates that AMP and PEP concentrations have decreased due to enzymatic activity, or that ADP/ATP concentrations have increased due to enzymatic activity, or that both of these activities have occurred to some degree. This is consistent with the occurrence of catalytic activity associated with both *EcADK* and PK, AMP and PEP concentrations would be decreased by the activities of *EcADK* and PK respectively while ADP and ATP concentrations would be increased by the activities of *EcADK* and PK respectively.

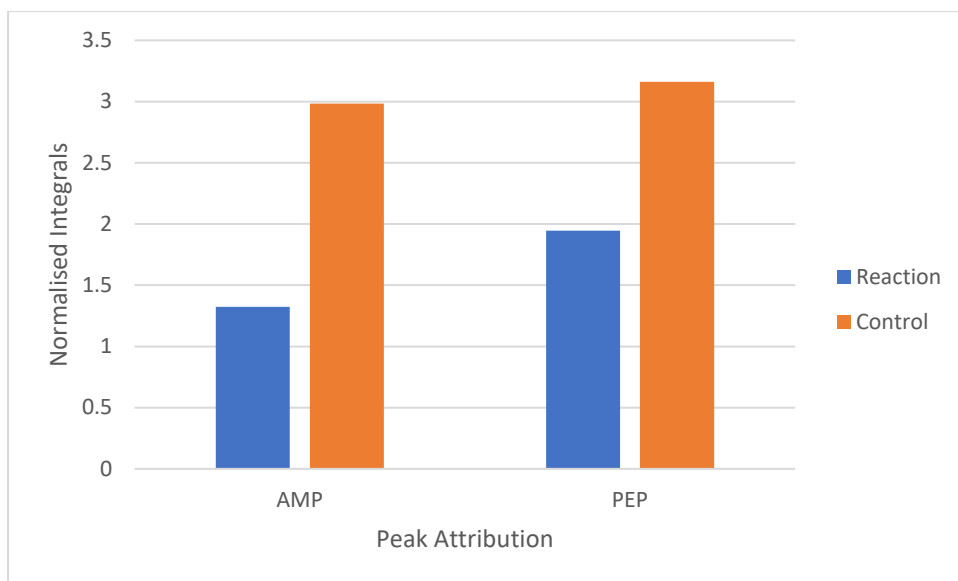


Figure 4.31: Comparative bar graph depicting difference in integrals of relevant peaks between reaction and control sample of ADK activity study. Full data described in Table 4.6.

Sample	Peak No.	Attribution	Range	Integral (Normalised)
Reaction	1	AMP	0.93 ... 0.82	1.322
	2	Free phosphate	0.66 ... 0.60	0.357
	3	PEP	-3.46 ... -3.57	1.945
	4	ADP (β)/ATP (γ)	-9.72 ... -9.94	0.617
	5	ADP (α)/ATP (α)	-10.49 ... -10.69	1.000
Control	1	AMP	0.86 ... 0.75	2.984
	2	Free phosphate	0.64 ... 0.58	0.258
	3	PEP	-3.60 ... -3.71	3.161
	4	ADP (β)/ATP (γ)	-9.71 ... -9.93	0.835
	5	ADP (α)/ATP (α)	-10.58 ... -10.78	1.000

Table 4.6: Data from ^{31}P NMR spectra of samples from ADK activity study. Peak attributions made as per observations described in Section 4.2. Relevant spectra can be seen in Appendix I.5. ^{31}P NMR analysis conducted as described in Section 2.7.1.2.

4.8.2 GUK

In order to assess whether the *Pf*GUK samples purified in Section 3.6.2 exhibited ribonucleotide monophosphate kinase activity, a reaction mixture comprising 12.5 mM AMP, 13.75 mM PEP, 2.5 mM ATP, 1.5 mg *Pf*GUK, and 3 mg PK was generated, had catalytic activity induced, and was processed for ^{31}P NMR analysis as described in Section 2.6.1 and Section 2.7.1.2 respectively. A negative control sample identical except lacking *Pf*GUK and PK addition was also generated in the same manner. ^{31}P spectra derived from these samples can be found in Appendix I.5.

As can be seen in Figure 4.32, when normalised from the peak attributed to the α -phosphate of ADP/ α -phosphate of ATP a clear decrease in integral value can be seen for both the AMP and PEP peaks from

the control to reaction sample spectra. This indicates that AMP and PEP concentrations have decreased due to enzymatic activity, or that ADP/ATP concentrations have increased due to enzymatic activity, or that both of these activities have occurred to some degree. This is consistent with the occurrence of catalytic activity associated with both *Pf*GUK and PK, AMP and PEP concentrations would be decreased by the activities of *Pf*GUK and PK respectively while ADP and ATP concentrations would be increased by the activities of *Pf*GUK and PK respectively.

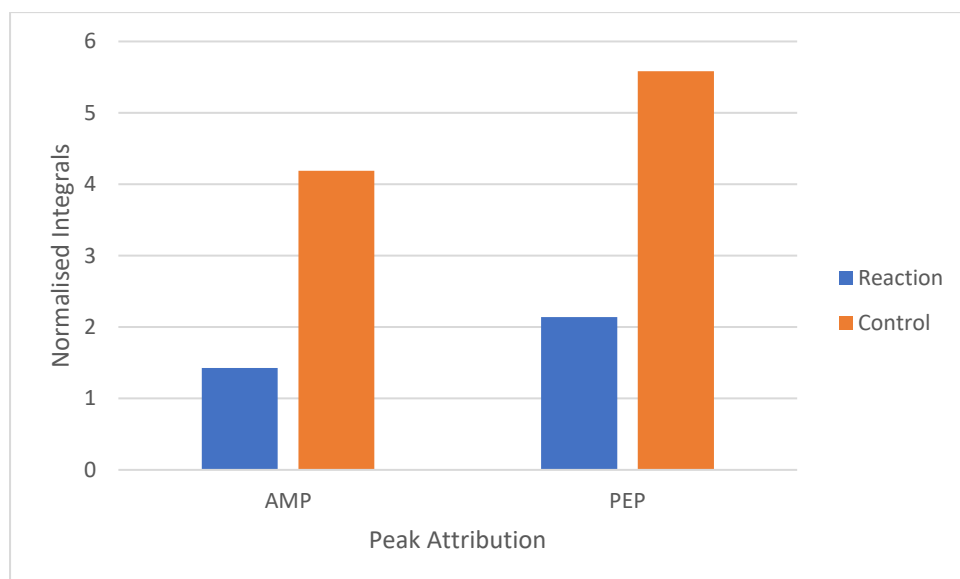


Figure 4.32: Comparative bar graph depicting difference in integrals of relevant peaks between reaction and control sample of GUK activity study. Full data described in Table 4.7.

Sample	Peak No.	Attribution	Range	Integral (Normalised)
Reaction	1	AMP	0.91 ... 0.81	1.429
	2	Free phosphate	0.64 ... 0.58	0.207
	3	PEP	-3.48 ... -3.59	2.140
	4	ADP (β)/ATP (γ)	-9.52 ... -9.74	0.577
	5	ADP (α)/ATP (α)	-10.48 ... -10.68	1.000
Control	1	AMP	0.83 ... 0.73	4.187
	2	Free phosphate	0.62 ... 0.56	0.303
	3	PEP	-3.63 ... -3.74	5.585
	4	ADP (β)/ATP (γ)	-9.48 ... -9.70	0.733
	5	ADP (α)/ATP (α)	-10.57 ... -10.77	1.000

Table 4.7: Data from ^{31}P NMR spectra of samples from GUK activity study. Peak attributions made as per observations described in Section 4.2. Relevant spectra can be seen in Appendix 1.5.

4.8.3 UCK1

In order to assess whether the human UCK1 samples purified in Section 3.3.2 exhibited rNK activity, a reaction mixture comprising 12.5 mM uridine, 13.75 mM PEP, 2.5 mM ATP, 1.5 mg UCK1, and 3 mg

PK was generated, had catalytic activity induced, and was processed for ^{31}P NMR analysis as described in *Section 2.6.1* and *Section 2.7.1.2* respectively. A negative control sample identical except lacking UCK1 and PK addition was also generated in the same manner. ^{31}P spectra derived from these samples can be found in *Appendix I.5*.

As can be seen in *Figure 4.33*, when normalised from the peak attributed to the α -phosphate of ADP/ α -phosphate of ATP a clear decrease in integral value of the peak attributed to PEP can be seen between the control and reaction sample spectra. The peak attributed to UMP cannot be seen in the control spectra. These results indicate that PEP concentration has been decreased due to enzymatic activity, and that UMP or a related NMP has been formed by enzymatic activity. This is consistent with the occurrence of catalytic activity associated with both UCK1 and PK, PEP concentration would be decreased by the catalytic activity of PK while UMP would be generated by the catalytic activity of UCK1.

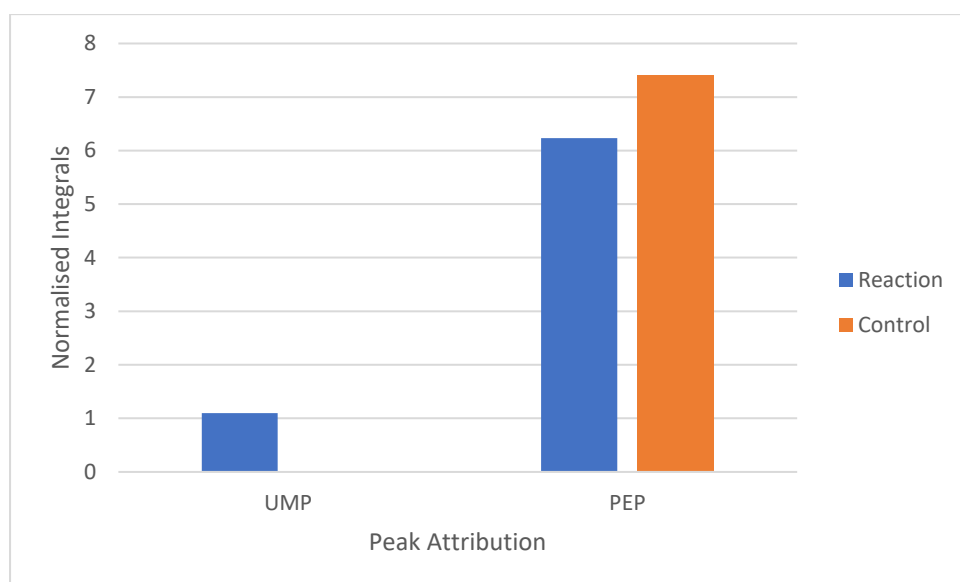


Figure 4.33: Comparative bar graph depicting difference in integrals of relevant peaks between reaction and control sample of UCK1 activity study. Full data described in Table 4.8.

Sample	Peak No.	Attribution	Range	Integral (Normalised)
Reaction	1	UMP	0.79 ... 0.68	1.097
	2	Free phosphate	0.63 ... 0.58	0.262
	3	PEP	-3.46 ... -3.63	6.232
	4	ADP (β)/ATP (γ)	-9.53 ... -9.69	0.690
	5	ADP (α)/ATP (α)	-10.48 ... -10.70	1.000
Control	1	UMP	N/A	0.000
	2	Free phosphate	0.60 ... 0.55	0.314
	3	PEP	-3.68 ... -3.85	7.401
	4	ADP (β)/ATP (γ)	-9.91 ... -10.07	1.294
	5	ADP (α)/ATP (α)	-10.63 ... -10.85	1.000

Table 4.8: Data from ^{31}P NMR spectra of samples from UCK1 activity study. Peak attributions made as per observations described in Section 4.2. Relevant spectra can be seen in Appendix I.5.

4.8.4 UCK2 (His-tag)

In order to assess whether the human UCK2 (His-tag) samples purified in Section 3.4.2.2 exhibited rNK activity, a reaction mixture comprising 12.5 mM uridine, 13.75 mM PEP, 2.5 mM ATP, 1.5 mg UCK2, and 3 mg PK was generated, had catalytic activity induced, and was processed for ^{31}P NMR analysis as described in Section 2.6.1 and Section 2.7.1.2 respectively. The same negative control was used for this reaction as the previously described UCK1 activity confirmation. ^{31}P spectra derived from these samples can be found in Appendix I.5.

As can be seen in Figure 4.34, when normalised from the peak attributed to the α -phosphate of ADP/ α -phosphate of ATP a decrease can be seen in the peak attributed to PEP between the control and reaction sample spectra. No UMP-attributed peak can be observed in either spectra. This indicates that PEP concentration has been decreased by enzymatic activity. This is consistent with PEP consumption via the catalytic activity of PK, although ADP is also required for this reaction to occur this may have been generated by the heat-mediated degradation of ATP. These results are also consistent with a lack of enzymatic activity by UCK2.

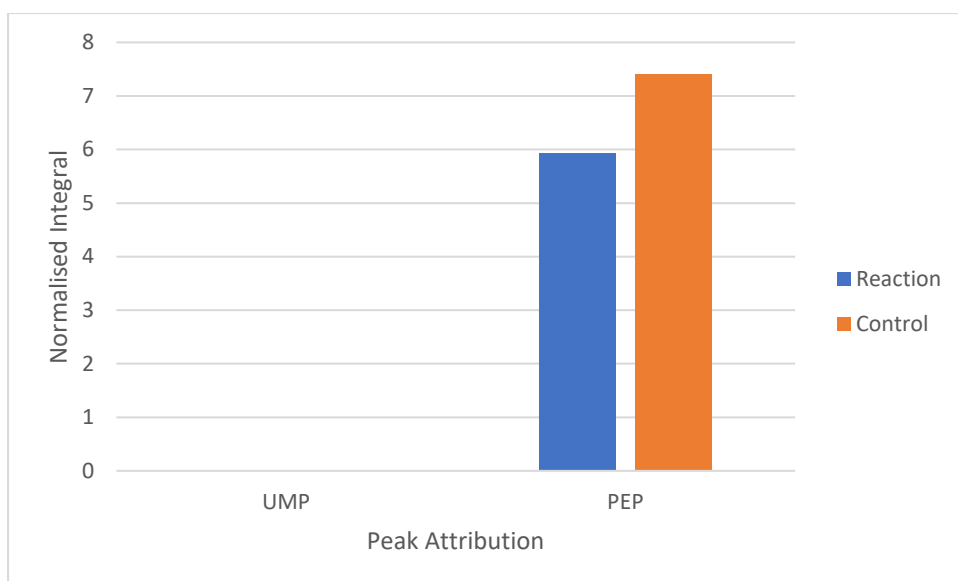


Figure 4.34: Comparative bar graph depicting difference in integrals of relevant peaks between reaction and control sample of UCK2 activity study. Full data described in Table 4.9.

Sample	Peak No.	Attribution	Range	Integral (Normalised)
Reaction	1	UMP	N/A	0.000
	2	Free phosphate	0.62 ... 0.57	0.217
	3	PEP	-3.63 ... -3.80	5.923
	4	ADP (β)/ATP (γ)	-9.58 ... -9.74	0.710
	5	ADP (α)/ATP (α)	-10.59 ... -10.81	1.000
Control	1	UMP	N/A	0.000
	2	Free phosphate	0.60 ... 0.55	0.314
	3	PEP	-3.68 ... -3.85	7.401
	4	ADP (β)/ATP (γ)	-9.91 ... -10.07	1.294
	5	ADP (α)/ATP (α)	-10.63 ... -10.85	1.000

Table 4.9: Data from ^{31}P NMR spectra of samples from UCK2 activity study. Peak attributions made as per observations described in Section 4.2. Relevant spectra can be seen in Appendix I.5.

4.8.5 CMPK (His-tag)

In order to assess whether the human CMPK (His-tag) samples purified in Section 3.7.2.2 exhibited ribonucleotide monophosphate kinase activity, a reaction mixture comprising 12.5 mM UMP, 13.75 mM PEP, 2.5 mM ATP, 1.5 mg CMPK, and 3 mg PK was generated, had catalytic activity induced, and was processed for ^{31}P NMR analysis as described in Section 2.6.1 and Section 2.7.1.2 respectively. A negative control identical except lacking CMPK and PK addition was also generated in the same manner.

Given the dramatic change in observable peaks between the reaction and control spectra of this experiment, visual analysis was used to detect enzymatic activity. It must be noted that the peaks

attributed to the γ - and β -phosphates of ATP cannot be seen in the ^{31}P spectra of the control sample, it may be the case that these peaks are obscured by the baseline noise at the working concentrations. In the ^{31}P spectra of the reaction sample (*Figure 4.36*), two pairs of doublet peaks can be seen one of which includes the ATP α -phosphate peak observed in the control sample. An isolated peak at a chemical shift of -19.0 ppm can also be seen in the reaction sample, this can likely be attributed to the β -phosphate of ATP. Due to the similarity it is unclear as to which peaks are which, however the new peaks can be attributed to the α - and β -phosphate groups of UDP, and the γ -phosphate of ATP. UDP is an expected product of the CMPK catalytic reaction and given the similarity the chemical environments of its phosphorus atoms to those of ADP it can be expected that the ^{31}P signals derived from these compounds are similar.

In the control sample spectrum (*Figure 4.35*) the peak at a chemical shift of approximately 0.7 ppm can be attributed to UMP while the peak at an approximate chemical shift of -3.5 ppm can be attributed to PEP. In the reaction sample (*Figure 4.36*) these peaks have shifted downfield, and the peak attributed to UMP can be observed to have decreased significantly in size. The peak attributed to PEP can also be observed to have decreased in size.

This indicates that UMP and PEP concentration have been decreased by enzymatic activity, and that UDP has been generated by enzymatic activity. This is consistent with the conversion of UMP to UDP via the catalytic activity of CMPK, and the consumption of PEP during ATP regeneration by PK.

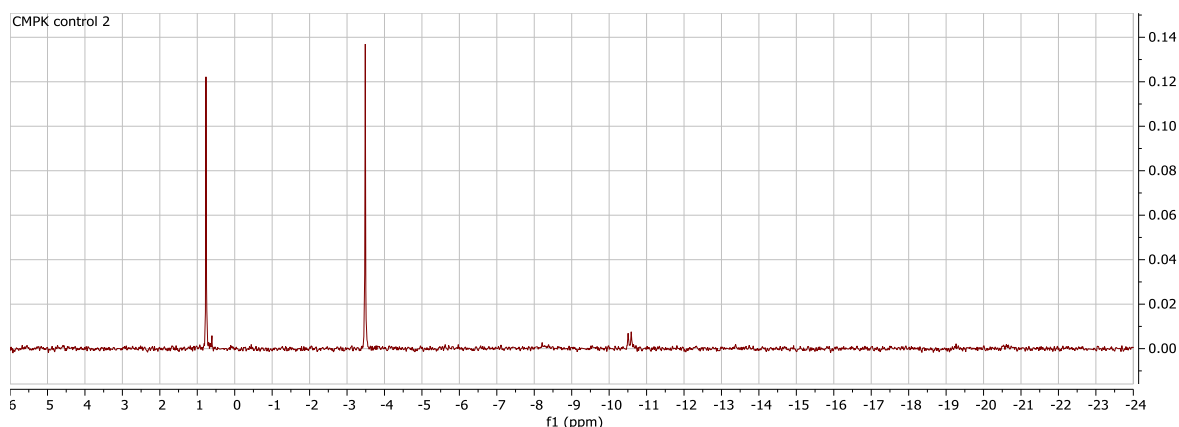


Figure 4.35: ^{31}P NMR spectrum derived from CMPK (His-tag) activity test negative control sample. Sample heated as described in Section 4.2.8. NMR analysis conducted as described in Section 2.7.1.2.

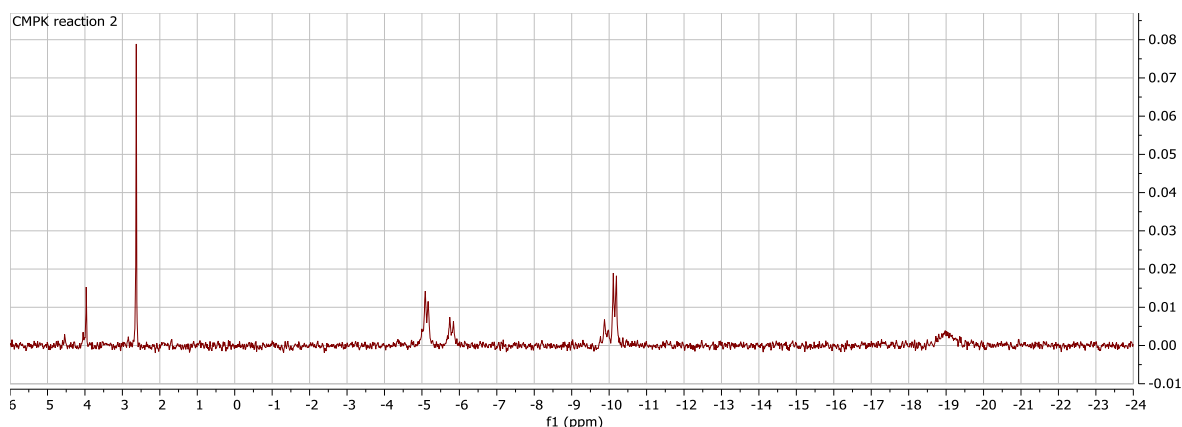


Figure 4.36: ^{31}P NMR spectrum derived from CMPK (His-tag) activity test reaction sample. Reaction conducted as described in Section 2.6.1. NMR analysis conducted as described in Section 2.7.1.2.

4.7 Quantification Model

4.7.1 NMR

In order to quantify the conversion of nucleoside to NMP mediated by rNK catalytic activity via ^{31}P NMR analysis, a quantification model was constructed as described in Section 2.7.2. Due to the consistency of the presence and intensity of the peak corresponding to the α -phosphate of ATP throughout the quantification curve spectra, this peak was selected for to normalise integrals of other peaks for curve construction and further quantification studies. ^{31}P spectra derived from these samples can be found in Appendix I.6.

As can be seen in Figure 4.37, as the concentration of UMP in the sample increases, simulating increasing catalytic activity by UCK1, the peak corresponding to the phosphate group of UMP is observed to increase at a rate proportional to concentration. A similar observation was observed for the peak corresponding to the phosphate group of PEP, as PEP concentration decreased the height of this peak decreased in a proportional manner. These peaks are also seen to exhibit a downfield shift as simulated substrate conversion increases, with the peak attributed to UMP occurring at a chemical shift of approximately 0.65 ppm in spectra simulating 5% uridine to UMP conversion while the corresponding peak in the spectra simulating 100% conversion occurs at an approximate chemical shift of 3.5 ppm (Figure A-I.35, Figure A-I.92). With regard to the peak attributed to PEP, at 0% conversion this peak occurs at a chemical shift of approximately -3.75 ppm while at 100% conversion it occurs at approximately -0.75 ppm (Figure A-I.32, Figure A-I.92).

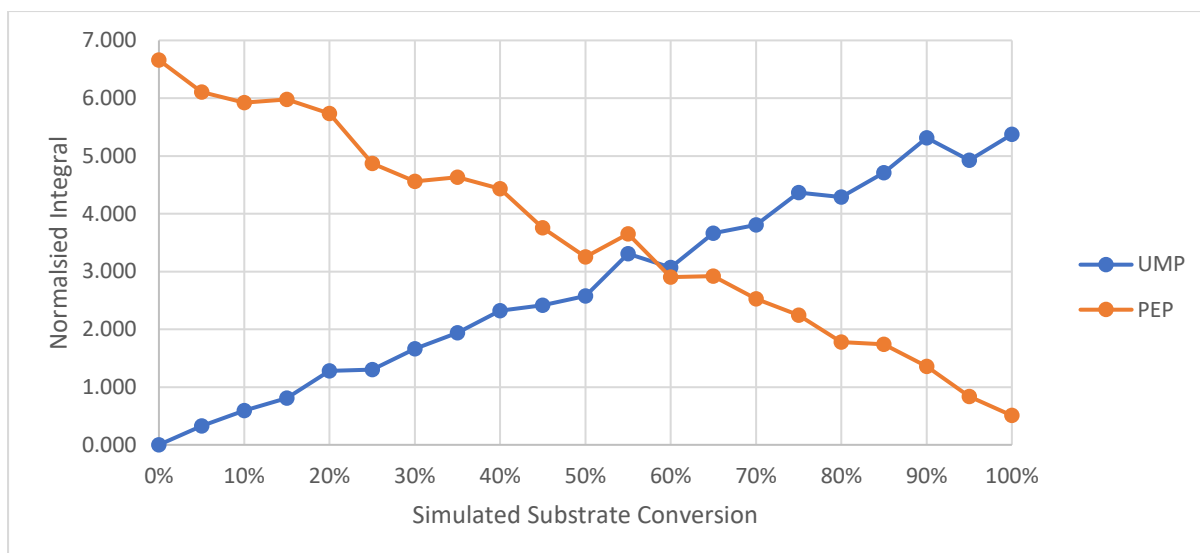


Figure 4.37: Changes in peak integrals of peaks attributed to UMP and PEP as simulated substrate conversion increases. Normalised from peak attributed to the α -phosphate of ATP.

This trend of peaks shifting downfield as the UMP:PEP ratio increases can also be seen in the peaks corresponding to the α -, β -, and γ -phosphate groups of ATP (Figure 4.38). The peak corresponding to the α -phosphate group is observed at a chemical shift of approximately -10.7 ppm at 0% conversion and at a chemical shift of approximately -10.1 ppm at 100% conversion. The peak corresponding to the β -phosphate group is observed at a chemical shift of approximately -21.9 ppm at 0% conversion and at a chemical shift of approximately -18.6 ppm at 100% conversion. The peak corresponding to the γ -phosphate group exhibits the most pronounced downfield shift with an increasing UMP:PEP ratio, it is observed at a chemical shift of approximately -10.0 ppm at 0% conversion and at a chemical shift of approximately -5.1 ppm at 100% conversion. The peaks corresponding to the β - and γ -phosphate groups of ATP become largely indistinguishable from the baseline noise of the spectra from about 50% conversion to about 80% simulated substrate conversion.

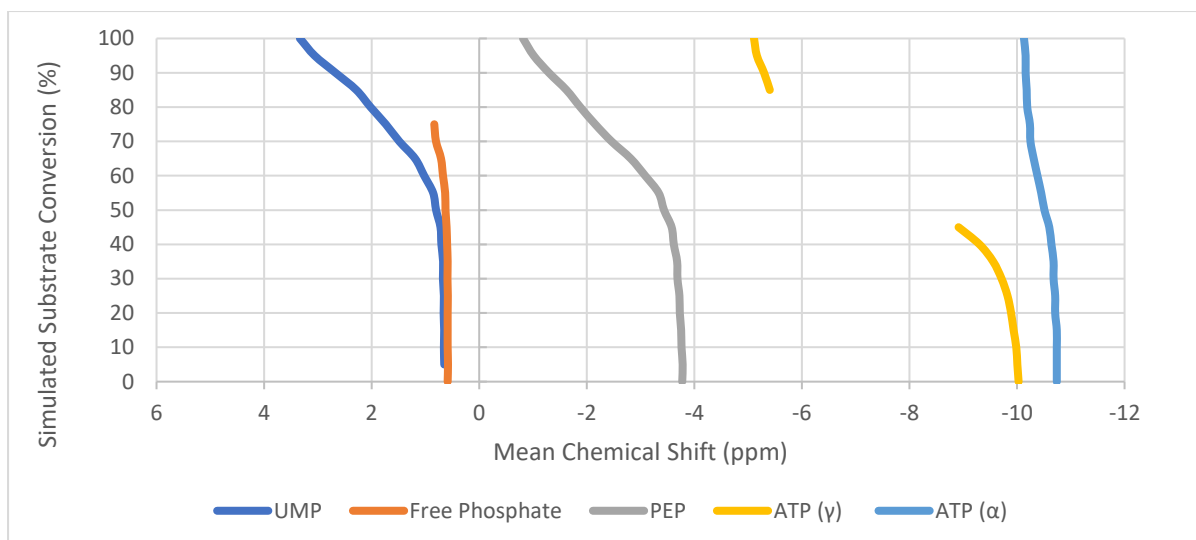


Figure 4.38: Changes in mean peak chemical shift as simulated substrate conversion increases. Chemical shift of each peak calculated as approximate midpoint of peak. Where peaks could not be reasonably identified no data has been entered. Peak attributed to β -phosphate of ATP not tracked due to consistent difficulty with identification.

4.7.2 Linear Regression Modelling

For each spectrum the peak ratio, x , was calculated through the following formula:

$$x = a / (a + b)$$

Where a describes the integrated value of the peak associated with the phosphate group of UMP and b describes the integrated value of the peak associated with the phosphate group of PEP.

As can be seen in *Figure 4.39* a linear relationship was observed between the peak ratio and the level of simulated substrate conversion, indicating that the data would be suitable for use in the generation of a linear model from which to calculate the substrate conversion in reaction samples.

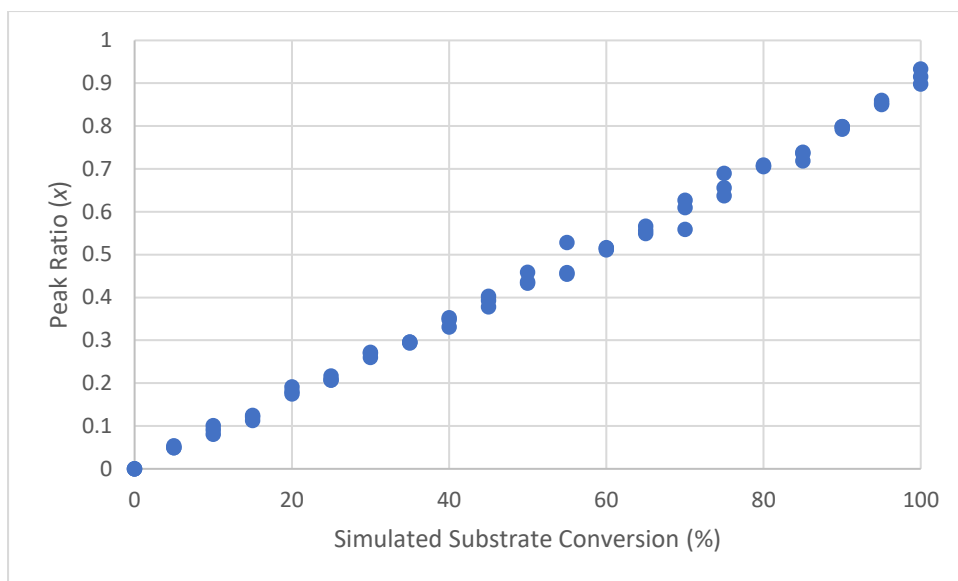


Figure 4.39: Relationship between peak ratio and simulated substrate conversion of samples of quantification curve. $x = a / (a + b)$. a = integral of UMP peak. b = integral of PEP peak.

Using x as a predictor with substrate conversion percentage as a target, a linear regression model was generated through the use of SPSS Statistics automatic linear modelling function, using a forward stepwise model selection method. The model was calculated to have an adjusted R^2 of 0.996. As can be seen in Figure 4.40, calculated conversion values were in close agreement with the actual known values, with mean error remaining within $\pm 4\%$ across the entire quantification range.

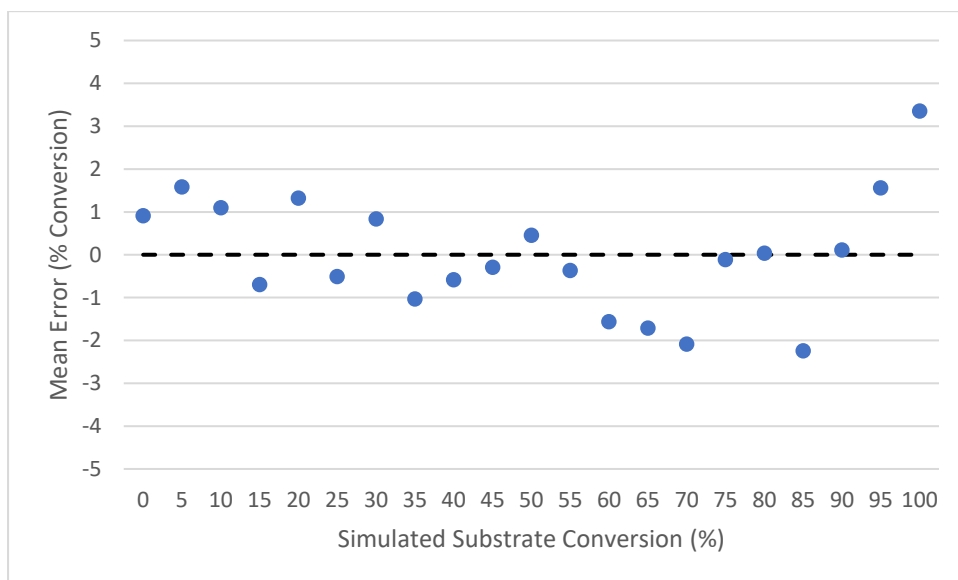


Figure 4.40: Change in mean error of calculated substrate conversion across full quantification curve. Mean error calculated as mean difference between calculated and actual known substrate conversion percentage.

Regression analysis provided a linear model that predicted NMP concentration in samples of known concentration with sufficient accuracy, thus this model was deemed suitable for use in calculating the conversion occurring in experimental samples.

4.7.3 Accuracy of Model at Higher Component Concentrations

It was theorised that as long as the ratio of phosphate containing reaction components was maintained the previously described quantification curve would be effective at calculating uridine to UMP conversion at different component concentration levels than used in the study. In order to assess this, a series of samples representing an initial uridine concentration of 25 mM, PEP concentration of 27.5 mM and ATP concentration of 5 mM was generated. The ^{31}P NMR spectra of these samples were analysed as described above, and the resulting data was processed using the previously described linear model. These samples were generated in 10% conversion iterations for a total of eleven samples, with a 10% conversion increase corresponding to a 2.5 mM increase in UMP concentration and a 2.5 mM decrease in both uridine and PEP concentration.

As can be seen in *Figure 4.41*, the predicted conversion generated from passing the data through the quantification curve model was in close agreement with the actual simulated conversion values. This supports the hypothesis that the previously described NMP conversion quantification model would maintain utility at different component concentrations as long the initial ratio of components in solution remained the same. These results also support the accuracy of the model in calculating substrate conversion from samples with unknown substrate monophosphate concentration.

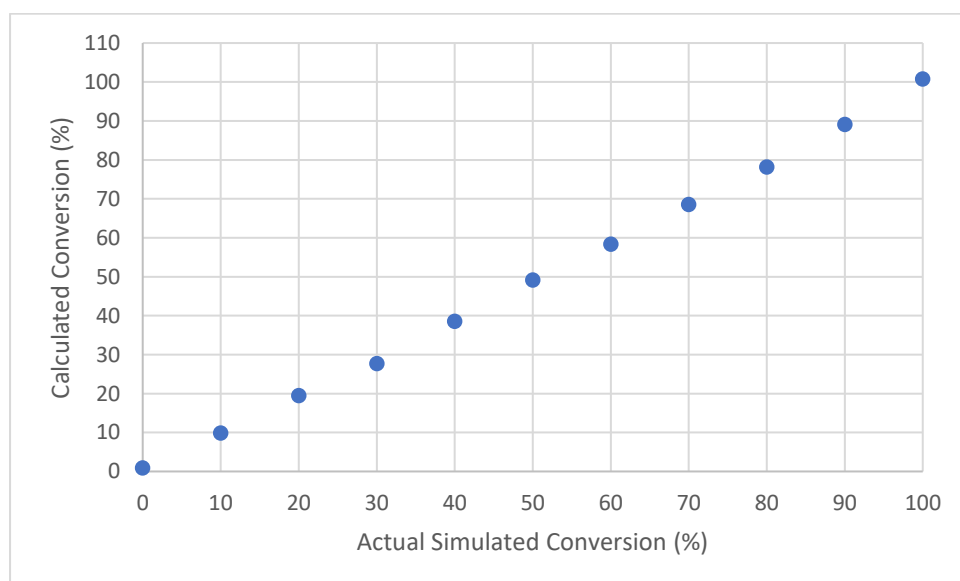


Figure 4.41: Effectiveness of substrate conversion quantification curve at calculating conversion at higher component concentrations at the same component ratio.

4.8 UCK1 Concentration Study

In order to assess the effect of UCK1 concentration within the reaction mixture on catalytic activity, a series of reactions across a range of UCK1 concentrations were conducted and analysed via ^{31}P NMR, as described in *Section 2.6.1* and *Section 2.7.1.2* respectively. These experiments were conducted in rNK reaction buffer, with 12.5 mM uridine, 13.75 mM PEP, and 2.5 mM ATP. Equivalent amount of PK and UCK1 were used in each reaction. Reactions were conducted in triplicate and enzymatic conversion of uridine to UMP was assessed using the model described in *Section 4.7*. Full ^{31}P NMR data can be found in *Appendix I.8*.

As can be seen in *Figure 4.42*, mean estimated conversion of uridine to UMP by human UCK1 increased with increasing enzyme concentration in a linear manner from 0.75 mg/mL to 1.5 mg/mL, at a rate of approximately 4.08% per 1 mg/mL increase. As enzyme concentration rose above this level the rate of mean estimated conversion increase appeared to slow, with an approximate rate of 2.39% per 1 mg/mL increase between 1.5 mg/mL and 1.875 mg/mL decreasing to an approximate rate of increase of 1.49% per 1 mg/mL increase between 1.875 mg/mL and 2.25 mg/mL.

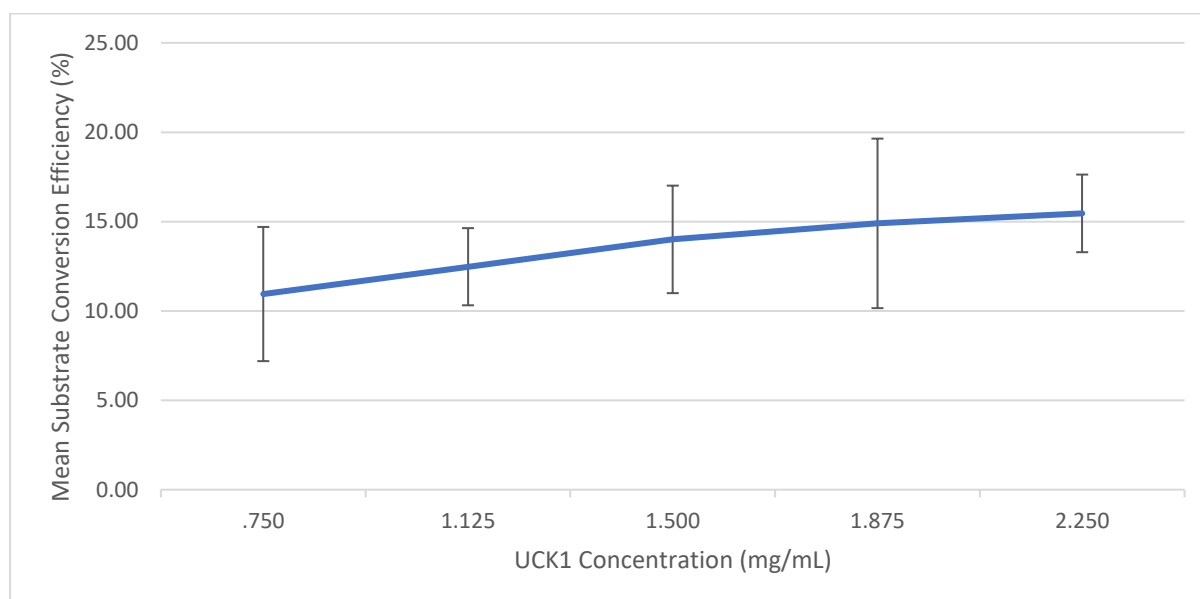


Figure 4.42: Change in mean substrate conversion efficiency (% of total substrate in solution phosphorylated) of UCK1 against uridine with change in UCK1 concentration. Error bars are 95% confidence intervals for mean.

One-way analysis of variance (ANOVA) of the data revealed that there was a statistically significant difference in mean calculated substrate conversion between samples with different UCK1 concentrations, $F(4, 10) = 5.727$, $p = 0.012$. All assumptions of the one-way ANOVA were found to have held. Post-hoc analysis via Tukey's honestly significant difference (HSD) test indicated that there was statistically significant difference between the mean calculated substrate conversion at 0.75 mg/mL

UCK1 and both 1.875 mg/mL ($p = 0.030$) and 2.25 mg/mL ($p = 0.013$) UCK1. Full results of statistical analysis can be found in *Appendix III.1*.

Although the low sample size and relatively high degree of variation between samples makes drawing firm conclusions difficult, the results of these experiments indicate that increases in enzyme concentration above 1.5 mg/mL result in diminishing returns with regard to increasing substrate conversion. Given this, and the practicalities involved with producing sufficient amounts of human UCK1 for further experiments, the optimal concentration for human UCK1 in the reactions of the present study was identified as 1.5 mg/mL.

4.9 PK Concentration Study

In order to assess whether the concentration of PK relative to UCK in the reaction mixture was affecting the catalytic activity of UCK1, a series of reactions with increasing PK concentration relative to UCK1 concentration were conducted and analysed via ^{31}P NMR, described in *Section 2.6.1* and *Section 2.7.1.2* respectively. These experiments were conducted in rNK reaction buffer with 12.5 mM uridine, 13.75 mM PEP, and 2.5 mM ATP. UCK1 concentration of 1.5 mg/mL was used in each reaction. Reactions were conducted in triplicate and enzymatic conversion of uridine to UMP was assessed using the model described in *Section 4.7*. Data from the previously described UCK1 concentration study (*Section 4.8*), from those reactions with UCK1 concentration of 1.5 mg/mL, was used as the 1:1 UCK1:PK ratio control. Full ^{31}P NMR data can be found in *Appendix I.9*.

One-way ANOVA analysis of the data revealed that there was a statistically significant difference in mean calculated substrate conversion between samples with different PK:UCK1 concentration ratios, $F(2, 6) = 50.262$, $p < 0.001$. All assumptions of the one-way ANOVA were found to have held. Post-hoc analysis via Tukey's HSD test indicated that there was statistically significant difference between the mean calculated substrate conversion at all levels of PK:UCK1 ratio. The results of this analysis support the hypothesis that increasing the ratio of PK to UCK1 in solution would result in a change in the amount of uridine converted to UMP. Full results of statistical analysis can be found in *Appendix III.2*.

As the ratio of PK to UCK1 concentration in the reaction mixture was increased the mean estimated substrate conversion was observed to increase from 14.01% at a 1:1 ratio to 23.22% at a 3:1 ratio (*Figure 4.43*). Given these results, and the practicalities involved with producing the necessary amount of PK for further experiments, the optimal mass ratio of PK to human UCK1 was decided to be 2:1 representing a PK concentration of 3 mg/mL in the reaction mixture when applied to the previously identified UCK1 concentration of 1.5 mg/mL.

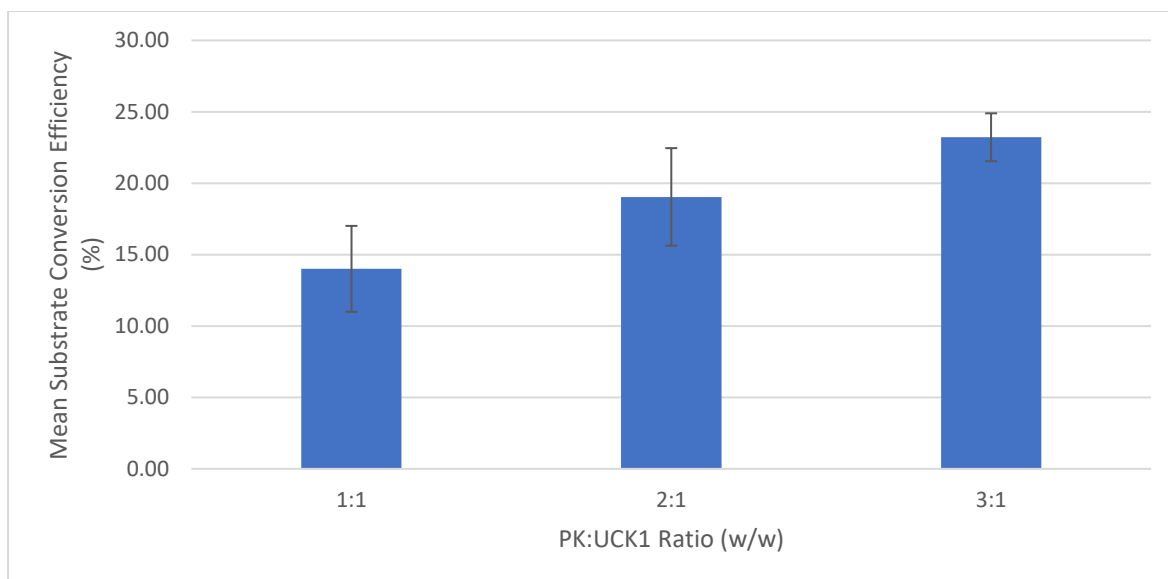


Figure 4.43: Mean substrate conversion efficiency (% of total substrate in solution phosphorylated) of UCK1 against uridine across different weight to weight ratios of PK to UCK1 in solution. Error bars are 95% confidence intervals for mean.

4.10 Addition Strategy Study

In order to determine if enzyme turnover number was a limiting factor in the conversion of uridine to UMP by human UCK1, the effect of incremental vs fixed addition was assessed via ^{31}P NMR spectroscopy, described in *Section 2.6.1* and *Section 2.7.1.2* respectively. Incremental addition involved the addition of UCK1 in three iterations of equal mass spaced 10 minutes apart, beginning at the initiation of reaction, to the same final amount. 1.5 mg of UK1 and 1.5 mg of PK were used in each reaction. Fixed addition involved the addition of the complete amount of UCK1 at the initiation of reactions, as described in *Section 2.6.1*. Data from the previously described UCK1 concentration study (*Section 4.8*), from those reactions with UCK1 concentration of 1.5 mg/mL, was used as fixed addition control. Reactions were conducted in triplicate and enzymatic conversion of uridine to UMP was assessed using the model described in *Section 4.7*. Full ^{31}P NMR data can be found in *Appendix I.10*.

As can be seen in *Figure 4.44*, the mean estimated conversion of samples subject to incremental human UCK1 addition (13.41%) appeared to be lower than the mean estimated conversion of those samples subjected to fixed addition (14.01%), although the large margin of error and relatively small difference between these groups makes drawing statistical conclusions difficult.

Analysis of the data via an independent samples t-test revealed that there was no statistically significant difference in mean calculated substrate conversion between samples with different addition strategies ($t(4) = 0.797$, $p = 0.470$). All assumptions of the t-test were found to have held. Due to this lack of evidence that an incremental UCK1 addition strategy would increase substrate conversion, it was decided to maintain the fixed addition strategy utilised in the previously described experiments for further studies. Full results of statistical analysis can be found in *Appendix III.3*.

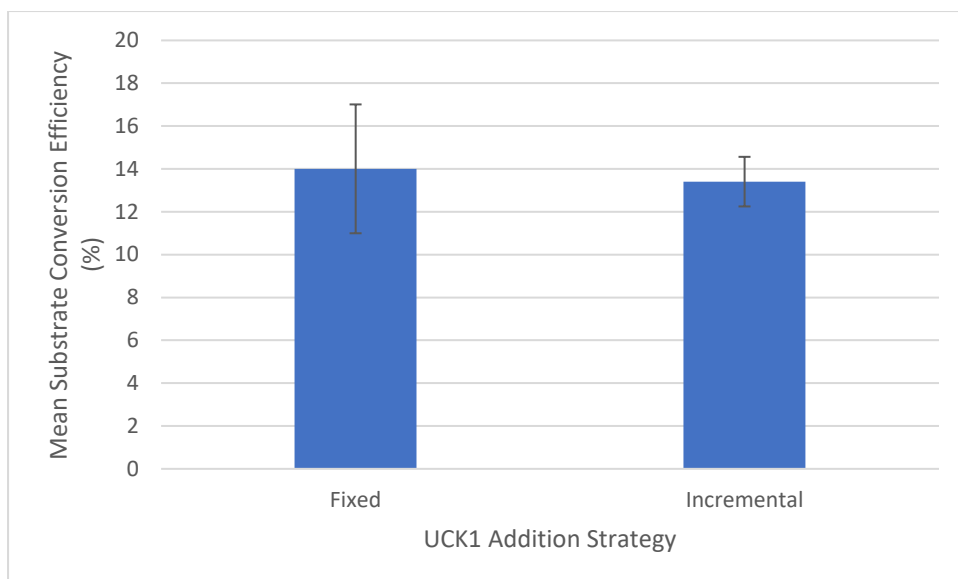


Figure 4.44: Mean substrate conversion efficiency (% of total substrate in solution phosphorylated) of UCK1 against uridine across different UCK1 addition strategies. Error bars are 95% confidence interval for mean.

4.11 Identification of Optimised Conditions

In accordance with the results of the previously described studies, an optimised reaction system for use in activity testing against unnatural nucleosides was specified. This reaction system involved component concentrations of 12.5 mM uridine, 13.75 mM PEP, and 2.5 mM ATP. For each sample, reaction was initiated by the addition of 1.5 mg UCK1 and 3 mg PK followed by heating to 37 °C. All other factors were as described in *Section 2.6.1*.

5.0 Results: Activity Against Unnatural Nucleosides

5.1 Introduction

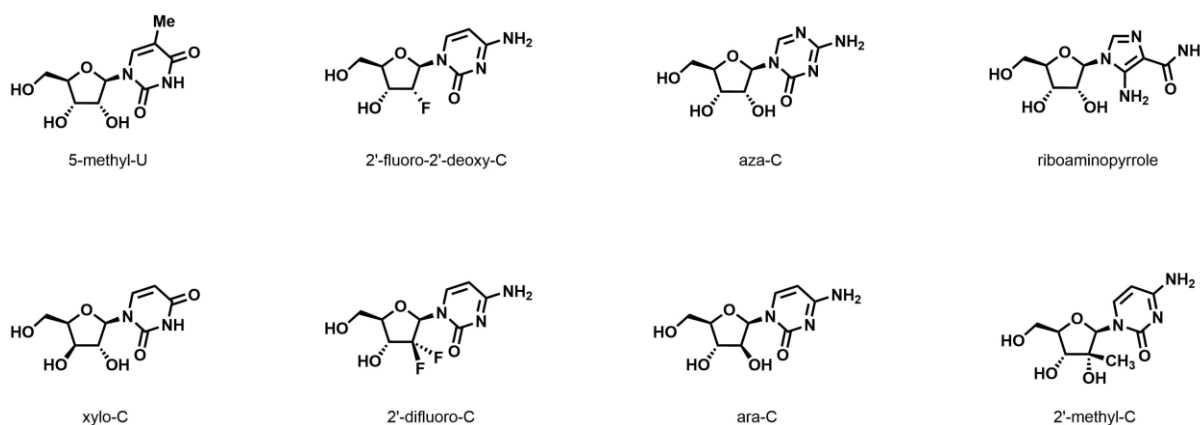


Figure 5.1: Molecular structures of unnatural nucleosides used in the present study.

The unnatural nucleosides utilised in the present study were selected from a range of nucleobase and sugar-modified pyrimidine nucleosides synthesised by scientists of the Ferrier Research Institute (*Figure 5.1*). Those compounds that were selected for use were done so based primarily on availability, but care was taken to ensure that the compounds used exhibited a range of different sugar and base modifications. The natural substrates of human UCK, uridine and cytidine, were used as positive controls with which to compare activity against unnatural substrates. Negative controls were produced for each compound, involving reaction mixtures comprising identical chemical ingredients but lacking UCK and PK. All controls were subject to the same heating and filtration process as reaction samples before analysis by NMR and LCMS.

5.2 Activity Against Natural Substrates

Although initial activity tests of the purified human UCK2 (His-tag) samples of the present study, described in *Section 4.8.4*, indicated a lack of catalytic activity it was decided that further testing was warranted given the potential utility of the enzyme against the target unnatural substrates. To this end, human UCK2 was included in the initial studies of enzymatic activity against uridine and cytidine.

As previously described, initial in-depth activity tests investigated the activity of human UCK against their natural substrates. The results of these investigations would be used as a positive control for the comparative assessment of activity against the previously described unnatural substrates.

In order to assess the activity of both human UCK1 and UCK2 against uridine and cytidine, a series of reaction mixtures comprising 12.5 mM substrate, 13.75 mM PEP, 2.5 mM ATP, 1.5 mg UCK, and 3

mg PK in rNK reaction buffer were generated and had catalytic activity induced as described in *Section 2.6.1*. Each enzyme was assessed against each substrate individually, and each reaction was done in triplicate. In the case of the assessment of the activity of UCK1 and UCK2 against uridine, the previously described confirmation of activity tests (*Section 4.8*) were considered as part of these triplicate reactions given the identical reaction conditions used. Control samples were generated comprising identical components but lacking UCK or PK addition, also in triplicate.

5.2.1 Analysis via ^{31}P NMR

^{31}P NMR peak attributions identified and described in *Section 4.2* were applied to the spectra derived from the presently described experiments to identify the compounds present in solution. For each reaction, data as to the relevant ^{31}P peaks was gathered and processed as described in *Section 2.7.1.2*. The previously described enzyme turnover quantification model (*Section 4.7*) was applied to the data of the present experiment to calculate the proportion of substrate in solution successfully converted to its monophosphate derivative.

As expected, a lack of phosphorylative activity was observed in each of the non-enzyme-containing negative control samples (*Appendix I.11*).

As can be seen in *Figure 5.2*, the purified human UCK2 did not appear to have any activity against either uridine or cytidine when assessed via ^{31}P NMR analysis. Human UCK1 however was found to exhibit phosphorylative activity against both cytidine and uridine. UCK1 was able to convert cytidine (3.04 mg, 12.5 mM) to CMP (2.90 mg, 8.96 mM) with much greater efficiency than uridine (3.05 mg, 12.5 mM) to UMP (0.57 mg, 1.77 mM), resulting in mean calculated conversions of 71.68% and 14.12% of total substrate respectively. There was also more variation in the observed catalytic activities of human UCK1 against uridine, with a standard deviation of 6.20% as opposed to that the standard deviation of 1.65% calculated from the cytidine reactions (*Appendix III.4*).

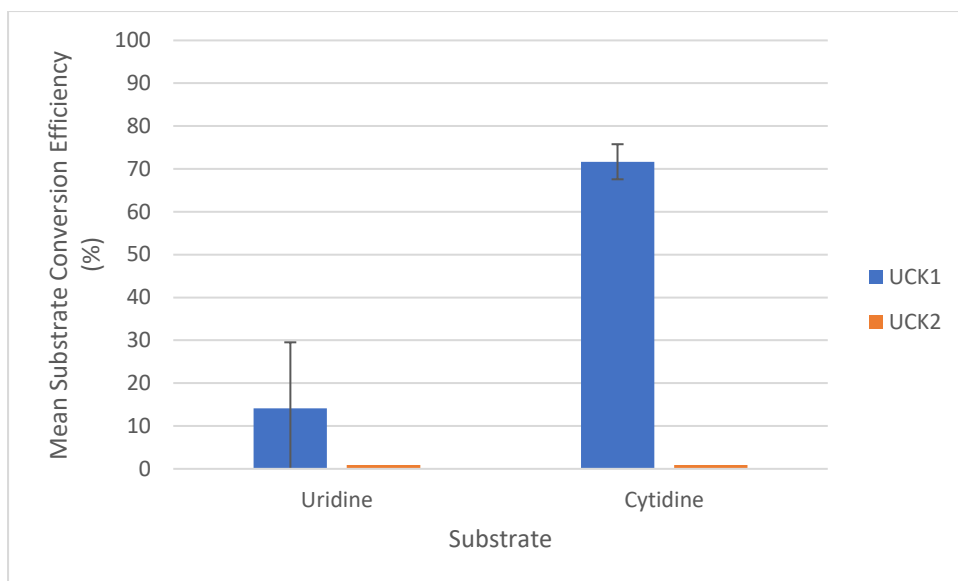


Figure 5.2: Mean substrate conversion efficiency (% of total substrate in solution phosphorylated) of UCK1 and UCK2 against uridine and cytidine. Error bars are 95% confidence interval of the mean.

To confirm that the observed differences in conversion efficiencies were statistically significant an independent samples t-test was performed. As no conversion was observed in any sample derived from the reaction of UCK2 against either cytidine or uridine, thus there was zero variance within these groups, only UCK1 reactions against uridine and cytidine were included in this analysis. The results of Levene's test of the homogeneity of variances found that this assumption had been violated ($F = 8.010$, $p = 0.047$). All other relevant assumptions were found to have held. The results of an independent samples t-test revealed that the mean observed conversion efficiency of human UCK1 was significantly greater for cytidine as the substrate ($71.68 \pm 1.65\%$) than uridine as the substrate ($14.12 \pm 6.21\%$), $t(2.281) = -15.525$, $p = 0.002$. Full results of statistical analysis can be found in *Appendix III.4*.

5.2.2 Analysis via LCMS

Following ^{31}P NMR analysis, the NMR samples were transferred into LCMS vials and analysed via LCMS as described in *Section 2.7.1.1*. Initial analysis of LCMS data focused on the identification of the retention times and mass charges of key compounds of the reaction mixture. This identification was achieved through extracted ion chromatogram (EIC) analysis of the data of each sample, with target mass charges rationally calculated from compound molecular weights (*Table 5.1*). The presence of substrate monophosphate was confirmed through comparison of EIC spectra derived from reaction and control samples, as can be seen in *Figure 5.3*.

Compound	Molecular Weight (g/mol)	Target Mass Charge (m/z)	Approx. Retention Time (min)
ATP	507.18	508.0	23
ADP	427.20	428.0	21
PEP	168.04	169.0	19.5
Uridine	244.20	245.0	4
UMP	324.18	325.0	16
Cytidine	243.21	244.0	5
CMP	323.20	324.0	18.5

Table 5.1: Identification details of key compounds of enzymatic reaction mixture. Compounds identified via EIC analysis targeting target mass charge ± 0.5 . Full data in Appendix II.

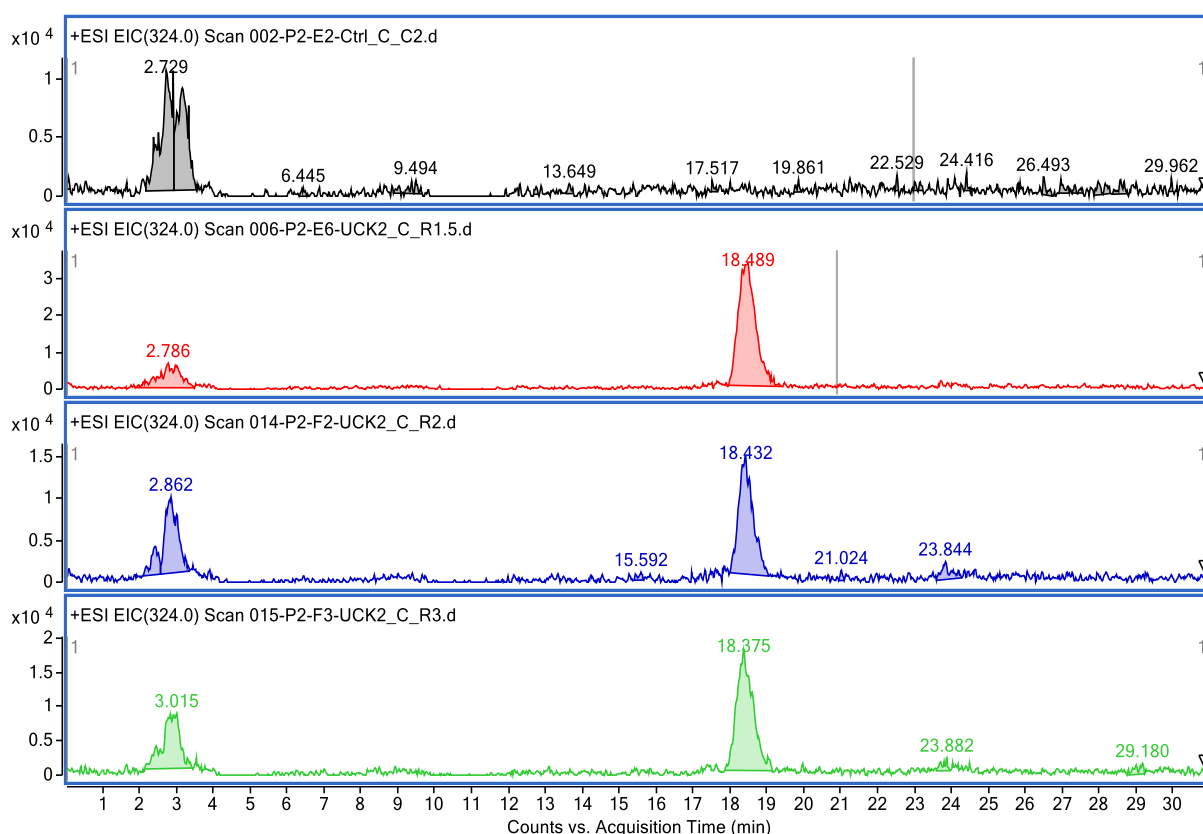


Figure 5.3: Comparison of CMP-targeting EIC spectra of UCK2-cytidine reactions and cytidine control sample. Black – cytidine control sample 1. Red – UCK2 cytidine reaction sample 1. Blue – UCK2 cytidine reaction sample 2. Green – UCK2 cytidine reaction sample 3. All IEC extraction done targeting m/z value of 324.0 ± 0.5 . Peaks at approx. 18.5 min retention time include ion fragment at m/z = 324.1 that was identified as CMP. LC-MS analysis conducted as described in Section 2.7.1.1.

As expected, substrate monophosphates were not identified in any negative control sample via LCMS analysis.

The presence of ADP, a product of the phosphorylation reaction catalysed by rNKs, was observed in all samples in which substrate monophosphates were also detected. ADP was also detected in samples in which both ^{31}P NMR and LCMS analysis failed to detect catalytic activity; this was not unexpected due to the inherent instability of ATP and resultant breakdown into ADP and free phosphate.

Following the identification of the target NMP compounds within each of the relevant spectra, peaks relating to these compounds were located and integrated (*Table 5.2*).

Enzyme	Substrate	Replicate	Substrate Monophosphate		
			m/z (± 0.5)	Retention Time (min)	Peak Area
UCK1	Uridine	1	325.0	15.783	9.40×10^6
		2	325.0	15.859	9.63×10^6
		3	325.0	16.012	3.31×10^6
UCK1	Cytidine	1	324.0	18.508	5.08×10^7
		2	324.0	18.527	4.64×10^7
		3	324.0	18.451	4.60×10^7
UCK2	Uridine	1	325.0	N/A	N/A
		2	325.0	N/A	N/A
		3	325.0	N/A	N/A
UCK2	Cytidine	1	324.0	18.429	1.11×10^6
		2	324.0	18.432	3.82×10^5
		3	324.0	18.375	5.43×10^5

Table 5.2: Results of EIC analysis of LCMS data aimed at detecting phosphorylated substrate in natural substrate reaction samples. Control data has not been included as no substrate monophosphate was detected in any sample. N/A has been entered where no relevant distinguishable peaks were observed. Full data in Appendix II.

As can be seen in *Figure 5.4*, LCMS analysis of the samples largely supported the conclusions of ^{31}P NMR analysis. With regard to the activity of UCK1 the mean area of the relevant NMP peaks was larger with cytidine (4.77×10^7) as the substrate compared to uridine as the substrate (7.44×10^6), indicating that cytidine was a more efficiently phosphorylated substrate than uridine for UCK1. With regard to the activity of UCK2, despite the lack of detection of phosphorylative activity via ^{31}P NMR analysis molecular fragments with masses correlating to CMP were observed in analysis of spectra derived from UCK2-cytidine reactions. This suggests that the UCK2 used within these reactions did in fact have phosphorylative activity against cytidine, albeit at a low enough rate to go undetected by ^{31}P NMR. No distinguishable peaks relating to UMP were observed in the spectra relating to UCK2-uridine reactions indicating a lack of phosphorylative activity, supporting the results of the previously described ^{31}P NMR analysis.

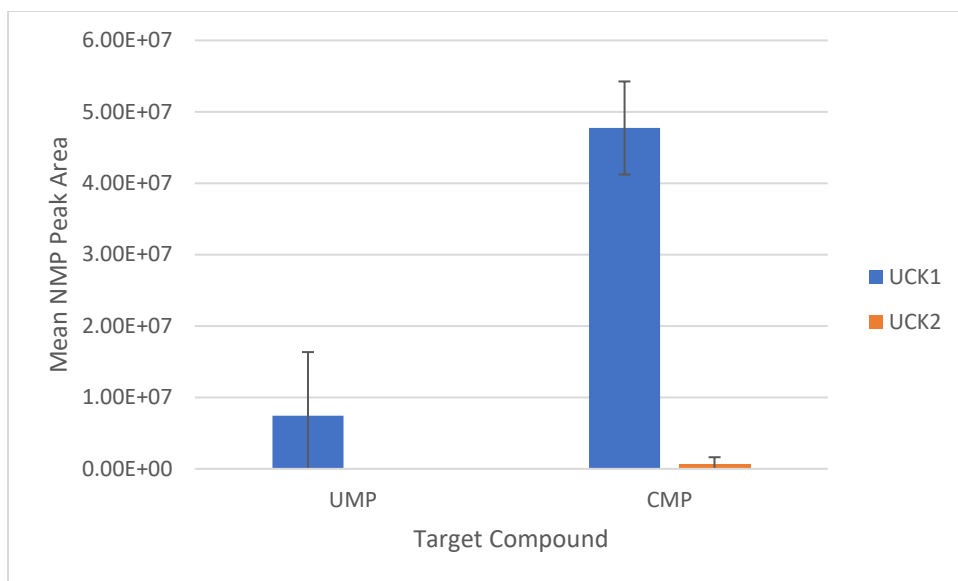


Figure 5.4: Mean areas of integrated nucleoside monophosphate LCMS peaks in reactions of UCK1 and UCK2 against uridine and cytidine as substrates. Error bars are 95% confidence interval of mean. Controls not included as no relevant peaks were observed. Peaks identified through EIC analysis of data derived through LCMS analysis of relevant reaction samples. Compounds identified via EIC analysis targeting target mass charge ± 0.5 .

Statistical analysis was undertaken to confirm that the observed differences in conversion efficiencies were statistically significant. As no conversion was observed in any sample derived from the reaction of UCK2 against uridine, there was zero variance within these groups therefore these reactions were excluded from analysis. The results of Levene's test of the homogeneity of variances found that this assumption had been violated ($F = 6.392$, $p = 0.033$). All other relevant assumptions were found to have held. The results of a Welch's ANOVA revealed that there was a statistically significant difference in mean peak area between the different reactions, $F(2, 2.751) = 382.861$, $p < 0.001$. Post-hoc analysis via a Games-Howell test revealed that mean NMP peak area was significantly greater in UCK1-cytidine reactions than in UCK1-uridine and UCK2-cytidine reactions. This test also indicated that the difference in mean NMP peak area between the UCK1-uridine and UCK2-cytidine reactions was not statistically significant, thus the observed activity of UCK1 against uridine cannot be considered as greater than the observed activity of UCK2 against cytidine based on the results of this LCMS analysis. Full results of statistical analysis can be found in *Appendix III.4*.

Given the lack of activity observed with human UCK2 against uridine and the low activity observed against cytidine, it was decided that UCK2 would not be used in further tests.

5.3 Activity Against Unnatural Substrates

Human UCK1 was assessed for activity against each of the eight different unnatural nucleosides described in *Section 5.1*. Experiments were conducted as described in *Section 2.6.1*, with ingredient

concentrations being 12.5 mM substrate, 2.5 mM phosphate donor, and 13.75 mM PEP. 1.5 mg of UCK1 and 3 mg of PK were used in each reaction. Each reaction was conducted in triplicate. Negative control samples were generated with identical componentry and reaction process, but neither UCK nor PK was included in the reaction mixture. Singular controls were generated to preserve substrate compound.

5.3.1 Analysis via ^{31}P NMR

For each reaction, data as to the relevant ^{31}P peaks was gathered and processed as described in *Section 2.7.1.2*. ^{31}P NMR peak attributions identified and described in *Section 4.2* were applied to the spectra derived from the presently described experiments to identify the compounds present in solution. The linear model generated from the previously described enzyme turnover quantification curve was applied to the data of the present experiments to calculate the proportion of substrate in solution successfully converted to its monophosphate derivative.

As expected, a lack of phosphorylative activity was observed in each of the non-enzyme-containing negative control samples (*Appendix I.12*). NMP production via UCK1 catalytic activity was only observed for one of the eight unnatural substrates tested, 5-methyl-U. For the reactions of UCK1 against 5-methyl-U, catalytic activity was observed in only two of the three. This indicates that there was a failure to induce catalytic activity in the reaction sample in which no activity was observed at the timescale of reaction. There was significant variability in the observed substrate conversions of the remaining UCK1/5-methyl-U reactions, with calculated conversions of 19.60% and 7.74%. Excluding the failed reaction, the mean calculated conversion of 5-methyl-U was 13.67%. The variability of the data between these samples, in particular the failure to observe activity via ^{31}P NMR analysis in one of the three, makes further statistical analysis redundant.

As can be seen in *Figure 5.5*, 5-methyl-U appears to have been phosphorylated by UCK1 with a similar conversion efficiency to uridine and markedly less efficiency than cytidine, although there is more variability in the results of UCK1/5-methyl-U reactions than those with uridine or cytidine.

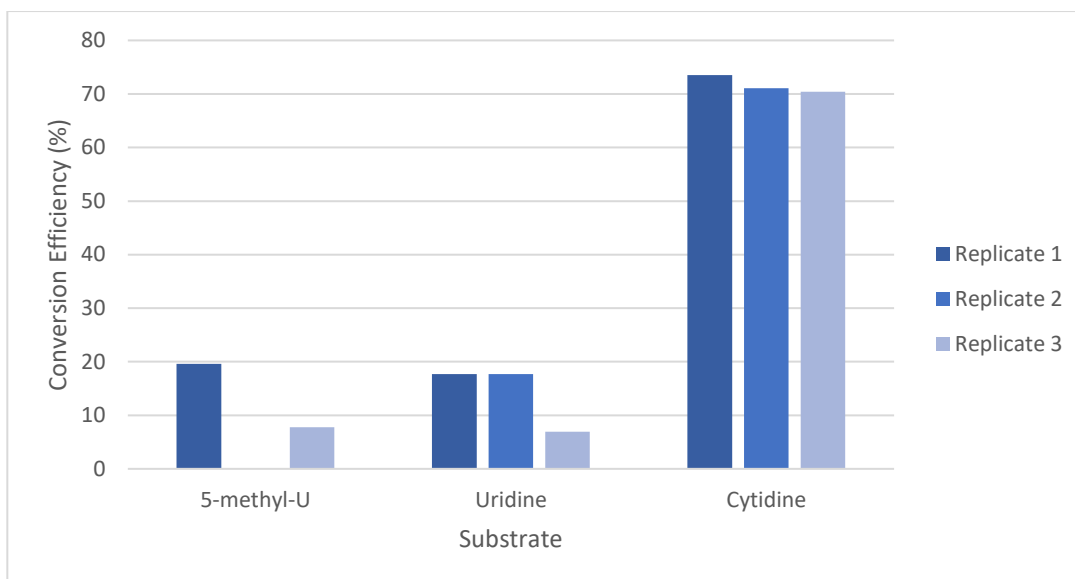


Figure 5.5: Comparison of substrate conversion efficiency (% of total phosphorylated substrate in solution) of UCK1 against 5-methyl-U, uridine, and cytidine. Conversion efficiency of each reaction sample presented individually.

5.3.2 Analysis via LCMS

Following ^{31}P NMR analysis, NMR samples were transferred into amberised LCMS vials and analysed via LCMS as described in *Section 2.7.1.1*. As in *Section 5.2.2*, initial analysis of LCMS data focused on the identification of the retention times and mass charges of key compounds of the reaction mixture, in this case the unnatural substrates and their monophosphate derivatives. This was achieved through EIC analysis of the data of each sample, with target mass charges rationally calculated from compound molecular weights (*Table 5.3*). Visual comparison of control and reaction EIC spectra was used to confirm that any peaks of appropriate mass charges that were observed did in fact relate to the presence of the target substrate monophosphate.

Compound	Molecular Weight (g/mol)	Target Mass Charge (m/z)	Approx. Retention Time (min)
5-methyl-U	258.23	259.0	3
5-methyl-U monophosphate	338.21	339.0	16
2'-fluoro2'deoxy-C	245.21	246.0	3.5
2'-fluoro2'deoxy-C monophosphate	325.91	326.0	N/A
aza-C	244.21	245.0	4
aza-C monophosphate	324.19	325.0	18
riboaminopyrrole	258.23	259.0	3.5
riboaminopyrrole monophosphate	338.21	339.0	18
xylo-C	244.20	245.0	4
xylo-C monophosphate	324.18	325.0	N/A
2'-difluoro-C	263.20	264.0	3
2'-difluoro-C monophosphate	343.18	344.0	N/A
ara-C	243.22	244.0	5
ara-C monophosphate	323.20	324.0	N/A
2'-methyl-C	257.25	258.0	4
2'-methyl-C monophosphate	337.23	338.0	N/A

Table 5.3: Identification details of unnatural substrates and monophosphate derivatives thereof in enzymatic reaction mixtures. Compounds identified via EIC analysis targeting target mass charge ± 0.5 . N/A has been given as retention time where compound could not be identified in any spectra. Full data in Appendix II.

As expected, substrate monophosphates were not identified in any negative control sample via LCMS analysis. Following the identification of the target NMP compounds within each of the relevant spectra, peaks relating to these compounds were located and integrated (Table 5.4).

Substrate	Replicate	Substrate Monophosphate		
		m/z (± 0.5)	Retention Time (min)	Peak Area
5-methyl-U	1	339.0	15.402	6.00×10^6
	2	339.0	15.440	3.43×10^5
	3	339.0	16.469	4.67×10^6
2'-fluoro-2'-deoxy-C	1	326.0	N/A	N/A
	2	326.0	N/A	N/A
	3	326.0	N/A	N/A
aza-C	1	325.0	17.898	9.46×10^5
	2	325.0	N/A	N/A
	3	325.0	N/A	N/A
riboaminopyrrole	1	339.0	17.422	4.39×10^5
	2	339.0	N/A	N/A
	3	339.0	18.451	4.66×10^5
xylo-C	1	325.0	N/A	N/A
	2	325.0	N/A	N/A
	3	325.0	N/A	N/A
2'-difluoro-C	1	344.0	N/A	N/A
	2	344.0	N/A	N/A
	3	344.0	N/A	N/A
ara-C	1	324.0	N/A	N/A
	2	324.0	N/A	N/A
	3	324.0	N/A	N/A
2'-methyl-C	1	338.0	N/A	N/A
	2	338.0	N/A	N/A
	3	338.0	N/A	N/A

Table 5.4: Results of EIC analysis of LCMS data aimed at detecting phosphorylated substrate in unnatural substrate reaction samples. Control data has not been included as no substrate monophosphate was detected in any sample. N/A has been entered where no relevant distinguishable peaks were observed. Full data in Appendix II.

As can be seen in *Figure 5.6*, substrate monophosphate was detected via LCMS analysis in samples relating to the reaction of UCK1 against the substrates 5-methyl-U, aza-C, and riboaminopyrrole. The presence of substrate monophosphate peaks in LCMS spectra relating to these samples indicates that UCK1 is somewhat active against 5-methyl-U, aza-C, and riboaminopyrrole as substrates. With regard to aza-C and riboaminopyrrole, the lack of detection of activity via ^{31}P NMR analysis indicates that this activity is occurring at an efficiency below the level of detection of the NMR methodology utilised in the present study. There is significant variation in the integrated substrate monophosphate peak areas within the reaction sets for these substrates, indicating variability in the activity of UCK1 in these experiments. The area of peaks corresponding to 5-methyl-U monophosphate appear to be greater than the peak areas corresponding to aza-C monophosphate and riboaminopyrrole monophosphate, supporting the ^{31}P NMR results that indicated a greater activity of UCK1 for 5-methyl-U than aza-C or riboaminopyrrole. The variability of the data between these samples, in particular inconsistency as to whether UCK1 activity is observed at all, makes further statistical analysis of this data redundant.

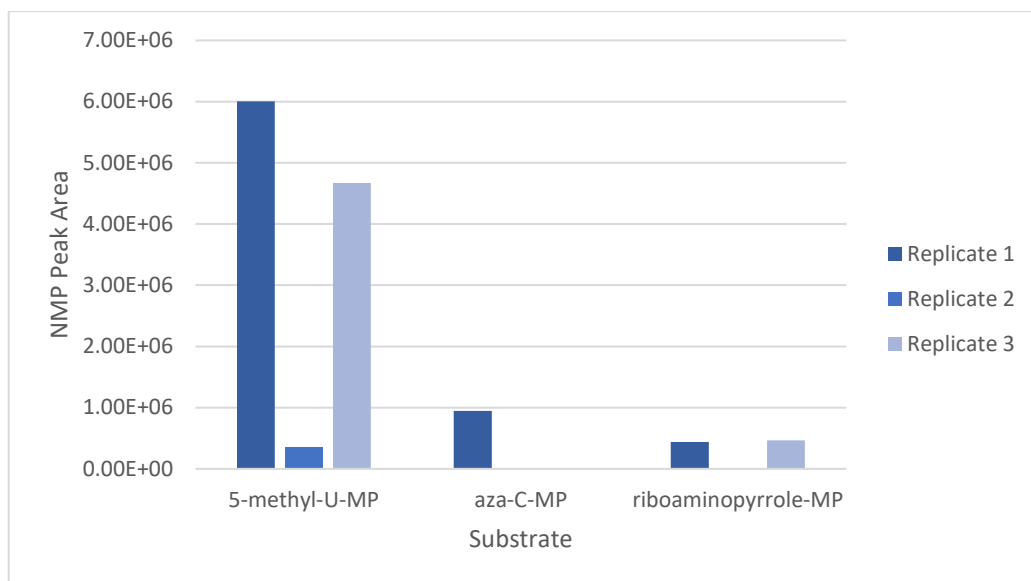


Figure 5.6: Areas of integrated nucleoside monophosphate LCMS peaks in reactions of UCK1 against unnatural substrates. Controls not included as no relevant peaks were observed. MP = monophosphate. Only substrates against which phosphorylative activity by UCK1 was observed have been included. Peaks identified through EIC analysis of data derived through LCMS analysis of relevant reaction samples. Compounds identified via EIC analysis targeting target mass charge \pm 0.5.

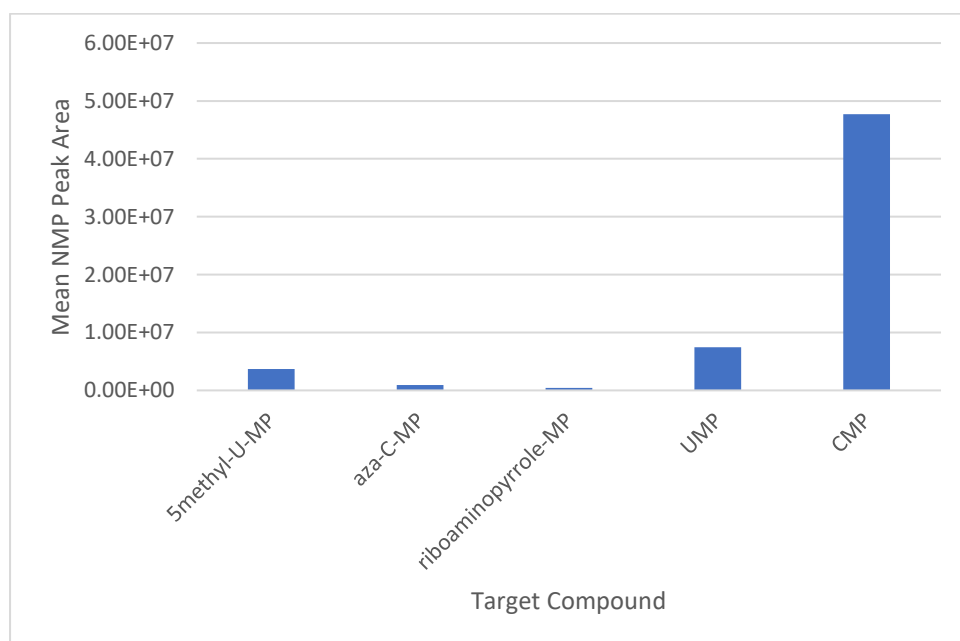


Figure 5.7: Comparison of mean nucleoside monophosphate peak area of UCK1 against unnatural and natural substrates. Substrates against which no activity was observed have been excluded. For substrates in which activity was not observed in all samples, samples in which no activity was observed have been excluded from calculations of mean peak area.

Comparison of the LCMS data derived from those unnatural substrates against which UCK1 exhibited activity with data derived from natural substrate UCK1 reactions indicates that the quantity of 5-methyl-U monophosphate produced was similar to production of UMP (Figure 5.7), in agreement with the results of ^{31}P NMR analysis. The production of aza-C monophosphate and riboaminopyrrole

monophosphate appears to be much lower than for the other substrates, supporting the hypothesis that the lack of activity seen in ^{31}P NMR analysis is due to the activity occurring at a level below the sensitivity of the methodology.

6.0 Discussion

6.1 Protein Production

6.1.1 Heterologous Protein Expression

The amount and quality of DNA used will affect the likelihood of success when attempting to transform competent cells with plasmid DNA.¹¹² The initial failure of transformation of BL21 *E. coli* cells described in *Section 3.2.1* was likely due to the degradation of the target plasmid on the filter paper whereon it had been stored. DNA is known to degrade faster at higher temperatures thus should the sample have been improperly stored prior to acquisition by the researchers of the present study this may have resulted in a reduction in DNA quality.¹¹³ Experimental observation in the laboratory has shown that the in-house produced BL21 *E. coli* cells are less chemically competent than the commercially sourced Stellar™ *E. coli* cells. This reduced competency may have resulted in an increased sensitivity to any reduction in DNA quality of the AgAK plasmid that had occurred.

6.1.2 Mode of Bacterial Lysis

Sonication-based and chemical-based lysis methodologies have been recently shown as having different bactericidal efficiencies in the lysis of cyanobacterial cultures.¹¹⁴ Although these results do not necessarily translate to the lysis of *E. coli* cultures as part of a protein production process, it suggests that analysis of the mode of cell lysis may represent a point of optimisation in which the production efficiencies of target protein could be improved.

Although no specific comparative analysis of lysis methodology was conducted, thus one's ability to draw conclusions is severely limited, a retrospective assessment of protein purification efficiency differences between the modes of lysis used in the present study may be a useful means of predicting the value of further investigation.

In the present study both chemical and sonication lysis were used in the purification process of the proteins AgAK, human UCK1, and PfGUK (*Section 3.0*). With regard to AgAK and PfGUK, both proteins were unable to be purified in useful amounts through purification processes that utilised either chemical or sonication lysis. As can be seen in *Figure 6.1*, human UCK1 purification efficiency was much higher from bacterial culture lysed chemically (18.27 µg/mL) than from culture lysed via sonication (9.75 µg/mL). It must be noted here that significantly different bacterial culture volumes were used in the protein purifications discussed here, the purification process involving chemical lysis used a 150 mL culture volume while the purification process involving sonication lysis used a 6000 mL culture volume. Thus, the discrepancy in protein production efficiencies observed here may be due to

factors independent of lysis mode and no scientific conclusions may be drawn from this data alone. It does however suggest that there may be value in further investigation into the impact of lysis mode on protein purification efficiency.

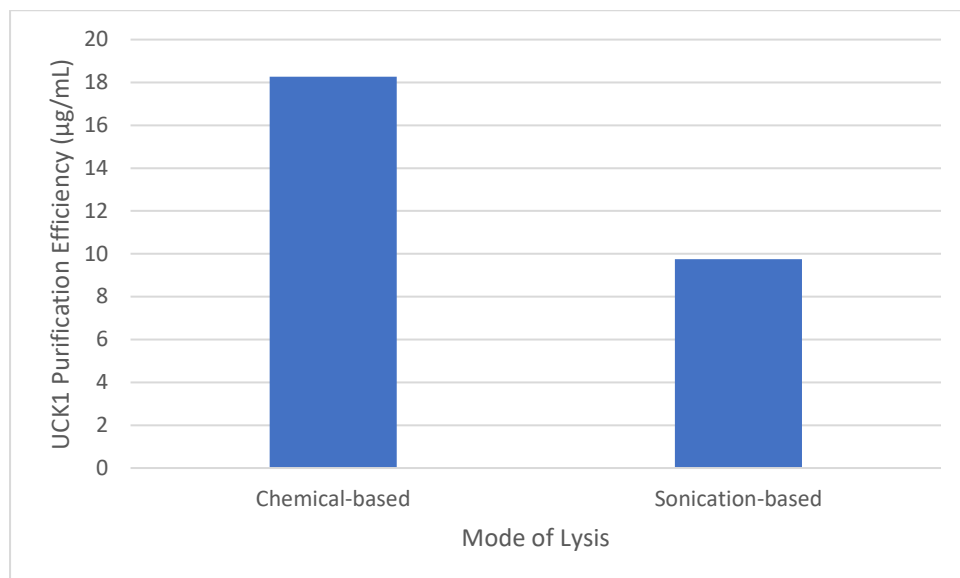


Figure 6.1: Comparison of protein purification efficiencies of UCK1 purifications utilising different modes of lysis. UCK1 purification efficiency given as µg of protein purified per mL of bacterial culture lysed. Relevant protein purification processes described in Section 3.3.2.

6.1.3 IMAC Protein Purification

Neither AgAK nor PfGUK were able to be successfully purified from cell lysate via IMAC in quantities sufficient for further analysis, despite the inclusion of a terminal His-tag in the amino acid sequences of both proteins. This failure of purification may have been caused by low protein expression by the relevant transformed BL21 cell strains, or by a failure of the IMAC methodology employed in the present study. Future investigations seeking to improve the production efficiency of these proteins should first investigate the source of this purification failure.

Recombinant proteins such as AgAK and PfGUK may be poorly expressed in the heterologous host if their expression results in toxicity to the cell.^{115, 116} Overexpression of recombinant protein may also result in an increased ‘metabolic burden’ on the heterologous host thus decreasing the bacterial growth rate and overall protein production.¹¹⁷ In this case it is unlikely that an increased ‘metabolic burden’ derived from protein overexpression influenced protein purification efficiency as no significant difference in growth rate was observed between any of the transformed cell strains described in Section 3.0. Further investigation is required to assess whether protein-induced toxicity impacted expression. In the case that the observed low protein purification efficiencies were in fact due to poor expression, a potential means of mitigating this would be the transformation of alternate bacterial strains with the

relevant plasmids and attempt of expression in and purification from these novel transformed strains. It has also been suggested that the removal of periplasmic material from *E. coli* cultures prior to lysis can increase yields of poorly expressed recombinant proteins.¹¹⁸

The IMAC process may be the failure point of protein production when the His-tag is insufficiently exposed within the tertiary structure of the recombinant protein thus cannot effectively interact with the chromatography column.¹¹⁹ This can be mitigated through analysis of the protein structure prior to design of the recombinant plasmid, and rational choice of the terminal on which the His-tag is to be located based on the relative likelihoods of exposure of each terminal to the column. An insufficiently exposed His-tag is unlikely to be the cause of the failure of AgAK purification as this recombinant protein has been successfully purified via IMAC previously.⁶³

6.1.4 IEC Protein Purification

Due to the non-selective nature of IEC purification, this methodology was not able to be successfully employed as a means to effectively purify FLAG-tagged human UCK2 and CMPK from bacterial lysate in the present study. The failure to purify these proteins was mitigated through the sourcing of plasmid constructs encoding the relevant enzymes in vectors that would incorporate a terminal His-tag into the protein. Another potential means of purifying the FLAG-tagged proteins would have been to use a FLAG-resin column.⁷⁵ In the case of the present study, the high cost of materials required for the immunoaffinity chromatography purification of FLAG-tagged proteins prohibited the use of such methodology.

An IEC protein purification methodology was also employed as a means of mitigating the previously discussed failure of IMAC purification of AgAK and PfGUK. The elution fractions derived from IEC purification were heavily contaminated with non-target protein, due to the non-selective nature of IEC. It was theorised that using the elution fragments containing target protein for a second IEC protocol with an extended gradient may increase the separation between the elution points of different proteins thus provide a purer sample of target protein. This double-IEC methodology did not have the desired effect as elution fractions containing target protein derived from the second run remained heavily contaminated. This indicates that IEC is an ineffective methodology to employ when attempting to purify specific recombinantly expressed proteins.

6.2 Optimisation of Catalytic Activity

6.2.1 Choice of Phosphate Donor

An aspect of the catalytic reaction of UCK that was not explored within the present study was the effect of different phosphate donor compounds on reaction efficiency. Non-human isoforms of UCK have been shown to be able to utilise purine NTPs other than ATP as phosphate donors, albeit at lower efficiency than with ATP, but little information was found regarding the UCKs used within the present study and non-ATP phosphate donor compounds.^{82, 120} Given this lack of information, further investigation into the use of such compounds as phosphate donors may provide a means of increasing NMP production by UCK. Pyrimidine NTPs have been shown to have inhibitory effect on UCK activity, thus are likely not useful as phosphate donors for this enzyme.^{120, 121}

6.2.2 Utility of Phosphate Donor Regeneration

A significant proportion of the optimisation experiments of the present study were done without the presence of the phosphate donor regeneration enzyme PK due to supply issues brought on by the Covid-19 pandemic. Due to this, the assessment of the enzymatic activity of these samples via ³¹P NMR spectroscopy was largely futile and the presence of such activity was not able to be determined. These results reinforce the importance of coupling nucleoside kinase reactions to phosphate regeneration systems if analysis is to be achieved in this way. The ease and speed of ³¹P NMR analysis makes this analytical methodology extremely efficient for iterative experiments such as a reaction optimisation process.

Enzymes other than PK can also be utilised as phosphate donor regenerators in enzymatic reaction systems such as used in the present study. Acetate kinase can be used to regenerate guanosine triphosphate in solution through consumption of guanosine diphosphate and acetyl phosphate, and has been shown to function effectively alongside the UCK catalytic reaction.^{82, 122} Polyphosphate kinase can catalyse the transfer of phosphate from polyphosphate to ADP to regenerate ATP thus may have utility as a phosphate donor regenerator in the presently discussed reaction system, although the chelation of Mg²⁺ by polyphosphate may inhibit utility given the ions importance in UCK catalytic activity.^{59, 123}

This variety of possible phosphate donor regeneration systems represents an additional point of optimisation within the discussed catalytic reaction, future research could investigate whether utilising alternate phosphate donor regenerators would further increase reaction efficiency.

6.2.3 Observed Activity of Nucleoside Monophosphate Kinases

The results of the *EcADK* activity test described in *Section 4.8.1* seemed to indicate that ribonucleotide monophosphate kinase catalytic activity was occurring in the reaction sample, as comparison of normalised peak integrals suggested a decrease in AMP and PEP concentration and/or an increase in ADP concentration from control to reaction sample. A similar pattern was also observed in the activity test of *PfGUK* described in *Section 4.8.2*. It must however be considered that these changes in integral size alone may not necessarily be indicative of ADP production. In the earlier *EcADK* activity test described in *Section 4.3.1* novel doublet peaks were observed in the reaction sample indicating the presence of ADP and catalytic activity by *EcADK*. Furthermore, in the spectra of the *CMPK* activity test described in *Section 4.8.5*, the presence of the product of *CMPK* catalytic activity UDP resulted in the appearance of two novel doublet peaks distinct from those of ATP. Thus, although the changes in peak size seen in the results of the experiments described in *Section 4.8.1* and *Section 4.8.2* may be consistent with the catalytic activity of *EcADK* and *PfGUK*, the lack of novel doublet peaks in the reaction spectra may imply that ADP is in fact not being produced as a result of enzymatic activity. Furthermore, the similarity in amplitude of peak integral changes between the *EcADK* and *PfGUK* experiments is not consistent with the differing affinities for AMP as a substrate that has been reported for these enzymes in the literature.^{101, 104}

6.2.4 Duration of Reaction

The thirty-minute duration of reaction utilised throughout the reaction optimisation process and activity tests was largely chosen due to the practicalities of performing all the necessary experiments within the timeframe allowed for the presently discussed project, although this reaction duration has also been successfully utilised for *UCK* activity testing in the past.⁶⁰ The translation of the optimised reaction of the present study into a synthetic tool would likely involve extending this duration, high yields have been seen in enzyme-catalysed nucleotide synthesis systems with reaction durations between twelve and nineteen hours.^{82, 83}

6.2.5 Potential Phosphate Contamination

Some of the previously described *UCK1* catalytic reaction optimisation experiments had been erroneously conducted using *PK* samples purified using phosphate-containing buffer thus the reaction samples themselves may have had phosphate contamination. This contamination, had it occurred, would result in the presence of free phosphate in solution and the appearance of a small peak with size relative

to PK concentration of the sample (*Section 4.2.8*). In samples known to contain free phosphate this peak seems to consistently exist slightly upfield of the peak attributed to the phosphate group of UMP.

The particular experiments affected by this potential contamination were the UCK1 concentration study, the PK concentration study, and the addition strategy study described in *Section 4.8*, *Section 4.9*, and *Section 4.10* respectively. In some of the ^{31}P spectra of these samples a small peak can be observed slightly downfield of the peak that was attributed to the phosphate group of UMP (*Figure 6.2*). Given the previously described spatial relationship between the free phosphate and UMP-phosphate peaks, there is potential that the peak that has been attributed to UMP-phosphate may in fact be due to free phosphate contamination while the minor peak downfield of this is representative of a very slight amount of phosphorylative activity. If this is the case then there has been very little enzymatic activity in any sample, and the results of these experiments cannot be used to draw further conclusions regarding optimal reaction conditions.

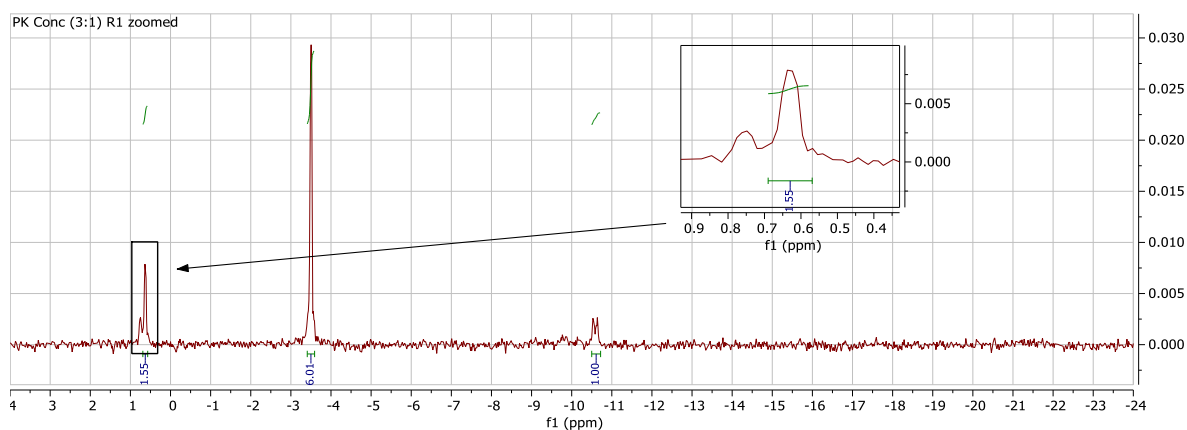


Figure 6.2: Representative ^{31}P NMR spectra depicting UMP and phosphate peaks in potentially phosphate-contaminated experiments. Spectra derived from PK concentration study 3:1 ratio sample 1 (*Section 4.9*) with zoom region depicting relevant peaks. Full spectra provided in Appendix I.9.

It has however been observed that there can be considerable variation in chemical shift of phosphate peaks appearing on ^{31}P NMR spectra (*Section 4.7*), thus it is entirely possible that the free phosphate peak has exhibited a minor downfield change in chemical shift in these spectra and that phosphate contamination is not responsible for the large peak that had been attributed to UMP-phosphate. This interpretation of the presently discussed results is congruent with the results of the UCK1-uridine reactions described in *Section 5.2*, the mean calculated substrate conversion of these was $14.12 \pm 6.21\%$, the ‘optimal’ results of each of the potentially contaminated experiments all fall within this range (14.00%, 19.04%, 14.01%). It is relevant to note that the experiments described in *Section 5.2* used a different source of PK known to not have phosphate contamination. In the case of the UCK1

concentration study, the observed increased activity with increasing enzyme concentration is consistent with what previous studies involving UCK have reported.⁸²

It is likely that the phosphate contamination that may have occurred in these experiments did not majorly influence the results, although it is essential that any further optimisation of the UCK1 catalytic reaction described herein involves repetition of these experiments to ensure the veracity of the results.

6.2.6 Choice of Component Concentration

Many studies aimed at assessing the activity of nucleoside kinase enzymes have used substrate concentrations at or below 1 mM, often in concert with a stoichiometric excess of ATP.^{60, 103, 106} The 12.5 mM substrate concentration used in the catalytic activity tests of the present study was chosen with the ultimate goal of employing the reaction methodology synthetically. This strategy of utilising high substrate concentrations in synthetic reaction mixtures has been successfully employed previously.⁸² Another key difference in the component concentrations used in the present study and those typically used during the assessment of activity of similar enzymes is concentration of the phosphate donor compound. Many studies have used phosphate donor concentrations stoichiometrically equivalent to or in excess of substrate concentration, in some cases such a strategy has been utilised even with the presence of a phosphate donor regeneration enzyme.^{60, 83, 103} The present study utilised an ATP concentration equivalent to one fifth of substrate concentration representing an excess of substrate. Although this strategy is less commonly seen in the literature, it has been successfully employed in studies aimed at both synthesis and the characterisation of enzymatic activity.^{82, 124} It is worth noting that in both studies referenced in the previous statement, a phosphate donor regeneration system was used within the reaction mixtures.

With regard to enzyme concentration, the amounts of UCK used in the presently discussed study were far in excess of any reported in the literature that was reviewed. Although the enzyme concentrations used in this study were selected following the results of optimisation experiments, this discrepancy indicates that further investigation into the optimal enzyme concentration within such a reaction mixture may be warranted. Fehlau et al. (2010) for example were able to achieve up to 99% conversion of nucleoside to NTP in a multi-enzyme ‘one-pot’ system with rNK concentration approximately eight-fold lower than used in the present study, albeit with a nineteen hour reaction duration.⁸³ It is relevant to note here that substrate concentrations used in the previously mentioned study were approximately twelve-fold lower than what was used in the present study. The substrate concentration used in the present study was chosen with the ultimate goal of producing synthetically useful quantities of product compound in mind.

6.3 Activity Against Unnatural Substrates

6.3.1 Predicted Utility of Ribonucleoside Kinases

Of the six different rNKs selected for use in the present study, three catalyse the addition of an α -phosphate to their substrate nucleosides (AgAK, human UCK1, human UCK2) while three catalyse the addition of a β -phosphate to their substrate NMPs (*Ec*ADK, *Pf*GUK, human CMPK). The unnatural nucleosides involved in the present study all have pyrimidine nucleobases with the exception of riboaminopyrrole which bears a pyrrole nucleobase. UCK1 and UCK2 thus have the strongest likelihood of exhibiting activity against the unnatural substrates of the present study given their affinity for natural pyrimidine nucleosides and AgAK's lack thereof.^{60, 63} With regard to β -phosphate addition, should future investigations continue the research of the present study CMPK would seem to have the most potential utility, again due to the greater affinity for natural pyrimidine NMPs possessed by the enzyme over *Ec*ADK and *Pf*GUK.^{101, 104, 125, 126}

6.3.2 Impact of Substrate Solubility

The solubility of some of the unnatural nucleosides used in the presently discussed experiments may have affected the observed lack of activity of UCK1 against them. The compounds 2'-fluoro-2'-deoxy-C and 2'-difluoro-C both resisted dissolution in dH₂O at room temperature, requiring heating to approximately 60 °C before complete dissolution when generating a 125 mM 10 × stock solution. The reduced solubility exhibited by these compounds is likely due to the fluorine substitutions each of these compounds bear, the presence of fluorine atoms is known to increase the lipophilicity of nucleoside analogues.¹²⁷

This reduced solubility, when compared to the other nucleosides of the present study, may have resulted in precipitation of the compound during the 30 minutes of 37 °C heating during the reaction process. Should this precipitation have been occurring, the true concentration of substrate in solution would have been less than expected in those samples which may have impacted the observed enzymatic activity. Visual monitoring of the reaction solutions throughout the reaction process could be utilised in future studies involving these compounds to assess whether precipitation is in fact occurring.

6.3.3 Activity of UCK1

In the presently discussed experiments, UCK1 was observed to exhibit a phosphorylation efficiency against cytidine that was approximately 500% of the phosphorylation efficiency of the enzyme for uridine. The observed marked difference in activity between these natural substrates conflicts with the

results of Van Rompay et al. (2001), who found that human UCK1 phosphorylated cytidine with an efficiency approximately 120% of the enzyme for uridine.⁶⁰ This discrepancy may be due to the different reaction conditions used in these studies, although further investigation would be required to confirm this. It must be noted that the timescale used in the previously mentioned paper is identical to that used in the reactions of the present study.

5-methyl-U was the only unnatural substrate of the present study which human UCK1 was able to phosphorylate with activity detectable by ³¹P NMR analysis of the reaction mixture (*Section 5.3.1*). Application of the substrate conversion quantification model, described in *Section 4.7*, to the ³¹P NMR spectra derived from UCK1/5-methyl-U reactions revealed mean estimated conversion of 13.67% of total substrate in solution. It must be noted that this calculation excludes the reaction sample in which enzymatic activity was not observed via ³¹P NMR, thus the reliability of this mean may be weak. These results are in conflict with the observations of Van Rompay et al. (2001), who found that the phosphorylation efficiency of human UCK1 against 5-methyl-U was less than 5% that of the enzyme against uridine.⁶⁰ The differences in UCK1 activity against these substrates may again be explained by the different reaction conditions used in the studies, although further investigation would be required to confirm this.

Another unnatural nucleoside which UCK1 was tested against in both the present study and that of Van Rompay et al. (2001) is aza-C, referred to in the Van Rompay et al. study as 5-azacytidine. In this case the results of these studies are in agreement, UCK1 activity against aza-C was observed to be less than 5% of that of the enzyme against uridine by Van Rompay et al. and in the present study activity was below the limit of detection of the ³¹P NMR methodology employed.⁶⁰ Aza-C is however known to be phosphorylated by UCK enzymes in models of leukaemia, although it is unclear which isoform is responsible for this.¹²⁸

The lack of activity of UCK1 against the unnatural substrates observed in the present study may be due to the mechanism of substrate binding to the enzyme. Of the eight unnatural nucleosides tested, only those with modifications to the nucleobase moiety were observed to have had any phosphorylative activity by any analytical method. Those compounds against which no activity whatsoever was observed all had modifications to the sugar moiety. A study of the crystal structure of UCK2 by Suzuki et al. (2004) suggested that the sugar moiety of substrate binds to the active site initially then induces a conformational change resulting in binding of the base moiety.⁵⁹ This mode of binding requires tight binding of the sugar moiety, thus the lack of activity observed against sugar-modified nucleosides may be due to the strength of this initial binding and fit of the sugar moiety into the active site. Although the study in question refers to UCK2 and the present study assessed UCK1 activity, the similarity of activity of these enzymes suggests a similarity of active sites and infers that this importance of the sugar moiety structure may also apply to UCK1.⁶⁰

6.3.4 Activity of UCK2

Human UCK2 has been shown to have good activity against not only uridine and cytidine, but also a range of both sugar and base-modified unnatural nucleosides.^{60, 87, 88} The markedly reduced activity against natural substrates of human UCK2 compared to UCK1 observed in the present study is in stark contrast to the increased affinity of UCK2 that has previously been reported in the literature.⁶⁰ This discrepancy indicates that the IMAC-purified samples of UCK2 may have contained a largely non-functional form of the enzyme, as its presence in solution was supported by PAGE analysis (*Section 3.4.2.2*). The inclusion of a terminal His-tag in a polypeptide, although a common and generally impact-free strategy, has been shown to in some cases affect the structure, function, and stability of proteins.¹²⁹⁻¹³³ Thus, the His-tag incorporated into the sequence of the recombinant UCK2 of the present study may be responsible for this lack of function.

It may also be that the protein fragment approximately 30 kDa in size observed via PAGE analysis was not entirely due to the presence of human UCK2 in solution. The low level of phosphorylative activity observed towards cytidine as a substrate via LCMS analysis (*Section 5.2.2*) indicates that UCK2 is indeed present in the discussed samples, however it may be that a co-eluted protein of similar size is also present thus making the actual UCK2 concentration lower than expected. The presence of UCK in said samples could be further supported through Western blot analysis.¹³⁴

Given the utility that UCK2 has previously shown for the phosphorylation of unnatural nucleosides, it would be valuable for future research aimed at further developing the synthetic utility of the reaction system described herein to focus on the production of a functional variant of human UCK2 against which the unnatural substrates could be tested.

6.4 Quantification Curve

The NMP conversion quantification model developed in the present study could represent a useful tool for the assessment of enzymatic NMP production by nucleotide kinases beyond those of the present study. Although ³¹P NMR spectroscopy has been used for the quantification of nucleotides previously, the present study seems to represent the first reporting of the use of a ³¹P NMR based statistical model to quantify nucleoside kinase activity.¹³⁵⁻¹³⁸ Given the similarity in the ³¹P NMR signals derived from different NMPs, as observed with AMP and UMP in the present study, it is likely that the utility of this model could extend to calculating the conversion of nucleosides other than uridine to their monophosphate derivatives. This extended utility could be validated through the generation of a series of samples of known ingredient concentration with nucleosides other than uridine and assessment of the model's calculated conversion against the known value, in a similar manner as described in *Section 4.7.3*.

The concept developed here may also be able to be applied to the quantification of activity of nucleoside monophosphate kinases such as CMPK and ADK, by replacing the nucleoside and NMPs of the samples with NMPs and NDPs respectively. Given the similarities in ^{31}P NMR spectra of NDP and NTP compounds, quantification of target NDP production by nucleoside monophosphate kinase enzymes through this methodology may be prohibitively difficult.

6.5 Limitations of Present Study

A major limitation of the present study was a lack of access to PK throughout early stages of experimental work. This lack of access was largely caused by supply chain delays resulting from the impact of the global response to the Covid-19 pandemic on said supply chains.

Without the ATP regeneration provided by PK, the required ATP concentration in the reaction mixture was higher. This resulted in the ^{31}P NMR signals of the phosphate groups of ATP masking those of any substrate monophosphates that may have occurred as a result of enzymatic activity. As can be seen in *Section 4.5* and *Section 4.6*, this masking effect was not able to be overcome through increasing the duration of reaction or providing substrate in stoichiometric excess to phosphate donor concentration. The inability of these experiments to overcome this masking effect reinforces the importance of including a phosphate donor regeneration enzyme such as PK in the reaction mixture when using ^{31}P NMR analysis to detect rNK action.

Another limitation of the present study was the lack of variety of rNK enzymes that were able to be successfully purified, proven functional, and tested against the unnatural substrates. Although the methods used to source plasmids encoding the target proteins fit the purposes of the present study, future investigations could utilise specifically designed plasmid constructs such as described in *Section 3.4.2.1* and *Section 3.7.2.1*. This approach may serve to improve overall protein purification efficiencies and enzymatic activity as it would allow the choice of expression vectors known to function well with the methodology utilised in this study and the design of constructs in a manner conducive to catalytic activity.

6.6 Future Development

6.6.1 Synthetic Utility

Within the time constraints of the present study, it was not possible to attempt the successful isolation of target phosphorylated nucleoside from the reaction mixture following the termination of catalytic activity. Methods of achieving this isolation using automated flash chromatography with an ion

exchange methodology have been developed by researchers involved with the wider project that the present study is part of. This methodology has been successfully employed in the isolation of compounds similar to those described in the present study, however further development may still be necessary to optimise function for the presently discussed reaction system.

In order to validate the use of rNKs such as UCK for synthetic use, the reaction methodology employed in the present study must be proven to function at sufficient scale so as to produce synthetically useful amounts of product compound. Using 5-methyl-U as an example and assuming that 100 mg of 5-methyl-U monophosphate is required, with the reaction conditions used and yields observed in the present study the reaction would need to be conducted on a 227.27 mL reaction mixture scale to produce the required amount. This calculation also assumes that no target compound loss occurs during isolation and work-up, that the reaction is perfectly scalable, and that the mean substrate conversion calculated from the two 5-methyl-U reactions in which catalytic activity was observed is correct. It must be noted (as previously stated) that increasing the duration of reaction may be an alternate means of increasing product compound production thus reducing the magnitude of scale increase needed to produce the required amount of compound.

There are also many reaction condition variables that were not assessed for optimisation during the present study. Increasing the yield of reaction through increasing reaction efficiency would serve to reduce the necessary magnitude of scale increase while also potentially increasing the economic efficiency as well. Further optimisation of reaction conditions could explore factors such as the duration of reaction, the concentration of Mg^{2+} in solution, the temperature of reaction, and the buffer compound used in the reaction buffer.

6.6.2 ‘One-pot’ Reaction Development

The experimental work described in the present study could be furthered through the inclusion of CMPK and a NDPK in the reaction mixture and subsequent optimisation of this process.⁸³ Previously developed ‘one-pot’ enzymatic synthesis processes such as this have shown utility in the production of 5'-triphosphate derivatives of both base- and sugar-modified nucleoside analogues, although substrate concentrations used within these studies were approximately ten-fold lower than in the present study.⁸³

¹³⁹ Given the high substrate concentration of the optimised reaction of the present study, and observed conversion efficiencies for conversion of both natural and unnatural nucleosides to their monophosphate derivatives, the development of the strategy of the present study into a fully coupled ‘one-pot’ synthetic system could result in a major increase in yield for such systems as applies to unnatural nucleosides. If nucleoside diphosphate is the desired product, similar systems have also been employed for the enzymatic synthesis of these compounds.¹⁴⁰

7.0 Concluding Remarks

The present study aimed to assess the utility of a range of nucleoside kinase enzymes in the synthesis of 5'-phosphorylated nucleoside analogues, as progress towards the ultimate goal of developing a scalable 'one-pot' methodology for the enzyme-catalysed production of nucleoside mono, di, and triphosphates. Further to this, the study also aimed to develop an efficient and effective method for the quantification of nucleoside kinase substrate turnover.

The substrate conversion quantification model developed in this study represents a facile means of calculating the catalytic activity of nucleoside kinase enzymes through ^{31}P NMR spectroscopy. ^{31}P NMR analysis is a relatively fast methodology to perform thus use of this model allows for large amounts of samples to be processed in a short timeframe. The quantification model was also shown to be accurate against increased substrate concentrations.

An optimised reaction process was developed for human UCK1, the optimal reaction conditions identified in the present study utilised a UCK concentration of 1.5 mg/mL, a PK concentration of 3 mg/mL, and a fixed UCK addition strategy. Human UCK1 was shown to have phosphorylative activity against a range of nucleobase-modified nucleoside analogues including 5-methyl-U, riboaminopyrrole, and aza-C. The lack of activity observed against sugar-modified nucleoside analogues reinforced the importance of the sugar moiety in nucleoside binding to UCK and indicates a low tolerability of the enzyme for modifications at this moiety.

The reaction process developed in the present study represents a significant step towards the development of an efficient means of synthesising phosphorylated derivatives of nucleoside analogues through enzyme-catalysed reaction. Future efforts on this research should focus on the development of an effective means of isolating product compound from the reaction mixture and increasing the scale of reaction to produce synthetically useful amounts of the target product compound. The scope of nucleoside analogues assessed against the enzymes of the present study could also be expanded.

References

1. Nelson, D. L.; Cox, M. M., *Principles of Biochemistry*. 6th ed.; W. H. Freeman,: New York, NY, 2013.
2. Seley-Radtke, K. L.; Yates, M. K., The evolution of nucleoside analogue antivirals: A review for chemists and non-chemists. Part 1: Early structural modifications to the nucleoside scaffold. *Antiviral Res.* **2018**, *154*, 66-86.
3. Lodish, H.; Berk, A.; Matsudaira, P.; Kaiser, C. A.; Krieger, M.; Scott, M. P.; Zipursky, L.; Darnell, J., *Molecular Cell Biology*. 5th ed.; W. H. Freeman,: New York, NY, 2003.
4. Rothwell, P. J.; Waksman, G., Structure and mechanism of DNA polymerases. *Adv. Protein Chem.* **2005**, *71*, 401-440.
5. Steitz, T. A., A mechanism for all polymerases. *Nature* **1998**, *391* (6664), 231-232.
6. Durmuş, S.; Ülgen, K. Ö., Comparative interactomics for virus–human protein–protein interactions: DNA viruses versus RNA viruses. *FEBS Open Bio* **2017**, *7* (1), 96-107.
7. Cann, A. J., Replication of Viruses. In *Encyclopedia of Virology*, 3rd ed.; Mahy, B. W. J.; Van Regenmortel, M. H. V., Eds. Academic Press: Cambridge, MA, 2008; pp 406-412.
8. Chinchar, V., Replication of Viruses. In *Encyclopedia of Virology*, 2nd ed.; Granoff, A.; Webster, R. G., Eds. Academic Press: Cambridge, MA, 1999; pp 1471-1478.
9. Leyssen, P.; De Clercq, E.; Neyts, J., Molecular strategies to inhibit the replication of RNA viruses. *Antiviral Res.* **2008**, *78* (1), 9-25.
10. McDonald, S. M., RNA synthetic mechanisms employed by diverse families of RNA viruses. *Wiley Interdiscip. Rev. RNA* **2013**, *4* (4), 351-367.
11. Ng, K. K.-S.; Arnold, J. J.; Cameron, C. E., Structure-function relationships among RNA-dependent RNA polymerases. In *RNA Interference*, Paddison, P. J.; Vogt, P. K., Eds. Springer Berlin Heidelberg: Berlin, Germany, 2008; pp 137-156.
12. Warren, T. K.; Wells, J.; Panchal, R. G.; Stuthman, K. S.; Garza, N. L.; Van Tongeren, S. A.; Dong, L.; Retterer, C. J.; Eaton, B. P.; Pegoraro, G., Protection against filovirus diseases by a novel broad-spectrum nucleoside analogue BCX4430. *Nature* **2014**, *508* (7496), 402-405.

13. Gizzi, A. S.; Grove, T. L.; Arnold, J. J.; Jose, J.; Jangra, R. K.; Garforth, S. J.; Du, Q.; Cahill, S. M.; Dulyaninova, N. G.; Love, J. D., A naturally occurring antiviral ribonucleotide encoded by the human genome. *Nature* **2018**, 558 (7711), 610-614.
14. Thomas, E.; Ghany, M. G.; Liang, T. J., The application and mechanism of action of ribavirin in therapy of hepatitis C. *Antiviral Chemistry and Chemotherapy* **2012**, 23 (1), 1-12.
15. Venkataraman, S.; Prasad, B. V. L. S.; Selvarajan, R., RNA dependent RNA polymerases: insights from structure, function and evolution. *Viruses* **2018**, 10 (2), 76.
16. Panjkovich, A.; Daura, X., Assessing the structural conservation of protein pockets to study functional and allosteric sites: implications for drug discovery. *BMC Struct. Biol.* **2010**, 10 (1), 1-14.
17. Zvereva, M. I.; Shcherbakova, D. M.; Dontsova, O. A., Telomerase: structure, functions, and activity regulation. *Biochem. (Mosc.)* **2010**, 75 (13), 1563-1583.
18. Svarovskaia, E. S.; Cheslock, S. R.; Zhang, W.-H.; Hu, W.-S.; Pathak, V. K., Retroviral mutation rates and reverse transcriptase fidelity. *Front. Biosci.* **2003**, 8 (4), d117-134.
19. Ceccherini-Silberstein, F.; Gago, F.; Santoro, M.; Gori, C.; Svicher, V.; Rodríguez-Barrios, F.; d'Arrigo, R.; Ciccozzi, M.; Bertoli, A.; Monforte, A. d. A., High sequence conservation of human immunodeficiency virus type 1 reverse transcriptase under drug pressure despite the continuous appearance of mutations. *J. Virol.* **2005**, 79 (16), 10718-10729.
20. Poch, O.; Sauvaget, I.; Delarue, M.; Tordo, N., Identification of four conserved motifs among the RNA-dependent polymerase encoding elements. *EMBO J.* **1989**, 8 (12), 3867-3874.
21. Gao, G.; Orlova, M.; Georgiadis, M. M.; Hendrickson, W. A.; Goff, S. P., Conferring RNA polymerase activity to a DNA polymerase: a single residue in reverse transcriptase controls substrate selection. *Proc. Natl. Acad. Sci. U.S.A* **1997**, 94 (2), 407-411.
22. Cihlar, T.; Ray, A. S., Nucleoside and nucleotide HIV reverse transcriptase inhibitors: 25 years after zidovudine. *Antiviral Res.* **2010**, 85 (1), 39-58.
23. Furuta, Y.; Komeno, T.; Nakamura, T., Favipiravir (T-705), a broad spectrum inhibitor of viral RNA polymerase. *Proc. Jpn. Acad. Ser. B, Phys. Biol. Sci.* **2017**, 93 (7), 449-463.
24. Appleby, T.; Shih, I.-h.; Zhong, W., Viral RNA Polymerase Inhibitors. In *Viral Genome Replication*, Raney, K. D.; Gotte, M.; Cameron, C. E., Eds. Springer US: Boston, MA, 2009; pp 527-548.

25. Payne, S., Chapter 10 - Introduction to RNA Viruses. In *Viruses*, Payne, S., Ed. Academic Press: 2017; pp 97-105.
26. De Clercq, E.; Neyts, J., Antiviral Agents Acting as DNA or RNA Chain Terminators. In *Antiviral Strategies*, Kräusslich, H.-G.; Bartenschlager, R., Eds. Springer Berlin Heidelberg: Berlin, Germany, 2009; pp 53-84.
27. Reid, R.; Mar, E. C.; Huang, E. S.; Topal, M. D., Insertion and extension of acyclic, dideoxy, and ara nucleotides by herpesviridae, human alpha and human beta polymerases. A unique inhibition mechanism for 9-(1, 3-dihydroxy-2-propoxymethyl) guanine triphosphate. *J. Biol. Chem.* **1988**, 263 (8), 3898-3904.
28. Piliero, P. J., Pharmacokinetic properties of nucleoside/nucleotide reverse transcriptase inhibitors. *J. Acquir. Immune Defic. Syndr.* **2004**, 37, S2-S12.
29. Sofia, M. J.; Chang, W.; Furman, P. A.; Mosley, R. T.; Ross, B. S., Nucleoside, nucleotide, and non-nucleoside inhibitors of hepatitis C virus NS5B RNA-dependent RNA-polymerase. *J. Med. Chem.* **2012**, 55 (6), 2481-2531.
30. Stein, D. S.; Moore, K. H. P., Phosphorylation of nucleoside analog antiretrovirals: a review for clinicians. *Pharmacotherapy* **2001**, 21 (1), 11-34.
31. Wermuth, C.-G.; Ganellin, C. R.; Lindberg, P.; Mitscher, L. A., Glossary of terms used in medicinal chemistry (IUPAC Recommendations 1998). *Pure Appl. Chem.* **1998**, 70 (5), 1129-1143.
32. Hajnal, K.; Gabriel, H.; Aura, R.; Erzsébet, V.; Blanka, S. S., Prodrug strategy in drug development. *Acta Med Marisiensis* **2016**, 62 (3), 356-362.
33. Pradere, U.; Garnier-Amblard, E. C.; Coats, S. J.; Amblard, F.; Schinazi, R. F., Synthesis of nucleoside phosphate and phosphonate prodrugs. *Chem. Rev.* **2014**, 114 (18), 9154-9218.
34. Van Rompay, A. R.; Johansson, M.; Karlsson, A., Phosphorylation of nucleosides and nucleoside analogs by mammalian nucleoside monophosphate kinases. *Pharmacol. Ther.* **2000**, 87 (2-3), 189-198.
35. Sofia, M. J.; Bao, D.; Chang, W.; Du, J.; Nagarathnam, D.; Rachakonda, S.; Reddy, P. G.; Ross, B. S.; Wang, P.; Zhang, H.-R., Discovery of a β -d-2'-deoxy-2'- α -fluoro-2'- β -C-methyluridine nucleotide prodrug (PSI-7977) for the treatment of hepatitis C virus. *J. Med. Chem.* **2010**, 53 (19), 7202-7218.

36. Hong Kang, S.; Sinhababu, A.; Cho, M. J., Synthesis and biological activity of bis (pivaloyloxymethyl) ester of 2'-azido-2'-deoxyuridine 5'-monophosphate. *Nucleosides Nucleotides* **1998**, *17* (6), 1089-1098.
37. Lefebvre, I.; Perigaud, C.; Pompon, A.; Aubertin, A.-M.; Girardet, J.-L.; Kirm, A.; Gosselin, G.; Imbach, J.-L., Mononucleoside phosphotriester derivatives with S-acyl-2-thioethyl bioreversible phosphate-protecting groups: intracellular delivery of 3'-azido-2', 3'-dideoxythymidine 5'-monophosphate. *J. Med. Chem.* **1995**, *38* (20), 3941-3950.
38. Mehta, R.; Chekmeneva, E.; Jackson, H.; Sands, C.; Mills, E.; Arancon, D.; Li, H. K.; Arkell, P.; Rawson, T. M.; Hammond, R.; Amran, M.; Haber, A.; Cooke, G.; Noursadeghi, M.; Kaforou, M.; Lewis, M.; Takats, Z.; Sriskandan, S., **2021**, Antiviral metabolite 3'-Deoxy-3',4'-didehydro-cytidine is detectable in serum and identifies acute viral infections including COVID-19. medRxiv doi:10.1101/2021.07.23.21260740
39. Helbig, K. J.; Beard, M. R., The Role of Viperin in the Innate Antiviral Response. *J. Mol. Biol.* **2014**, *426* (6), 1210-1219.
40. Ichikawa, E.; Kato, K., Sugar-modified nucleosides in past 10 years, a review. *Curr. Med. Chem.* **2001**, *8* (4), 385-423.
41. Mahmoud, S.; Hasabelnaby, S.; Hammad, S.; Sakr, T., Antiviral nucleoside and nucleotide analogs: a review. *J. Adv. Pharm. Res.* **2018**, *2* (2), 73-88.
42. Keating, G. M.; Vaidya, A., Sofosbuvir: First Global Approval. *Drugs* **2014**, *74* (2), 273-282.
43. Robinson, D. M.; Scott, L. J.; Plosker, G. L., Entecavir. *Drugs* **2006**, *66* (12), 1605-1622.
44. Sperling, R., Zidovudine. *Infect. Dis. Obstet. Gynecol.* **1998**, *6*, 372720.
45. Hervey, P. S.; Perry, C. M., Abacavir. *Drugs* **2000**, *60* (2), 447-479.
46. Buchanan, R. A.; Hess, F., Vidarabine (Vira-A®): pharmacology and clinical experience. *Pharmacol. Ther.* **1980**, *8* (1), 143-171.
47. Seth, A. K.; Misra, A.; Umrigar, D., Topical Liposomal Gel of Idoxuridine for the Treatment of Herpes Simplex: Pharmaceutical and Clinical Implications. *Pharm. Dev. Technol.* **2005**, *9* (3), 277-289.

48. Carmine, A. A.; Brogden, R. N.; Heel, R. C.; Speight, T. M.; Avery, G. S., Trifluridine: A Review of its Antiviral Activity and Therapeutic Use in the Topical Treatment of Viral Eye Infections. *Drugs* **1982**, *23* (5), 329-353.
49. Rabasseda, X., Brivudine: a herpes virostatic with rapid antiviral activity and once-daily dosing. *Drugs Today (Barc.)* **2003**, *39* (5), 359.
50. Johnson, D. C.; Widlanski, T. S., Overview of the synthesis of nucleoside phosphates and polyphosphates. *Curr. Protoc. Nucleic Acid Chem.* **2003**, *15* (1), 13.1. 1-13.1. 31.
51. Wu, W.; Bergstrom, D. E.; Davisson, V. J., A combination chemical and enzymatic approach for the preparation of azole carboxamide nucleoside triphosphate. *J. Org. Chem.* **2003**, *68* (10), 3860-3865.
52. Kimura, J.; Fujisawa, Y.; Yoshizawa, T.; Fukuda, K.; Mitsunobu, O., Studies on Nucleosides and Nucleotides, VII. Preparation of Pyrimidine Nucleoside 5'-Phosphates and N 3, 5'-Purine Cyclonucleosides by Selective Activation of the 5'-Hydroxyl Group. *Bull. Chem. Soc. Jpn.* **1979**, *52* (4), 1191-1196.
53. Sun, Q.; Gong, S.; Sun, J.; Wang, C.; Liu, S.; Liu, G.; Ma, C., Efficient synthesis of nucleoside 5'-triphosphates and their β , γ -bridging oxygen-modified analogs from nucleoside 5'-phosphates. *Tetrahedron Lett.* **2014**, *55* (13), 2114-2118.
54. Wood, J. M.; Evans, G. B.; Grove, T. L.; Almo, S. C.; Cameron, S. A.; Furneaux, R. H.; Harris, L. D., Chemical Synthesis of the Antiviral Nucleotide Analogue ddhCTP. *J. Org. Chem.* **2021**.
55. Marutzky, R.; Peterssen-Borstel, H.; Flossdorf, J.; Kula, M. R., Large scale enzymatic synthesis of nucleoside-5'-monophosphates using a phosphotransferase from carrots. *Biotechnol. Bioeng.* **1974**, *16* (11), 1449-1458.
56. Li, Z.; Ning, X.; Zhao, Y.; Zhang, X.; Xiao, C.; Li, Z., Efficient One-Pot Synthesis of Cytidine 5'-Monophosphate Using an Extremophilic Enzyme Cascade System. *J. Agric. Food Chem.* **2020**, *68* (34), 9188-9194.
57. Van Rompay, A. R.; Johansson, M.; Karlsson, A., Substrate specificity and phosphorylation of antiviral and anticancer nucleoside analogues by human deoxyribonucleoside kinases and ribonucleoside kinases. *Pharmacol. Ther.* **2003**, *100* (2), 119-139.
58. Schaertl, S.; Konrad, M.; Geeves, M. A., Substrate specificity of human nucleoside-diphosphate kinase revealed by transient kinetic analysis. *J. Biol. Chem.* **1998**, *273* (10), 5662-5669.

59. Suzuki, N. N.; Koizumi, K.; Fukushima, M.; Matsuda, A.; Inagaki, F., Structural basis for the specificity, catalysis, and regulation of human uridine-cytidine kinase. *Structure* **2004**, *12* (5), 751-764.
60. Van Rompay, A. R.; Norda, A.; Lindén, K.; Johansson, M.; Karlsson, A., Phosphorylation of uridine and cytidine nucleoside analogs by two human uridine-cytidine kinases. *Mol. Pharmacol.* **2001**, *59* (5), 1181-1186.
61. Boison, D., Adenosine kinase: exploitation for therapeutic gain. *Pharmacol. Rev.* **2013**, *65* (3), 906-943.
62. Kamat, S. S.; Burgos, E. S.; Raushel, F. M., Potent Inhibition of the C–P Lyase Nucleosidase PhnI by Immucillin-A Triphosphate. *Biochem.* **2013**, *52* (42), 7366-7368.
63. Cassera, M. B.; Ho, M.-C.; Merino, E. F.; Burgos, E. S.; Rinaldo-Matthis, A.; Almo, S. C.; Schramm, V. L., A high-affinity adenosine kinase from *Anopheles gambiae*. *Biochem.* **2011**, *50* (11), 1885-1893.
64. Park, J.; Gupta, R., Adenosine kinase and ribokinase—the RK family of proteins. *Cell. Mol. Life Sci.* **2008**, *65* (18), 2875-2896.
65. Panayiotou, C.; Solaroli, N.; Karlsson, A., The many isoforms of human adenylate kinases. *Int. J. Biochem. Cell Biol.* **2014**, *49*, 75-83.
66. Johansson, M.; Amiri, M.; Karlsson, A., Phosphorylation of 9-β-D-arabinofuranosylguanine monophosphate by *Drosophila melanogaster* guanylate kinase. *Biochem. Pharmacol.* **2005**, *70* (7), 987-992.
67. Agarwal, K. C.; Miech, R. P.; Parks, R. E., [64] Guanylate kinases from human erythrocytes, hog brain, and rat liver. In *Purine and Pyrimidine Nucleotide Metabolism*, Hoffee, P. A.; Jones, M. E., Eds. Academic Press: Cambridge MA, 1978; Vol. 51, pp 483-490.
68. Lascu, I.; Gonin, P., The catalytic mechanism of nucleoside diphosphate kinases. *J. Bioenerg. Biomembr.* **2000**, *32* (3), 237-246.
69. Janin, J.; Dumas, C.; Moréra, S.; Xu, Y.; Meyer, P.; Chiadmi, M.; Cherfils, J., Three-dimensional structure of nucleoside diphosphate kinase. *J. Bioenerg. Biomembr.* **2000**, *32* (3), 215-225.

70. Finan, P.; White, I.; Redpath, S.; Findlay, J.; Millner, P., Molecular cloning, sequence determination and heterologous expression of nucleoside diphosphate kinase from *Pisum sativum*. *Plant Mol. Biol.* **1994**, 25 (1), 59-67.
71. Lacombe, M.-L.; Wallet, V. r.; Troll, H.; Veron, M., Functional cloning of a nucleoside diphosphate kinase from *Dictyostelium discoideum*. *J. Biol. Chem.* **1990**, 265 (17), 10012-10018.
72. Ramos, C. R. R.; Abreu, P. A. E.; Nascimento, A. L. T. O.; Ho, P. L., A high-copy T7 *Escherichia coli* expression vector for the production of recombinant proteins with a minimal N-terminal His-tagged fusion peptide. *Braz. J. Med. Biol.* **2004**, 37 (8), 1103-1109.
73. Jeong, H.; Kim, H. J.; Lee, S. J., Complete genome sequence of *Escherichia coli* strain BL21. *Genome Announc.* **2015**, 3 (2).
74. Robichon, C.; Luo, J.; Causey, T. B.; Benner, J. S.; Samuelson, J. C., Engineering *Escherichia coli* BL21 (DE3) derivative strains to minimize *E. coli* protein contamination after purification by immobilized metal affinity chromatography. *Appl. Environ. Microbiol.* **2011**, 77 (13), 4634-4646.
75. Einhauer, A.; Jungbauer, A., The FLAGTM peptide, a versatile fusion tag for the purification of recombinant proteins. *J. Biochem. Biophys. Methods* **2001**, 49 (1), 455-465.
76. Lichty, J. J.; Malecki, J. L.; Agnew, H. D.; Michelson-Horowitz, D. J.; Tan, S., Comparison of affinity tags for protein purification. *Protein. Expr. Purif.* **2005**, 41 (1), 98-105.
77. Gorenstein, D. G., *Phosphorous-31 NMR: Principles and applications*. Academic Press: Cambridge, MA, 2012.
78. Gorenstein, D. G., Nucleotide conformational analysis by ³¹P nuclear magnetic resonance spectroscopy. *Annual Review of Biophysics and Bioengineering* **1981**, 10 (1), 355-386.
79. Rao, B. D. N.; Kayne, F. J.; Cohn, M., ³¹P NMR studies of enzyme-bound substrates of rabbit muscle pyruvate kinase. Equilibrium constants, exchange rates, and NMR parameters. *J. Biol. Chem.* **1979**, 254 (8), 2689-2696.
80. Rao, B. D. N.; Cohn, M.; Noda, L., Differentiation of nucleotide binding sites and role of metal ion in the adenylate kinase reaction by ³¹P NMR. Equilibria, interconversion rates, and NMR parameters of bound substrates. *J. Biol. Chem.* **1978**, 253 (4), 1149-1158.

81. Hooks, M. A.; Clark, R. A.; Nieman, R. H.; Roberts, J. K. M., Compartmentation of Nucleotides in Corn Root Tips Studied by ³¹P-NMR and HPLC 1. *Plant Physiol.* **1989**, *89* (3), 963-969.
82. Qian, Y.; Ding, Q.; Li, Y.; Zou, Z.; Yan, B.; Ou, L., Phosphorylation of uridine and cytidine by uridine–cytidine kinase. *J. Biotechnol.* **2014**, *188*, 81-87.
83. Fehlau, M.; Kaspar, F.; Hellendahl, K. F.; Schollmeyer, J.; Neubauer, P.; Wagner, A., Modular Enzymatic Cascade Synthesis of Nucleotides Using a (d)ATP Regeneration System. *Front. Bioeng. Biotechnol.* **2020**, *8* (854).
84. Ainsworth, S.; Macfarlane, N., A kinetic study of rabbit muscle pyruvate kinase. *Biochem. J.* **1973**, *131* (2), 223-236.
85. Song, Z.; Sims, A.; Eady, J.; Zhao, H.; Olubajo, O., Determining nucleotide acidity and cation binding constants by ³¹P NMR. *Canadian Journal of Analytical Sciences and Spectroscopy* **2008**, *53*, 45-51.
86. Hoffmann, R.; Reichert, I.; Wachs, W. O.; Zeppezauer, M.; Kalbitzer, H. R., ¹H and ³¹P NMR spectroscopy of phosphorylated model peptides. *Int. J. Pept. Protein Res.* **1994**, *44* (3), 193-198.
87. Sarkisjan, D.; Julsing, J. R.; Smid, K.; de Klerk, D.; van Kuilenburg, A. B. P.; Meinsma, R.; Lee, Y. B.; Kim, D. J.; Peters, G. J., The Cytidine Analog Fluorocyclopentenylcytosine (RX-3117) Is Activated by Uridine-Cytidine Kinase 2. *PLOS ONE* **2016**, *11* (9), e0162901.
88. Murata, D.; Endo, Y.; Obata, T.; Sakamoto, K.; Syouji, Y.; Kadohira, M.; Matsuda, A.; Sasaki, T., A Crucial Role of Uridine/Cytidine Kinase 2 in Antitumour Activity of 3'-Ethylnyl Nucleosides. *Drug Metab. Dispos.* **2004**, *32* (10), 1178-1182.
89. van Kuilenburg, A. B. P.; Meinsma, R., The pivotal role of uridine-cytidine kinases in pyrimidine metabolism and activation of cytotoxic nucleoside analogues in neuroblastoma. *Biochim. Biophys. Acta Mol. Basis Dis.* **2016**, *1862* (9), 1504-1512.
90. Boehm, J. S.; Zhao, J. J.; Yao, J.; Kim, S. Y.; Firestein, R.; Dunn, I. F.; Sjostrom, S. K.; Garraway, L. A.; Weremowicz, S.; Richardson, A. L.; Greulich, H.; Stewart, C. J.; Mulvey, L. A.; Shen, R. R.; Ambrogio, L.; Hirozane-Kishikawa, T.; Hill, D. E.; Vidal, M.; Meyerson, M.; Grenier, J. K.; Hinkle, G.; Root, D. E.; Roberts, T. M.; Lander, E. S.; Polyak, K.; Hahn, W. C., Integrative genomic approaches identify IKBKE as a breast cancer oncogene. *Cell* **2007**, *129* (6), 1065-79.

91. Schultheisz, H. L.; Szymczyna, B. R.; Scott, L. G.; Williamson, J. R., Pathway engineered enzymatic de novo purine nucleotide synthesis. *ACS Chemical Biology* **2008**, 3 (8), 499-511.
92. New England BioLabs Inc. Monarch® Plasmid DNA Miniprep Kit Protocol (NEB #T1010). <https://international.neb.com/protocols/2015/11/20/monarch-plasmid-dna-miniprep-kit-protocol-t1010> (accessed 4 Feb).
93. Merck BL21 Chemically Competent Cells. <https://www.sigmaaldrich.com/technical-documents/protocols/biology/bl21-chemically-competent-cells.html> (accessed 4 Feb).
94. Clontech Laboratories Inc. Stellar™ Competent Cells Protocol PT5055-2. <https://www.takarabio.com/documents/User%20Manual/PT5055/PT5055-2.pdf> (accessed 4 Feb).
95. Novagen BugBuster® Protein Extraction Reagent. https://www.merckmillipore.com/NZ/en/product/BugBuster-Protein-Extraction-Reagent,EMD_BIO-70584?ReferrerURL=https%3A%2F%2Fwww.google.com%2F#anchor_USP (accessed 4 Feb).
96. GE Healthcare His SpinTrap. <https://cdn.cytivalifesciences.com/dmm3bwsv3/AssetStream.aspx?mediaformatid=10061&destinationid=10016&assetid=13939> (accessed 10 Feb).
97. ThermoFisher Scientific Slide-A-Lyzer® Dialysis Cassette 12-30mL. https://www.thermofisher.com/document-connect/document-connect.html?url=https://assets.thermofisher.com/TFS-Assets%2FSLSG%2Fmanuals%2FMAN0011515_SlideALyzer_Dialy_Cassette_12_30mL_UG.pdf (accessed 10 Sep).
98. Appleby, T. C.; Larson, G.; Cheney, I. W.; Walker, H.; Wu, J. Z.; Zhong, W.; Hong, Z.; Yao, N., Structure of human uridine-cytidine kinase 2 determined by SIRAS using a rotating-anode X-ray generator and a single samarium derivative. *Acta Crystallogr. D* **2005**, 61 (3), 278-284.
99. Rogne, P.; Rosselin, M.; Grundström, C.; Hedberg, C.; Sauer, U. H.; Wolf-Watz, M., Molecular mechanism of ATP versus GTP selectivity of adenylate kinase. *Proc. Natl. Acad. Sci. U.S.A* **2018**, 115 (12), 3012-3017.
100. Kovermann, M.; Ådén, J.; Grundström, C.; Elisabeth Sauer-Eriksson, A.; Sauer, U. H.; Wolf-Watz, M., Structural basis for catalytically restrictive dynamics of a high-energy enzyme state. *Nat. Commun.* **2015**, 6 (1), 7644.

101. Kandeel, M.; Nakanishi, M.; Ando, T.; El-Shazly, K.; Yosef, T.; Ueno, Y.; Kitade, Y., Molecular cloning, expression, characterization and mutation of *Plasmodium falciparum* guanylate kinase. *Mol. Biochem. Parasitol.* **2008**, *159* (2), 130-133.
102. Segura-Peña, D.; Sekulic, N.; Ort, S.; Konrad, M.; Lavie, A., Substrate-induced conformational changes in human UMP/CMP kinase. *J. Biol. Chem.* **2004**, *279* (32), 33882-33889.
103. Lossani, A.; Torti, A.; Gatti, S.; Bruno, A.; Maserati, R.; Wright, G. E.; Focher, F., Thymidine kinase and uridine-cytidine kinase from *Entamoeba histolytica*: cloning, characterization, and search for specific inhibitors. *Parasitology* **2009**, *136* (6), 595-602.
104. Saint Girons, I.; Gilles, A.; Margarita, D.; Michelson, S.; Monnot, M.; Fermandjian, S.; Danchin, A.; Barzu, O., Structural and catalytic characteristics of *Escherichia coli* adenylate kinase. *J. Biol. Chem.* **1987**, *262* (2), 622-629.
105. Huss, R. J.; Glaser, M., Identification and purification of an adenylate kinase-associated protein that influences the thermolability of adenylate kinase from a temperature-sensitive adk mutant of *Escherichia coli*. *J. Biol. Chem.* **1983**, *258* (21), 13370-13376.
106. Xu, Y.; Johansson, M.; Karlsson, A., Human UMP-CMP kinase 2, a novel nucleoside monophosphate kinase localized in mitochondria. *J. Biol. Chem.* **2008**, *283* (3), 1563-1571.
107. Hsu, C.-H.; Liou, J.-Y.; Dutschman, G. E.; Cheng, Y.-C., Phosphorylation of cytidine, deoxycytidine, and their analog monophosphates by human UMP/CMP kinase is differentially regulated by ATP and magnesium. *Mol. Pharmacol.* **2005**, *67* (3), 806-814.
108. Hall, S. W.; Kühn, H., Purification and properties of guanylate kinase from bovine retinas and rod outer segments. *Eur. J. Biochem.* **1986**, *161* (3), 551-556.
109. Nardi-Schreiber, A.; Sapir, G.; Gamliel, A.; Kakhlon, O.; Sosna, J.; Gomori, J. M.; Meiner, V.; Lossos, A.; Katz-Brull, R., Defective ATP breakdown activity related to an ENTPD1 gene mutation demonstrated using ³¹P NMR spectroscopy. *ChemComm.* **2017**, *53* (65), 9121-9124.
110. Dong, Y.; McGown, L. B., Chiral selectivity of guanosine media in capillary electrophoresis. *Electrophoresis* **2011**, *32* (13), 1735-1741.
111. Kaucher, M. S.; Lam, Y. F.; Pieraccini, S.; Gottarelli, G.; Davis, J. T., Using diffusion NMR to characterize guanosine self-association: Insights into structure and mechanism. *Chem. Eur. J.* **2005**, *11* (1), 164-173.

112. Liu, X.; Liu, L.; Wang, Y.; Wang, X.; Ma, Y.; Li, Y., The Study on the factors affecting transformation efficiency of *E. coli* competent cells. *Cell* **2014**, *5*, x106.
113. Kim, Y.-T.; Choi, E.-H.; Son, B.-K.; Seo, E.-H.; Lee, E.-K.; Ryu, J.-K.; Ha, G.-W.; Kim, J.-S.; Kwon, M.-R.; Jae-Hoon Nam, Y.-J. K., Effects of storage buffer and temperature on the integrity of human DNA. *Korean J. Clin. Lab. Sci.* **2012**, *44* (1), 24-30.
114. Greenstein, K. E.; Zamyadi, A.; Wert, E. C., Comparative Assessment of Physical and Chemical Cyanobacteria Cell Lysis Methods for Total Microcystin-LR Analysis. *Toxins* **2021**, *13* (9), 596.
115. Dumon-Seignovert, L.; Cariot, G.; Vuillard, L., The toxicity of recombinant proteins in *Escherichia coli*: a comparison of overexpression in BL21(DE3), C41(DE3), and C43(DE3). *Protein. Expr. Purif.* **2004**, *37* (1), 203-206.
116. Miroux, B.; Walker, J. E., Over-production of Proteins in *Escherichia coli*: Mutant Hosts that Allow Synthesis of some Membrane Proteins and Globular Proteins at High Levels. *J. Mol. Biol.* **1996**, *260* (3), 289-298.
117. Bentley, W. E.; Mirjalili, N.; Andersen, D. C.; Davis, R. H.; Kompala, D. S., Plasmid-encoded protein: The principal factor in the “metabolic burden” associated with recombinant bacteria. *Biotechnol. Bioeng.* **1990**, *35* (7), 668-681.
118. Magnusdottir, A.; Johansson, I.; Dahlgren, L.-G.; Nordlund, P.; Berglund, H., Enabling IMAC purification of low abundance recombinant proteins from *E. coli* lysates. *Nat. Methods* **2009**, *6* (7), 477-478.
119. Bornhorst, J. A.; Falke, J. J., [16] Purification of proteins using polyhistidine affinity tags. In *Applications of Chimeric Genes and Hybrid Proteins Part A: Gene Expression and Protein Purification*, Thorner, J.; Emr, S. D.; Abelson, J. N., Eds. Academic Press: Cambridge, MA, 2000; Vol. 326, pp 245-254.
120. Lee, T.; Karon, M.; Momparler, R. L., Kinetic Studies on Phosphorylation of 5-Azacytidine with the Purified Uridine-Cytidine Kinase from Calf Thymus. *Cancer Res.* **1974**, *34* (10), 2482-2488.
121. Anderson, E. P., [40] Uridine-cytidine kinase from a murine neoplasm. In *Purine and Pyrimidine Nucleotide Metabolism*, Hoffee, P. A.; Jones, M. E., Eds. Academic Press: Cambridge, MA, 1978; Vol. 51, pp 314-321.

122. Zou, Z.; Ding, Q.; Ou, L.; Yan, B., Efficient production of deoxynucleoside-5'-monophosphates using deoxynucleoside kinase coupled with a GTP-regeneration system. *Appl. Microbiol. Biotechnol.* **2013**, *97* (21), 9389-9395.
123. Kameda, A.; Shiba, T.; Kawazoe, Y.; Satoh, Y.; Ihara, Y.; Munekata, M.; Ishige, K.; Noguchi, T., A novel ATP regeneration system using polyphosphate-AMP phosphotransferase and polyphosphate kinase. *J. Biosci. Bioeng.* **2001**, *91* (6), 557-563.
124. Elkin, S. R.; Kumar, A.; Price, C. W.; Columbus, L., A broad specificity nucleoside kinase from *Thermoplasma acidophilum*. *Proteins* **2013**, *81* (4), 568-582.
125. Pearman, A. T.; Castro-Faria-Neto, H. C.; McIntyre, T. M.; Prescott, S. M.; Stafforini, D. M., Characterization of human UMP-CMP kinase enzymatic activity and 5' untranslated region. *Life Sci.* **2001**, *69* (20), 2361-2370.
126. Pasti, C.; Gallois-Montbrun, S.; Munier-Lehmann, H.; Veron, M.; Gilles, A. M.; Deville-Bonne, D., Reaction of human UMP-CMP kinase with natural and analog substrates. *Eur. J. Biochem.* **2003**, *270* (8), 1784-1790.
127. Cavaliere, A.; Probst, K. C.; Westwell, A. D.; Slusarczyk, M., Fluorinated nucleosides as an important class of anticancer and antiviral agents. *Future Med. Chem.* **2017**, *9* (15), 1809-1833.
128. Li, L. H.; Olin, E. J.; Buskirk, H. H.; Reineke, L. M., Cytotoxicity and Mode of Action of 5-Azacytidine on L1210 Leukemia. *Cancer Res.* **1970**, *30* (11), 2760-2769.
129. Khan, F.; Legler, P. M.; Mease, R. M.; Duncan, E. H.; Bergmann-Leitner, E. S.; Angov, E., Histidine affinity tags affect MSP142 structural stability and immunodominance in mice. *Biotechnol. J.* **2012**, *7* (1), 133-147.
130. Wang, F.; Ren, X.-F.; Chen, Z.; Li, X.-L.; Zhu, H.-J.; Li, S.; Ou, X.-H.; Zhang, C.; Zhang, F.-X.; Zhu, B.-C., The N-terminal His-tag affects the triglyceride lipase activity of hormone-sensitive lipase in testis. *J. Cell. Biochem.* **2019**, *120* (8), 13706-13716.
131. Booth, W. T.; Schlachter, C. R.; Pote, S.; Ussin, N.; Mank, N. J.; Klapper, V.; Offermann, L. R.; Tang, C.; Hurlburt, B. K.; Chruszcz, M., Impact of an N-terminal Polyhistidine Tag on Protein Thermal Stability. *ACS Omega* **2018**, *3* (1), 760-768.
132. Carson, M.; Johnson, D. H.; McDonald, H.; Brouillette, C.; DeLucas, L. J., His-tag impact on structure. *Acta Crystallogr. D* **2007**, *63* (3), 295-301.

133. Spriestersbach, A.; Kubicek, J.; Schäfer, F.; Block, H.; Maertens, B., Chapter One - Purification of His-Tagged Proteins. In *Laboratory Methods in Enzymology: Protein Part D*, Lorsch, J. R., Ed. Academic Press: Cambridge, MA, 2015; Vol. 559, pp 1-15.
134. Mahmood, T.; Yang, P.-C., Western blot: technique, theory, and trouble shooting. *N. Am. J. Med. Sci.* **2012**, *4* (9), 429-434.
135. Finch, S. A.; Slater, T. F.; Stier, A., Nucleotide metabolism by microsomal UDP-glucuronyltransferase and nucleoside diphosphatase as determine by ³¹P nuclear-magnetic-resonance spectroscopy. *Biochem. J.* **1979**, *177* (3), 925-930.
136. Wehrli, S. L.; Palmieri, M. J.; Reynolds, R. A.; Segal, S., ³¹P NMR spectra of intact red blood cells: Quantitation of UDPGlucose and UDPGalactose. *Mag. Reson. Med.* **1993**, *30* (4), 494-497.
137. Williams, J. P.; Headrick, J. P., Differences in nucleotide compartmentation and energy state in isolated and in situ rat heart: Assessment by ³¹P-NMR spectroscopy. *Biochim. Biophys. Acta Bioenerg.* **1996**, *1276* (1), 71-79.
138. Hitchins, S.; Cieslar, J. M.; Dobson, G. P., ³¹P NMR quantitation of phosphorus metabolites in rat heart and skeletal muscle in vivo. *American Journal of Physiology-Heart and Circulatory Physiology* **2001**, *281* (2), H882-H887.
139. Hennig, M.; Scott, L. G.; Sperling, E.; Bermel, W.; Williamson, J. R., Synthesis of 5-Fluoropyrimidine Nucleotides as Sensitive NMR Probes of RNA Structure. *J. Am. Chem. Soc.* **2007**, *129* (48), 14911-14921.
140. Valino, A. L.; Iribarren, A. M.; Lewkowicz, E., New biocatalysts for one pot multistep enzymatic synthesis of pyrimidine nucleoside diphosphates from readily available reagents. *J. Mol. Catal., B Enzym.* **2015**, *114*, 58-64.